

Sea Surface Temperature Reconstruction (Sr/Ca) from Modern and Fossil Caribbean Holocene Corals

By:

Ángel L. Jiménez Arroyo

Thesis submitted in partial fulfillment of the requirements for the degree of

MASTER OF SCIENCE
In
GEOLOGY

UNIVERSITY OF PUERTO RICO
MAYAGÜEZ CAMPUS
2018

Approved by:

Wilson R. Ramírez, Ph.D.
Graduate Committee, chair

Date

Hernán Santos Ph.D.
Graduate Committee, member

Date

Stephen Hughes Ph.D.
Graduate Committee, member

Date

Enid Arcelay, Ph.D.
Graduate Studies Office Representative

Date

Lizzette Rodríguez Ph.D.
Chairperson of the Department

Date

Abstract

Previous studies suggest that recent global temperature rise has been driven by both anthropogenic activity and natural variability. The study of pre-historic climate change without anthropogenic influences should place natural climate variability into context. The focus of this study is to interpret tropical Sea Surface Temperature (SST) based on measured Sr/Ca ratios, through the Holocene from $\sim 9.0 \text{ K} \pm 200$ - $5.6 \text{ K} \pm 29$ ybp from five (5) fossil *Orbicella complex sp.* corals collected from different facies in a well-preserved reef (Cañada Honda) located on the slopes of Enriquillo Lake Valley, Dominican Republic. A Sr/Ca-Temperature calibration curve was developed using a modern *Orbicella complex sp.* coral from Barahona Bay, ~ 70 Km from the fossil Cañada Honda Reef. Temperatures derived from previous Sr/Ca data sets were re-calculated with our equation. Coral growth rates based on measurements from radiographs indicate slow growth of fossil corals (1.32 - 1.98 mm/year, n=5) relative to the modern Barahona location coral that show a growth rate of 7.34 mm/year. U-Th analyses indicate a mid-Holocene for the age corals ($8,365 \pm 25$ - $5,690 \pm 29$ ybp, n=5). Original aragonite mineralogy of the coral skeleton (i.e. no neomorphism to calcite) was corroborated by XRD analyses. The resulting Sr/Ca-Temperature calibration equation is $\text{Sr/Ca} = -0.0676 * \text{SST} + 10.7867$. The SST average values obtained were 27.8 ± 1.1 (°C) for modern coral, (18.79 ± 1.2 to 26.86 ± 2.0 °C) for fossil corals, and they provide snapshots of SST for early to mid-Holocene ages.

Resumen

Estudios previos sugieren que el reciente aumento global de la temperatura ha sido impulsado tanto por la actividad antropogénica como por la variabilidad natural. El estudio del cambio climático prehistórico sin influencias antropogénicas debe ubicar la variabilidad climática natural en su contexto. El objetivo de este estudio es interpretar la temperatura superficial del mar tropical (SST) basada en relaciones medidas de Sr / Ca, a través del Holoceno desde $\sim 9,0 \text{ K} \pm 200 - 5,6 \text{ K} \pm 29$ ybp de cinco (5) fósiles del complejo *Orbicella sp.* corales recolectados de diferentes facies en un arrecife bien conservado (Cañada Honda) ubicado en las laderas del Valle del Lago Enriquillo, República Dominicana. Se desarrolló una curva de calibración Sr / Ca-Temperature usando un complejo moderno de *Orbicella sp.* coral de la bahía de Barahona, a unos 70 km del fósil Cañada Honda Reef. Las temperaturas derivadas de los conjuntos de datos anteriores Sr / Ca se recalcularon con nuestra ecuación. Las tasas de crecimiento de corales basadas en mediciones de radiografías indican crecimiento lento de corales fósiles (1.32 - 1.98 mm / año, n = 5) en relación con la moderna ubicación de coral Barahona que muestra una tasa de crecimiento de 7.34 mm / año. Los análisis U-Th indican un Holoceno medio para los corales de edad ($8.365 \pm 25 - 5.690 \pm 29$ ybp, n = 5). La mineralogía de aragonita original del esqueleto coralino (es decir, no neomorfismo a la calcita) fue corroborada por análisis XRD. La ecuación de calibración de Sr / Ca-temperatura resultante es $\text{Sr} / \text{Ca} = -0.0676 * \text{SST} + 10.7867$. Los valores promedio de SST obtenidos fueron 27.8 ± 1.1 (° C) para los corales modernos (18.79 ± 1.2 a 26.86 ± 2.0 ° C) para los corales fósiles, y proporcionan instantáneas de SST para edades tempranas a medias del Holoceno.

© 2018

Ángel L. Jiménez Arroyo
ALL RIGHTS RESERVED

To my mom, my dad, my sister and my wife

Love you all.....

Acknowledgements

I would like to express my gratitude to several people that contributed in different ways and help through my path on this incredible journey. I will like to thank Dr. Wilson R. Ramírez for his support and trust by letting me be part of this amazing project. My gratitude to the members of the graduate committee, Dr. Hernan Santos and Dr. Stephen Hughes, who both contributed with their knowledge to this work. I will also like to thank the Geology Department staff, Marsha Irizarry and Catherine Perez for the patience and help they both gave me through my years in the department.

My highest gratitude to Dr. Julie Richey and Dr. Jennifer Flannery of the United States Geological Survey (USGS) St. Petersburg, Florida for all the knowledge shared the use of their laboratory and equipment to produce my project. Without your help I would not have been able to finish such a great project. I will be forever thankful. Special thanks to the Extramural Research Experience Award -Transformational Initiative for Graduate Education and Research (EREA-TIGER) at University of Puerto Rico, Mayagüez Campus for the funding provided (Department of Education, Title V Part B, Promoting Postbaccalaureate Opportunities for Hispanic Americans Program (PPOHA) under Award # P031M140035) during the summer 2017 that help me with the travel expenses in St. Petersburg, Florida, while I was doing the analytical work at Dr. Julie Richey's laboratory. Special thanks to Dr. Ali Pourmand, from the Rosenstiel School of Marine and Atmospheric Science, for the Uranium/Thorium dating of corals and San Antonio Hospital personnel in Mayagüez for radiographs taken.

I would also like to thank my parents, Mr. Ángel R. Jiménez and Ms. Gloria M. Arroyo for all the unconditional love and support they provided through all my life. My highest gratitude to my wife Ms. Zully Contreras who stole my heart since the day we met. Thanks for always been

there for me, for all the love, support, patience, for holding my hand always, for been by my side on my hardest days, and for always pushing to make me better, love you hun. I would like to thank also my dearest friend Mr. Ángel Adames for the support and for all great times we had together.

In loving memory for those who are no longer with us but are going to be always in our minds, both of my grandmothers Ms. Gloria A. García and Fidelina Cotte (mama Gloria & mama File) and Dr. Eugenio Asencio, for encouraging me to continue graduate studies. Today, I feel pride when I mention that at some point I was your graduate student.

Table of contents:

Abstract.....	ii
Resumen.....	iii
Copy right page.....	iv
Dedication.....	v
Acknowledgements.....	vi-vii
Table of contents.....	viii
List of tables.....	ix
List of Figures.....	x-xiii
List of appendixes.....	xiv
1.0 Introduction	1-3
1.1 Objective Statement.....	2-3
2.0 Study Area	3-11
3.0 Methodology	12-22
3.1 Field Work	12
3.1.1 Sample collection.....	12-16
3.1.2 Sample selection & sample preparation.....	17
3.2 Lab Work	17
3.2.1 X-rays and Growth Rates estimations.....	17-19
3.2.2 Determine preservation of coral skeleton	20
3.2.2.1 XRD.....	20
3.2.3 Paleoenvironmental Analysis	21-22
3.2.3.1 Fossil Coral Dating.....	21
3.2.3.2 Sr/Ca analysis.....	21
4.0 Results	22-54
4.1 Growth rates for Orbicella complex.....	22
4.2 Coral skeleton preservation state.....	22-24
4.3 Fossil coral radiogenic dates.....	24-25
4.4 Sr/Ca analysis from modern & fossil coral.....	25-34
4.5 SST Calculations from modern coral & fossil corals.....	35-53
5.0 Discussion	55-69
5.1 Growth Rates.....	54-60
5.2 XRD analysis.....	61
5.3 U/Th.....	61
5.4 Sr/Ca-T calculations.....	62-66
5.5 Cañada Honda SST Record from corals vs. the Holocene SST record.....	67-68
6.0 Conclusion	69-70
References.....	71-76
Appendix.....	77-109

List of tables

Table 1: List of coral samples used for this study

Table 2: Corals used on Morales (2014) study. Added to this study.

Table 3: Summary of Growth Rates for coral used for this study.

Table 4: Fossil coral ages

Table 5: Record of sample and the analysis applied.

List of Figures

- Figure 1.** Location of Cañada Honda reef exposure (green dot) and location from which the modern coral was collected (red dot). Neiba and Bahoruco mountain ranges are enclosed by dotted lines.
- Figure 2.** Mann et al., 1984 and Taylor et al., 1985 proposed there was an Enriquillo embayment ~10K ybp (top figure) associated with open marine waters from the Caribbean Sea. The closure of the embayment probably occurred due to a gradual input of sediments from Rio Yaque del Sur ~4.5K ybp (middle figure) and produced the Enriquillo Lake Modern Day Conditions (bottom figure).
- Figure 3.** Cañada Honda corals in growth position (top figure). A, B, C and D show images illustrating the pristine preservation of fossil corals in the Cañada Honda reef exposure. This unusual preservation is due to the dry climate of the region and the fact that the corals were buried fast due to the high sedimentation environment. (Summer 2016).
- Figure 4.** Diagram of the cross-sectional view of Cañada Honda reef exposure showing the facies distribution map proposed for Cañada Honda by Hubbard et al., 2004 (Modified after Hubbard et al., 2004).
- Figure 5.** Location from which the fossil coral samples were collected (Red stars), and corals used on Morales (2014) study (Modified after Hubbard et al., 2004).
- Figure 6.** Mouth location of Rio Yaque del Sur ~10 K ybp (Top) and the mouth location in modern day (Bottom).
- Figure 7.** Radiograph of the modern *Orbicella complex* coral skeleton collected in Barahona Bay, Dominican Republic. Image illustrates high and low-density banding.
- Figure 8.** Luminance analysis of modern coral. Radiographs analyzed with “Coral XDS” program (Helmle et al., 2002).
- Figure 9.** Diffractogram showing the 2θ location of the intensity peaks for the minerals calcite, dolomite and aragonite (from Xu et al., 2014).
- Figure 10.** XRD results for the MZ fossil coral sample indicating a 100% aragonitic composition. Purple arrow indicates the location of the signal peak of calcite and the absence of detection of calcite (No Lin counts). The detection limit for calcite is 0.90% (Kontoyannis et al., 2015).
- Figure 11.** Discontinuity Band Observed in fossil coral M3-1. Samples were taken below, on the band and on top of the band. No other mineralogy in this coral aside aragonite was detected (3 samples).
- Figure 12.** Sr/Ca ratios from the modern coral sample (B-20) collected in Barahona, Dominican Republic. This is a composite of several analytical paths sampled along the coral. Depth in mm, zero, represent the surface of the coral.
- Figure 13.** Composite of different analytical transects or paths made from the modern coral sample (B-20) collected in Barahona, Dominican Republic. Depth in mm, zero, represent the surface of the coral.
- Figure 14.** Analytical replicates or paths made on fossil coral sample MZ-172. Re-drilling paths were made to confirm that the drilling was made along the same thecal wall. If the Sr/Ca values are reliable the analytical replicates of every path should be reproduced within analytical error. Depth in mm, zero, represent the surface of the coral.
- Figure 15.** Sr/Ca values combined from several analytical paths and replicates for coral sample MZ-172. Depth in mm, zero, represent the surface of the coral.

- Figure 16.** Sr/Ca values from fossil coral sample M2-135. Depth in mm, zero, represent the surface of the coral.
- Figure 17.** Sr/Ca values obtained from M3-1 coral sample. Depth in mm, zero, represent the surface of the coral.
- Figure 18.** Sr/Ca ratios obtained from M3-4. Depth in mm, zero, represent the surface of the coral.
- Figure 19.** Sr/Ca ratios Obtained from M2-146 fossil coral sample plotted vs. Depth (from top of the coral slab). Depth in mm, zero, represent the surface of the coral.
- Figure 20.** HADISST data set starting in 1870 and reaching the present from Rayner et al. (2003).
- Figure 21.** Lineage rescaling of Sr/Ca using HADI SST as reference.
- Figure 22.** Scatter plot and linear regression Sr/Ca (mmol/Mol) vs. temperature (°C) obtained from the modern coral (B-20) collected alive from the Barahona Bay, Dominican Republic. The graph also shows the calibration equations obtained from the linear regression and the correlation for the equation ($R^2 = -0.83$).
- Figure 23.** SST calculations for Sr/Ca obtained from the modern coral (B-20) collected alive in Barahona Bay, Dominican Republic. The equation used for the SST calculations is the one developed by this study.
- Figure 24.** Comparisons of the SST (°C) vs. time (years) for the modern coral (B-20) calculated from Sr/Ca, using different equations (Swart 2002 (green); Flannery 2013 (gold); this study (blue)) and also measured SST obtained from HADI (red). When all the results are compared Flannery (2013) SST is about 3 degrees warmer in average and Swart (2002) shows a similar average with higher high and low values. SST from the equation produced in this study is the most compatible with the measured HADI values. The equation obtained on this study exhibits a temperature average of 27.8 ± 1.1 , with maximum, minimum temperatures values of 30.5 ± 1.1 and 23.7 ± 1.1 , respectively. Using Flannery's (2013) equation on the modern coral shows an average, maximum and minimum temperature values of 33.8 ± 1.5 , 37.6 ± 1.5 and 28.4 ± 1.5 , respectively. Using Swart's (2002) equation on the modern coral exhibits a temperature average of 27.4 ± 1.9 , with maximum and minimum temperature values of 32.3 ± 1.9 and 20.15 ± 1.9 respectively.
- Figure 25.** Sea Surface Temperature calculations for fossil coral sample MZ-172 using equations from Swart (2002), Flannery (2013), and this study. Flannery (2013) resulted in a warmer temperature while Swart (2002) resulted in a colder temperature relative to our equation. The temperature values obtained by this study's equation are more similar to Swart (2002).
- Figure 26.** Sea Surface Temperature calculations for fossil coral sample M2-135 using equations from Swart (2002), Flannery (2013), and this study. Flannery (2013) and Swart (2002) resulted in warmer and colder SST values respectively. The temperature values obtained by this study's equation for fossil coral MZ-172 are similar to Swart (2002) SST values.
- Figure 27.** Sea Surface Temperature calculations for fossil coral sample M3-1 using equations from Swart (2002), Flannery (2013), and this study. Flannery (2013) and Swart (2002) resulted in warmer and colder SST values respectively. The temperature values obtained by this study's equation for fossil corals are more similar to Swart (2002).
- Figure 28.** Sea Surface Temperature calculations for fossil coral sample M3-4 using equations from Swart (2002), Flannery (2013), and this study. Flannery (2013) and Swart (2002) resulted in warmer and colder SST values respectively. The temperature values

obtained by this study's equation for fossil coral M3-4 resulted in similarities with Swart (2002).

- Figure 29.** Sea Surface Temperature calculations for fossil coral sample M2-146 using equations from Swart (2002), Giry (2011), and this study. Flannery (2013) and Swart (2002) resulted in warmer and colder SST values respectively. The temperature values obtained by this study's equation for fossil coral M2-146 are colder than Flannery (2013)
- Figure 30.** Sea Surface Temperature calculations for fossil coral sample M1-Ba using equations from Swart (2002), Giry (2011), and this study. Flannery (2013) and Swart (2002) resulted in slightly colder and colder SST values respectively. It should be noted that SST calculations using this study's equation resulted in similarities with Flannery (2013)
- Figure 31.** Sea Surface Temperature calculations for fossil coral sample M1-2E analyzed by Morales (2014) using equations from Swart (2002), Flannery (2013), and this study. Swart (2002) resulted in colder temperatures. M1-2E with Flannery (2013) resulted in slightly colder SST values. With this study's equation M1-2E resulted in similarities with Flannery (2013).
- Figure 32.** Sea Surface Temperature calculations for fossil coral sample M1-Dc processed by Morales (2014) using equations from Swart (2002), Flannery (2013), and this study. Flannery (2013) resulted in slightly colder SST values and Swart (2002) resulted in colder SST values. The SST values produced by this study's equation resulted in similarities with Flannery (2013).
- Figure 33.** Sea Surface Temperature calculations for fossil coral sample M1-Ee processed by Morales (2014) using equations from Swart (2002), Flannery (2013), and this study. Flannery (2013) resulted slightly colder SST values, while Swart (2002) resulted in colder SST values. The SST values produced by this study's equation resulted with similarities with Flannery (2013).
- Figure 34.** Composite graph of all SST calculated from Sr/Ca using equations by Flannery (2013) (gold), Swart (2002) (light green), and this study (royal blue). Sr/Ca data set of Massive Coral 1 (M1) was sampled and analyzed by from Morales 2014. Samples M2, MZ, M3-1 and M3-4 were sampled and analyzed for Sr/Ca in this study. The graph also includes Sr/Ca -SST values from the modern coral B-20 collected in Barahona Bay and processed by this study.
- Figure 35.** Images that illustrate exaggerated foliated morphology on shallow water corals (~3 meters depth).
- Figure 36.** Modern (Parguera Shelf Edge, PR) vs. Fossil (Holocene Cañada Honda Reef RD) examples of similar morphologies in the coral *Montastrea cavernosa*. A) *Montastrea cavernosa* from the Cañada Honda reef assumed to have lived an estimated depth of ~3 meters water. B) *Montastrea cavernosa* from the Parguera Shelf Edge in Lajas, Puerto Rico observed at a water depth of ~30 meters. The exaggerated columnar morphology of the fossil coral colony's. The estimated depth where it grew suggests that environmental conditions in the Holocene Cañada Honda reef were not optimal at the time when coral facies M3 accreted (Wilson R. Ramírez -personal communication)
- Figure 37.** Modern Caribbean growth rates of *Orbicella complex*. A comparison between corals that were collected on previous studied at a water depth lesser than 10 meters in, St.

Croix, USVI; Jamaica & Bermuda; Costa Rica; Puerto Rico; Mexico, ((black) (data from Gladfelter et al. 1978; Fairbanks and Dodge, 1979; Cortés and Risk, 1985; Torres and Morelock, 2002; Cruz-Piñón et al. 2003, respectively). Corals collected greater than 10 meters in St. Croix, USVI (red) (Hubbard et al., 1985) and this study at 10 meters water depth (Blue) (Barahona Bay). Average growth rate was calculated for data set and are represented as green.

Figure 38. Image show growth rates acquired from previous studies such as: Viviana (2005), Cuevas (2005 & 2009), Morales (2014), Herrera (2018), Arana (2018) and Rodríguez (2018), and this study from Cañada Honda reef exposure. Data from were compiled. Blue data points represent growth rates acquired in this study.

Figure 39. Cross sectional view of Cañada Honda reef showing the U-Th dates acquired from corals collected for this study and also corals studied by Morales (2014). U-Th dating for coral sample M2-135 was not determined (see table 5).

Figure 40. Figure shows the distributions of Sr/Ca ratios acquired for fossil collected from Cañada Honda. M1-Ba, M1-2E, M1-Dc, M1-Ee coral sample were acquired by Morales (2014), while M2-146, Mz-172, M3-4, M3-1 and Modern coral were acquired by author. Data set was arranged based on the U/Th ages acquired from each coral (oldest to youngest) (see Table 4 & Figure 34).

List of appendixes

Appendix 1: Densitometry analysis of M2-135 fossil coral sample.

Appendix 2: Densitometry analysis of M2-146 coral sample.

Appendix 3: Densitometry analysis of M3-1 coral sample.

Appendix 4: Densitometry analysis of M3-4 coral sample.

Appendix 5: Densitometry analysis of MZ-172 coral sample.

Appendix 6: XRD results for MZ-157.

Appendix 7: XRD results for M3-4.

Appendix 8: XRD results for M2-128.

Appendix 9: XRD results for M3-1 band.

Appendix 10: XRD results for M3-1 bottom.

Appendix 11: XRD results for M3-1 top.

Appendix 12: Sample M3-1 data.

Appendix 13: Sample M2-146 data.

Appendix 14: Sample MZ-172 data.

Appendix 15: Sample M3-4 data.

Appendix 16: Modern coral data.

1.0 Introduction

Modern climate change is an important issue. The role of natural climate variability, together with recent climate change, is relevant since both factors seem to be triggering natural climate hazards such as hurricanes, floods, and sea level rise (Flannery and Poore, 2013). A warming trend and associated global rise in sea level has been documented in recent decades (Saenger et al., 2008). Regional climatic events, produced by natural variability during the last 1,000 ybp, such as the Little Ice Age (LIA, 500–100 ybp.), seem to overlay anthropogenic activity, causing a significant change in the modern climate (Saenger et al., 2008). It is important to study natural climate variability in order develop a better understanding of the magnitude of man-made in climate change (Saenger et al., 2008). High-resolution reconstructions of paleo-temperatures using proxies during times before human influences help calibrate the relative contributions of natural vs. anthropogenic climate variations. Examples of these proxies are massive coral skeletons with annual banding patterns that provide a chronological framework for the records of temperature obtained from their geochemistry (Brachert et al., 2006). Massive coral skeletons can provide data to create high-resolution records of local and regional paleo-oceanographic variables such as paleo- Sea Surface Temperatures (SST), and Sea Surface Salinity (SSS) (Grottoli et al., 2001; Felis and Pätzold, 2004; Flannery et al., 2017).

The most common paleo-thermometers used for Sea Surface Temperature (SST) reconstructions at decadal and centennial scales are derived from coral skeleton proxies and are based on the ratio of strontium to calcium (Sr/Ca) or on oxygen isotopic ($\delta^{18}\text{O}$) aragonite compositions (Gaetani et al., 2011). The relationship of Sr/Ca ratios in coral skeletal aragonite varies as a function of water temperature as the coral grows. Fossil corals are good tools for paleoclimate studies, however, interpretations can be complicated by diagenesis (neomorphism),

calcification differences in coral species, precipitation of secondary Aragonite (CaCO_3) on the skeletons, variability in analytical methods, and the different sources of temperature data (in situ vs. remote satellite measurements) (Corrège, 2006). Correlation of temperature data sets from different studies has shown that corals living in the same environment and, at the same temperature show variations in Sr/Ca within single and multiple coral species (*Orbicella faveolata* and *Porites sp.*) (Saenger et al., 2008; Gaetani et al., 2011). It is difficult to find fossil corals older than a few thousand years that do not show neomorphic alterations (transformation of original aragonite to calcite) due to the instability of aragonite (Felis et al., 2004; Brachert et al., 2006; Sayani et al., 2011). That is what makes Cañada Honda fossil reef unique, due to the remarkable preservation state.

1.1 Objective Statement

Morales (2014) reported paleotemperature calculations (SST) of coral skeletons from Canada Honda reef, Dominican Republic that dated from 8.0 to 8.9k ybp (Holocene). He used equations from Leder et al. (1996), Giry et al. (2011), and Felis et al. (2004) and suggested that both $\delta^{18}\text{O}$ and Sr/Ca were reacting to external variables. He proposed that a better calibration equation was needed to produce more reliable SST from the Cañada Honda paleo-reef corals. The main objective of this study was produce an Sr/Ca - Temperature calibration equation from a modern coral collected in a location that is as close as possible to the Cañada Honda fossil reef. A modern coral was collected from the Barahona Bay, located 70 kilometers southeast of Cañada Honda in the Dominican Republic (Figure 1). Also, this study applied this equation to produce Sr/Ca derived SST estimates in several Cañada Honda Holocene fossil corals from which Sr/Ca was obtained. This modern coral represents the best possible analog to the Cañada Honda corals due to several reasons. Barahona Bay is in the same geographic environment than the paleo-

Enriquillo Bay was approximately 10 K ybp. Barahona Bay is affected today by high sedimentation conditions produced by the Río Yaque del Sur, similar to the paleo-Enriquillo Bay. The modern coral was collected in the bay close to the Río Yaque del Sur where estuarine conditions are present due to the continuous influx of river water, similar to the Paleo-Enriquillo Bay, where the river was just a few kilometers away from the Cañada Honda Reef several millennia ago. Most studies collect modern corals as far as possible from terrestrial influences, and their “geochemical” complications, but in this case, corals deposited under high sedimentation and riverine influences are those that are the most appropriate for comparison with the Cañada Honda fossil corals.

2.0 Study Area

The area of interest in this study is the Enriquillo Lake located in southwestern Dominican Republic between Sierra de Neiba and Sierra de Bahoruco. The lake is approximately 50 Km from the Haitian border and ~70 Km from Barahona Bay (Figure 1). Enriquillo Lake measures are ~40 Km and ~12 Km. These measurements can vary, due to regular changes in water level (Buck et al., 2005; Méndez et al., 2016; Delanoy et al., 2017). During the early Holocene (~10k ybp), the Enriquillo Basin had an extensive shallow marine embayment connected with the Caribbean Sea that provided an environment suitable for corals to grow and coral reefs to accrete (Hubbard et al. 2008). The connection to the open water marine environment became restricted about 4,500 ybp, probably due to the input of large amount of sediments from the Rio Yaque del Sur (Mann et al., 1984; Taylor et al., 1985). Although tectonic events associated with the Enriquillo-Great Plantain Fault Zone (GPFZ) have affected the area, it is a possible explanation for the restriction of Enriquillo Bay ~4.5 K ybp, Mann et al., (1984) suggest that episodic input of sediments from the Rio Yaque del Sur is the most likely cause for the enclosure of paleo-Enriquillo Bay. Eventually,

around 3,000 years ago, the mouth of the Enriquillo Bay was completely closed and lost the connection to the Caribbean Sea. This assessment is based on the presence of *Lithophaga sp.* boring on corals, massive, foliated, and columnar corals on top of the Cañada Honda reef; alga tufa along the shoreline, together with radiocarbon dating, suggested a grow stop on the Cañada Honda reef around these ages (Mann et al., 1984; Taylor et al., 1985; Cuevas, 2005; Greer and Swart, 2006). This situation caused evaporation and lowering of the water level, giving the lake its modern hypersaline character and its modern-day morphology (Figure 2) (Taylor et al., 1985).

The level of Enriquillo Lake, relative to modern sea level, has fluctuated significantly during the last decades. Depending on meteorological events and the degree of evaporation affecting the region, Enriquillo Lake has been as high as 25 meters below sea level and as low as 45 meters below sea level (Mendez et al., 2016; Delanoy et al., 2017). Along the flanks of the embayment, erosion has formed gullies or “cañadas”. One of these gullies, Cañada Honda, cuts through one of the Holocene reefs that was present in the paleo-Enriquillo Bay, exposing a complete section of spectacularly preserved coral reef (Taylor et al., 1985; Hubbard et al., 2004; Cuevas, 2005; Greer et al., 2006; Morales, 2014). The Enriquillo Valley region has low mean annual precipitation, a feature that has led to the preservation of the scleractinean coral skeletons and makes them ideal for paleo-climate studies (Greer et al., 2006; Flannery et al., 2013; Morales, 2014) (Figure 3).

Siderastrea sp., *Orbicella sp.*, and *Colpophylia sp.* are the dominant corals along the reef exposure, however many other coral species are present (Greer et al., 2006; Hubbard et al., 2004; Cuevas, 2005). The reef exposure extends 450 meters and was subdivided by Hubbard et al. (2004) into five reef facies based on the coral species abundance, attitude, distribution, size, and morphology (Figure 4): Massive Corals Facies 1 (M1), Massive Corals Facies 2 (M2), Mixing

Zone Facies (MZ), Massive Corals Facies 3 (M3), and *Acropora cervicornis* Facies Zone. These facies are similar to the modern reefs facies and are indicative of general reef zonation. Facies equivalent to modern fore-reef coral facies with plate-like corals and facies equivalent to reef-crest facies with *Acropora cervicornis* replacing *Acropora palmata* (Hubbard et al., 2008). The base of the Cañada Honda paleo-reef is a shell layer composed of different mollusk species. This layer served as a substrate for corals to colonize and drove the development of the reef (Hubbard et al., 2004). The M1 facies is the base coral unit and includes; *Siderastrea siderea* (51.5 %), *Montastrea faveolata* (14.0 %), *Stephanocoenia interspts* (7.3 %), *Dichocoenia stokesii* (1.7 %), *Colpophyllia natans* (1.7 %) (Cuevas 2005). In addition to the corals, 16.2 % of the M1 surface is covered by sediments and 5.8 % of the MAD Layer. The M2 facies is similar to the M1 facies, but it is separated from the M1 facies by a coral rubble layer composed of *Madracis sp.* coral fragments (MAD Layer) embedded in a matrix of carbonate mud. This layer has been interpreted as an event layer and has an age of 9,000 (\pm 200) ybp, based on U/Th dating of internal *Madracis sp.* coral fragments (Hubbard et al., 2004). Coral abundance in M2 is; *Siderastrea siderea* (56.3 %), *Montastrea faveolata* (10.1 %), *Stephanocoenia intersetsps* (1.0%), *Colpophyllia natans* (3.3%), *Eusmilia fastigiana* (1.5 %). Additional 10 species of coral are present in smaller abundance and comprise 4.1 % of the corals present (Cuevas 2005). In addition to the corals 18.5 % of M2 surface is covered by sediments and 5.2 % of the MAD Layer. Above M2, the MZ facies seems to have been deposited during a time of favorable environmental conditions, evidenced by the presence of several species of branching corals along with massive corals (Hubbard et al., 2004). The coral distribution in MZ based quadrant point counts of multiple transects along the exposure is; *Siderastrea siderea* (38.1%), *Montastrea faveolata* (5.0%), *Undaria agaricites* (7.8%), *Colpophyllia natans* (4.1%), *Agaricia lamarcki* (2.1%), *Porites porites* (7.6%), *Acropora*

cervicornis (1.1 %), *Montastrea cavernosa* (3.8%), *Eusmilia fastigiana* (5.8%), *Undaria tenuifolia* (1.1%), Additional 10 species of coral are present in smaller abundance and comprise 4.0 % of the corals present and 19.5 % of MZ surface is covered by sediments. The M3 facies includes abundant massive corals of considerable size, many with platy or foliated morphology (Hubbard et al., 2004). The coral abundance measured on M3 is; *Siderastrea siderea* (14.7 %), *Colpophyllia natans* (10.7 %), *Montastrea faveolata* (5.1 %), *Undaria agaricites* (8.4 %), *Porites porites* (8.1 %), *Monstastrea franksi* (26.7 %), *Montastrea cavernosa* (8.3 %), *Eusmilia fastigiana* (1.1 %). Additional 7 species of coral are present in smaller abundance and comprise 1.2 % of the corals present and 15.7 % of the outcrop surface is covered by sediments. Near the northernmost section of the reef (probably close to the paleo-shore) is 13 meters in size of *Acropora cervicornis* (Hubbard et al., 2004). The branching corals that compose this unit are in growth position. Finally, at the top of the sequence *Serpulid worm* mounds are present. These *Serpulid worm* mounds that are several meters size and line the whole embayment and are very useful as a marker. The *Serpulid worm* species that form the mounds live in shallow brackish water environments (Greer et al., 2006). The mounds are also useful as a marker of modern sea level since they are present around the Enriquillo embayment at the same elevation and that elevation is plus or minus 1 meter above modern sea level (Figure 4) (Winsor et al., 2006).

Barahona Bay its located ~70 Km southeast from the Cañada Honda Holocene reef. It is the closest location to Cañada Honda where modern corals grow. In addition, it has a similar environment than the one formerly present in the paleo-Enriquillo Bay with high sedimentation input from the Río Yaque del Sur (same river) and the high relief of Sierra de Neiba and Sierra de Bahoruco mountain ranges and association to marine waters from the Caribbean Sea. The proximity and similarity of modern Barahona Bay to the paleo-Enriquillo Bay, makes this location

the most appropriate to collect modern coral skeletons to produce Sr/Ca-Temperature calibrations for Cañada Honda fossil coral skeletons.

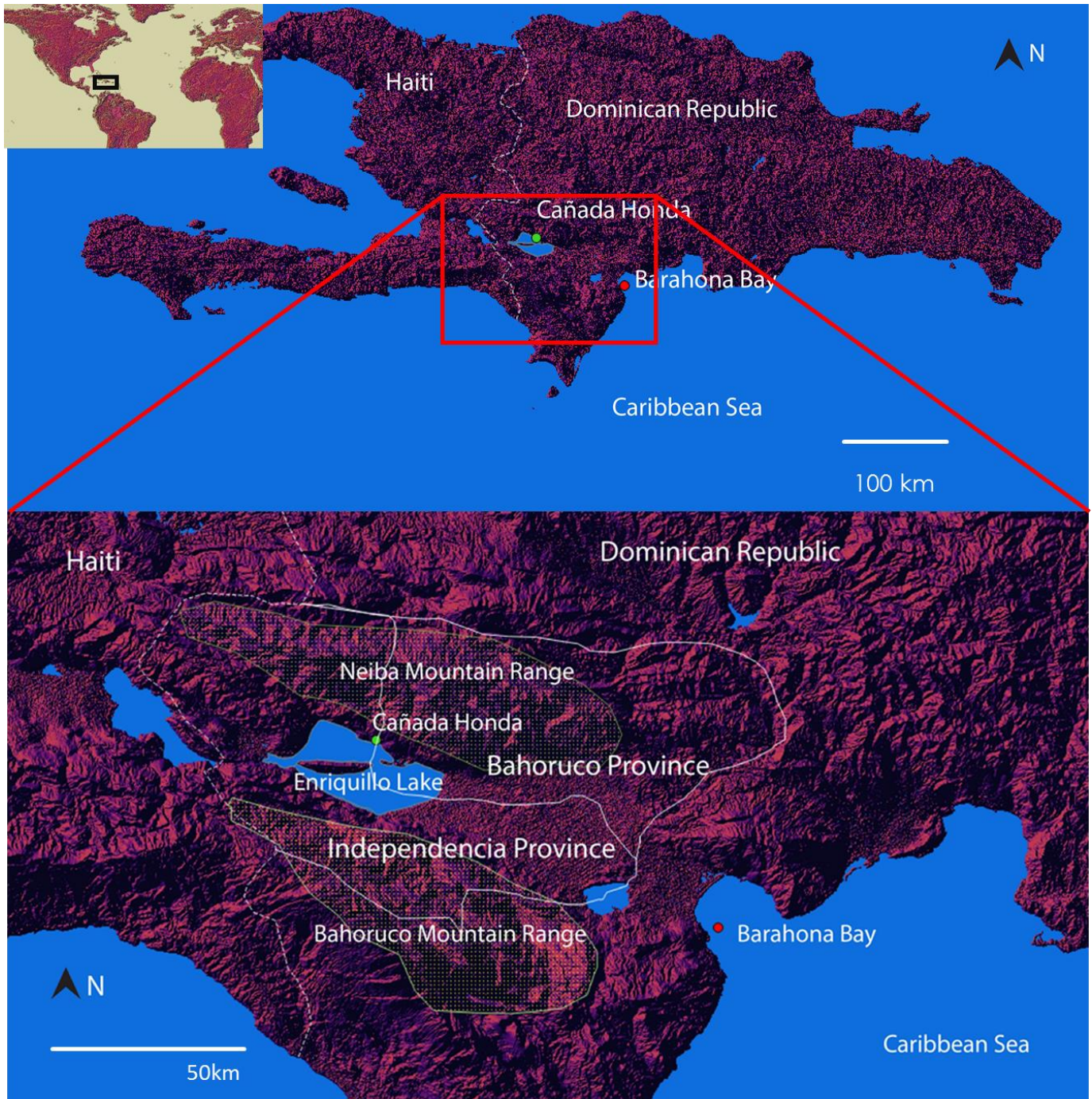


Figure 1. Location of Cañada Honda reef exposure (green dot) and location from which the modern coral was collected (red dot). Neiba and Bahoruco mountain ranges are enclosed by dotted lines.

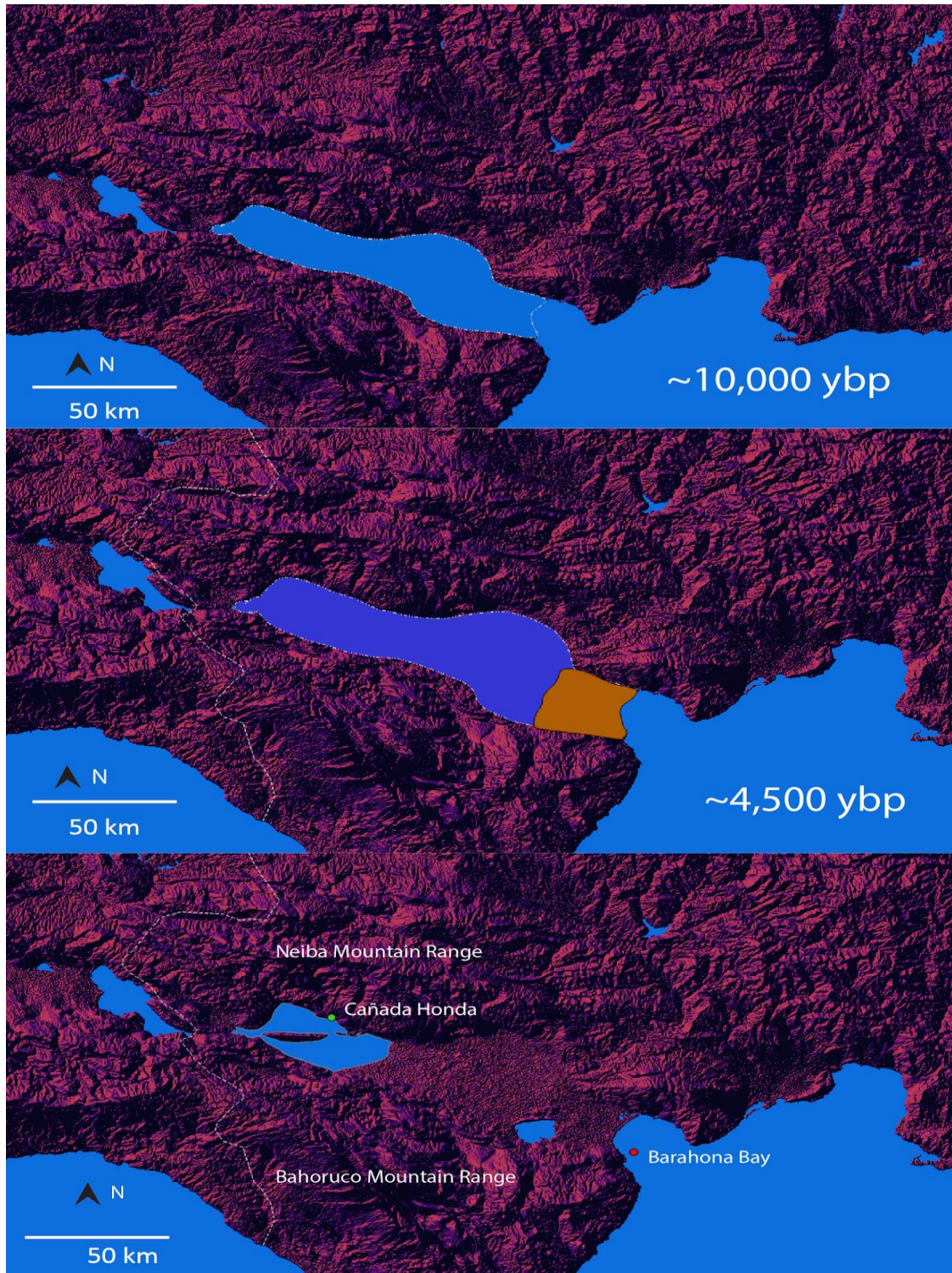


Figure 2. Mann et al., (1984) and Taylor et al., (1985) proposed there was an Enriquillo embayment ~10K ybp (top figure) associated with open marine waters from the Caribbean Sea. The closure of the embayment probably occurred due to a gradual input of sediments from Rio Yaque del Sur ~4.5K ybp (middle figure) and produced the Enriquillo Lake modern day conditions (bottom figure).

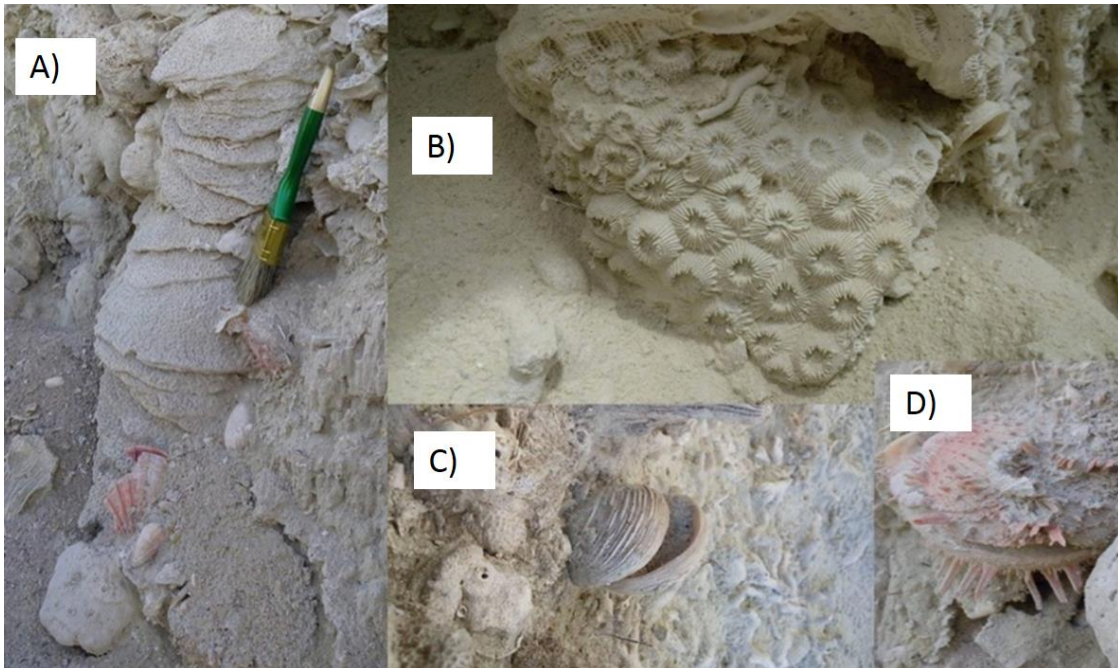


Figure 3. Cañada Honda corals in growth position (top figure). A, B, C and D show images illustrating the pristine preservation of fossil corals in the Cañada Honda reef exposure. This unusual preservation is due to the dry climate of the region and the fact that the corals were buried rapidly due to the high sedimentation environment. (Photos by: Author).

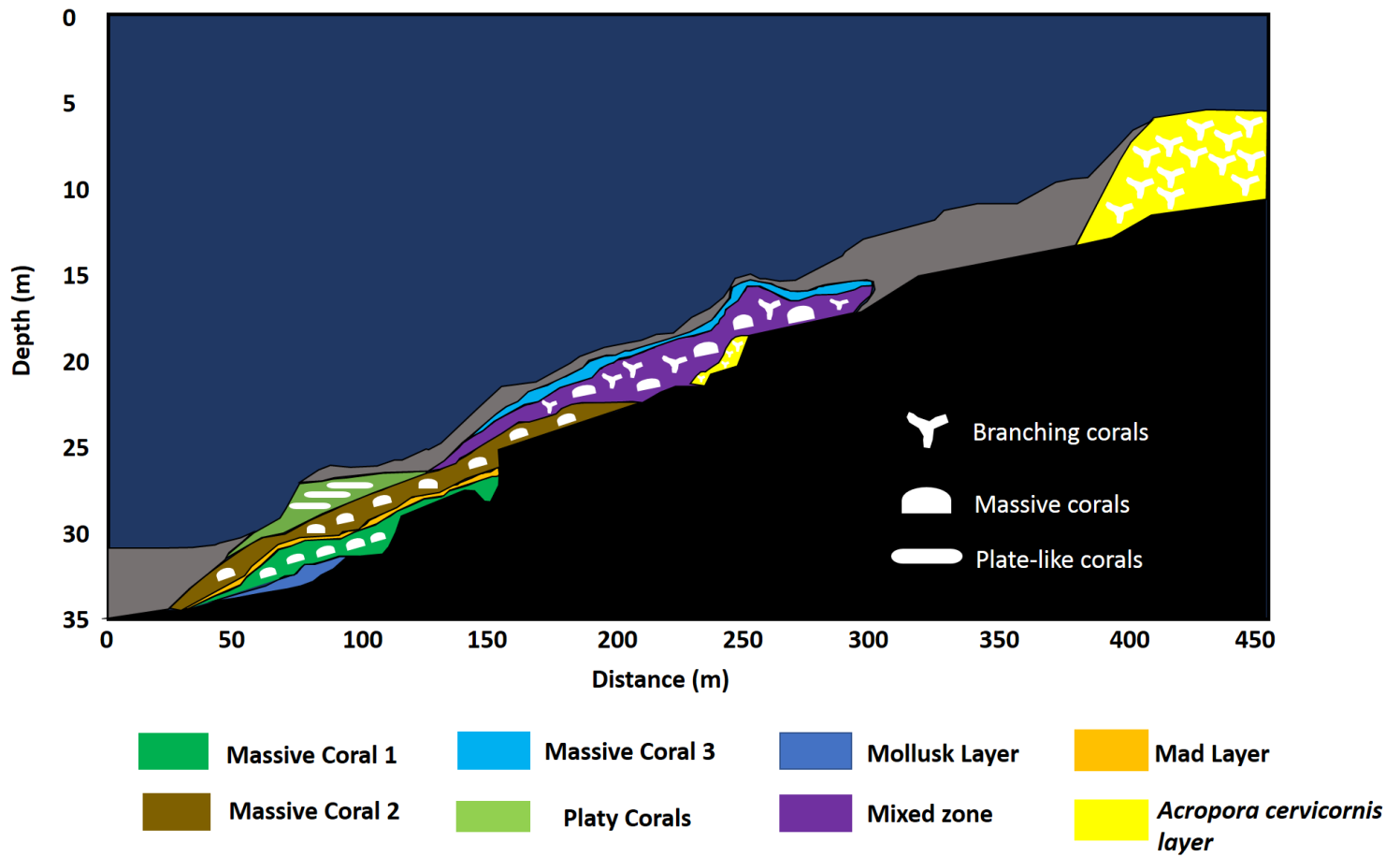


Figure 4. Diagram of the cross-sectional view of Cañada Honda reef exposure showing the facies distribution map proposed for Cañada Honda (Modified after Hubbard et al., 2004).

3.0 Methodology

3.1 Field Work

3.1.1 Sample Collection

The genus *Montastrea annularis* was first established in 1786 and in 1918 as *Madrepora annularis* and *Montastraea 'annularis'* complex, respectively (Ellis & Solander, 1786; Vaughan, 1918; Budd et al., 2012). In 2012 was re-classified into *Orbicella* (Budd et al., 2012). This family complex comprehends corals such as: *Orbicella faveolata*, *Orbicella annularis* and *Orbicella franksi* (Medina et al., 1999; Budd et al., 2012). *Orbicella annularis*, *Orbicella faveolata* and *Orbicella franksi* are the most important and dominant coral reef builders through the Caribbean and Western Atlantic (Medina et al., 1999; Toller et al., 2001). Previous studies suggest that *O. annularis*, *O. faveolata* and *O. franksi* are commonly referred as siblings, due to similarities shared among them, which can often lead to confused them when naked eye observations are applied (Medina et al., 1999; Toller et al., 2001). The difference comes down to molecular analysis and genes characterization and classification (Rowan et al., 1995; Medina et al., 1999; Toller et al., 2001). Within the three proposed siblings, there are different types of symbiodinium (zooxanthella) groups denoted as (A, B, C) (Medina et al., 1999; Toller et al., 2001). Depending on the zonation where the coral is situated and percentages of zooxanthella's A, B, C that colonize the coral colony, will result in the different coral morphology and therefore, into different *Orbicella*'s (Rowan et al., 1995; Medina et al., 1999; Toller et al., 2001). Only one *Orbicella franksi* (deep water coral) resulted to be colonize entirely by symbiodinium group C, while the most common case for *O. franksi* is to have all 3-zooxanthella's group but with high percentage of group C (Medina et al., 1999; Vize, 2006). Since (1) in Cañada Honda paleo-reef was observed all 3 *Orbicella*'s; (2) the similarities and characteristic that they share; and (3) since this study did

not realize molecular or genetical analyzes, the nomenclature used for this study was *Orbicella complex*, which can refer to all there *Orbicella sp.*

This study utilized six fossil *Orbicella complex* coral skeletons from the Cañada Honda exposure: two from the M2 facies, two from the MZ facies, two from M3 facies and one modern *Orbicella complex* coral sampled in Barahona Bay, Dominican Republic (Table 1) (Figure 5). In addition, results from Sr/Ca measured in 4 corals processed by Morales (2014) were also recalculated in this study using our new Sr/Ca-Temperature equation (Table 2). The six fossil *Orbicella complex* corals were collected in 2012 & 2014, and the modern *Orbicella complex* coral was collected in 2015, by Dr. Wilson R. Ramírez-Martínez. Each fossil coral sample name was based on its original geographic and horizontal (stratigraphic) position along the Cañada Honda exposure. The first part of the name refers to the facies from which the coral was collected (M1, M2, MZ, M3). The second part consists of a number that describes the distance, in meters, from a fixed location equivalent to the 2014 lake shoreline. This location, at coordinates 18°31'57" N, 71°37'04" W, was arbitrarily designated as the starting point or 0 meters, because it is close to the end of farthest southward extension of the reef exposure. From this 0 point the erosional gully that exposed the reef extends for 450 meters towards the north before reaching a concrete dam and the road (Joaquín Aybar Avenue, Road 48) (Figure 4). The third part of the sample name consists of a number that corresponds to the elevation, in meters, from the base of the reef exposure at the time of the collection of the sample (2012). This basal elevation coordinate changes through time since the gully geomorphology changes continuously (erosion and/or deposition of sediments) along its profile (Ramírez-Martínez, personal communication). Only fossil corals in growth position were collected. The modern coral of the *Orbicella complex* was collected from Barahona Bay approximately 8 km away from the mouth of the Río Yaque del Sur at a depth of

approximately 10 meters. The mouth of the Río Yaque del Sur was approximately 60 km from the Cañada Honda Reef in the Holocene paleo-Enriquillo Bay (~10k ybp). The fossil Cañada Honda reef was influenced by the sediments from same river and the river was at a similar distance, close enough to have a significant impact on the environment, same as in the modern Barahona Bay Reefs (Figure 6).

Table 1: List of coral samples:

Samples	Location
M2-146.7, 0.7	Cañada Honda
M2-135, 1.0	Cañada Honda
MZ-172.2, 1.0	Cañada Honda
MZ-157.3, 3.0	Cañada Honda
M3-1	Cañada Honda
M3-4	Cañada Honda
B-20 (modern coral)	Barahona Bay

Table 2: Corals used on Morales (2014) study. Added to this study.

Samples	Location
M1-1Ee	Cañada Honda
M1-1Dc	Cañada Honda
M1-2E	Cañada Honda
M1-2Ba	Cañada Honda

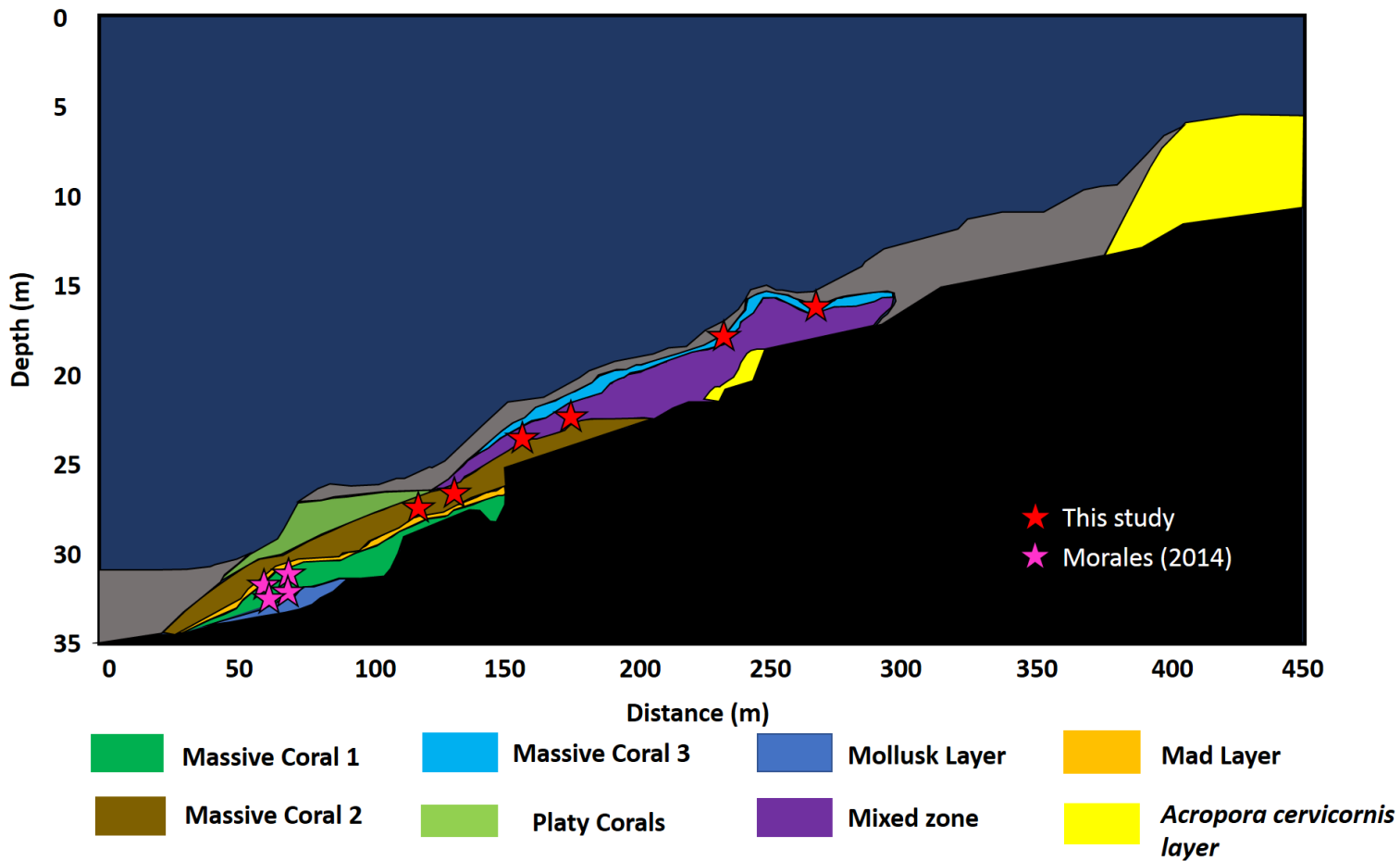


Figure 5. Location from which the fossil coral samples were collected (Red stars), and corals used on Morales (2014) study (Modified after Hubbard et al., 2004).

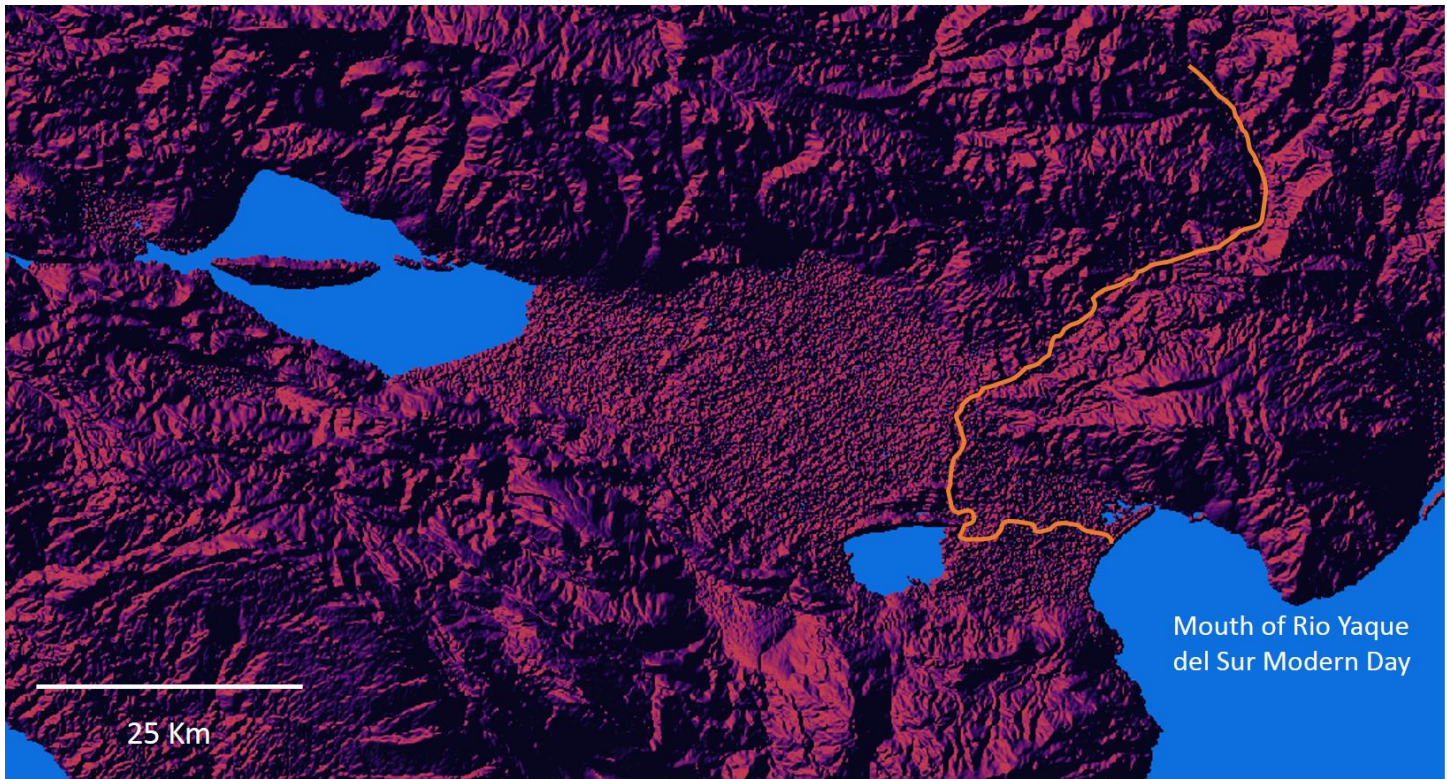
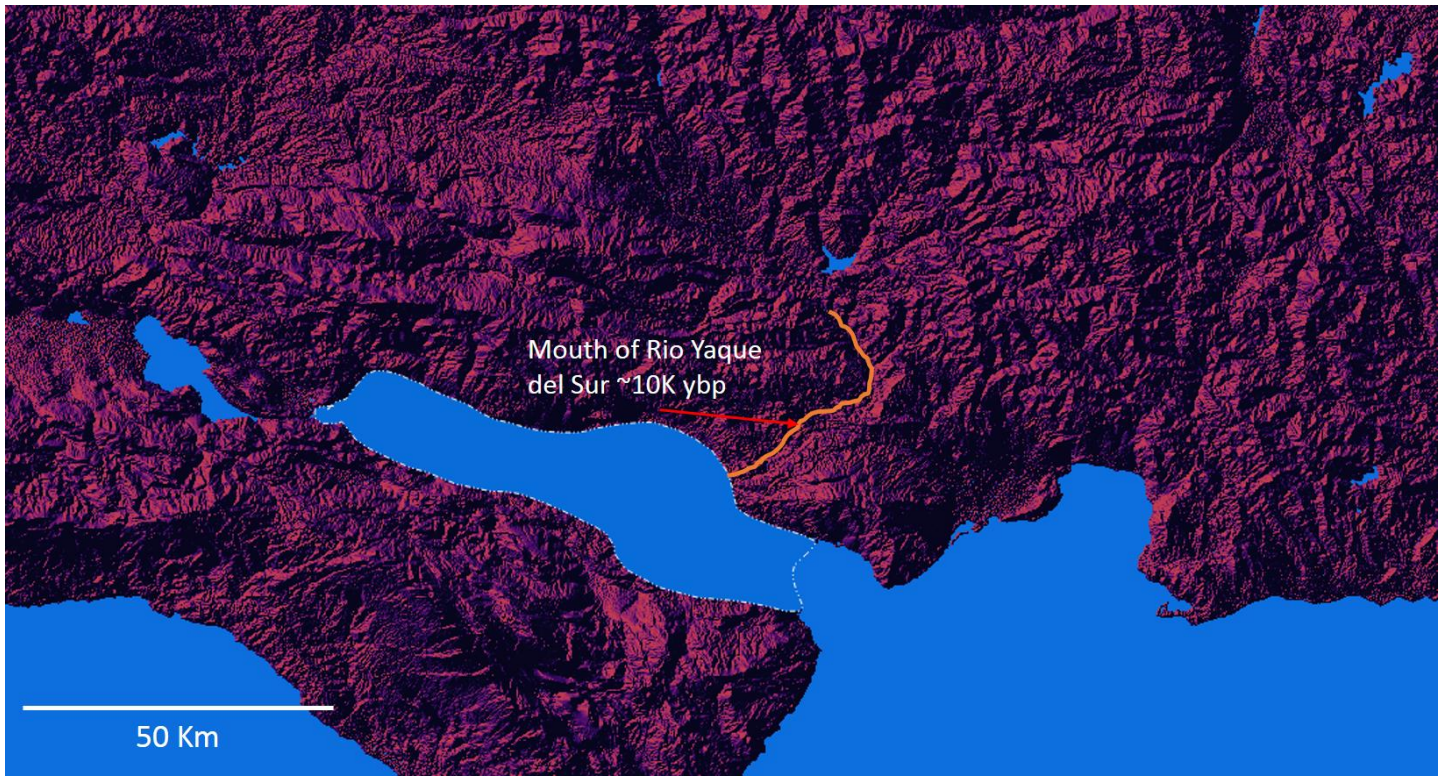


Figure 6. Mouth location of Rio Yaque del Sur ~10 K ybp (Top) and the mouth location in modern day (Bottom).

3.1.2 Sample selection & sample preparation

Fossil corals from different facies and different time intervals were selected in the field. The central longitudinal section or core of the coral skeletons was preserved by cutting the outer edges of the coral parallel to the growth direction using a portable concrete saw. This was necessary to reduce the volume and weight of the coral sample for transportation. At the rock-processing laboratory of the Geology Department in University of Puerto Rico, Mayaguez Campus, the coral skeletons cores were cut parallel to the growth direction in slabs with thicknesses of ~5 mm.

3.2 Lab Work

3.2.1 X-rays and Growth Rates Estimations

X-Ray images were obtained from the ~5 mm coral slabs at the San Antonio Hospital in Mayagüez, P.R. and at the United States Geological Survey laboratory facilities of St. Petersburg, Florida. The radiographs taken from the coral slabs were scanned to produce digital images (Figure 7). The digitized radiographs were analyzed using the software Coral XDS (Helmle et al., 2002) that identifies changes in luminosity. Based on the changes in luminosity, the high and low density (HD, LD) sections in the skeleton are separated and measured. The output is a spreadsheet with the measurements of HD and LD separately and the average (couplets) of HD and LD combined (Figure 8). Growth rate estimations are calculated using Equation 1. The HD and LD bands within the coral skeleton are interpreted as variations related to the amount of calcification in the skeletons produced by differences in environmental parameters (e.g. temperature) and/or biologic influences (e.g. reproduction) (Barnes and Devereux, 1984; Barnes and Lough, 1992; Cruz-Piñón et al., 2003). Abundant studies have shown that in many cases the HD and LD bands are the result of seasonal changes (Winter et al., 2000). Commonly, HD bands produce higher values of SST and are interpreted to be deposited during the summer. LD bands usually produce lower values of SST

and are interpreted to be deposited during the winter (Winter et al., 2000; Hubbard et al., 2008). Since the bands are interpreted to be produced by seasonal variability, the coupling of HD and LD bands is commonly assumed to represent a single year. If these assumptions and conditions are true, it becomes possible to measure the number of years of growth and the annual growth rates from coral skeletons.

$$\text{Equation 1: Growth rates} = \frac{\text{annual linear growth } \left(\frac{\text{mm}}{\text{year}}\right)}{\text{number of year}}$$

Hubbard (1985) suggested that water depth and bottom slope control growth rate within different coral species. Studies have measured *Orbicella complex* growth rates and they vary from 0.6 mm/year at a water depth of 36 meters, to 12 mm/ year at a water depth of 12 meters (Hubbard et al. 1985). These measurements and depths were compared to the growth rates and depths of the corals obtained from Cañada Honda reef corals since estimates of the depth where they grew are possible to be derived from preserved paleo-topography and relative position to modern sea level. High density and low-density bands were also used as chronometric guidelines for the $\delta^{18}\text{O}$ and Sr/Ca analysis and calculated SST values.

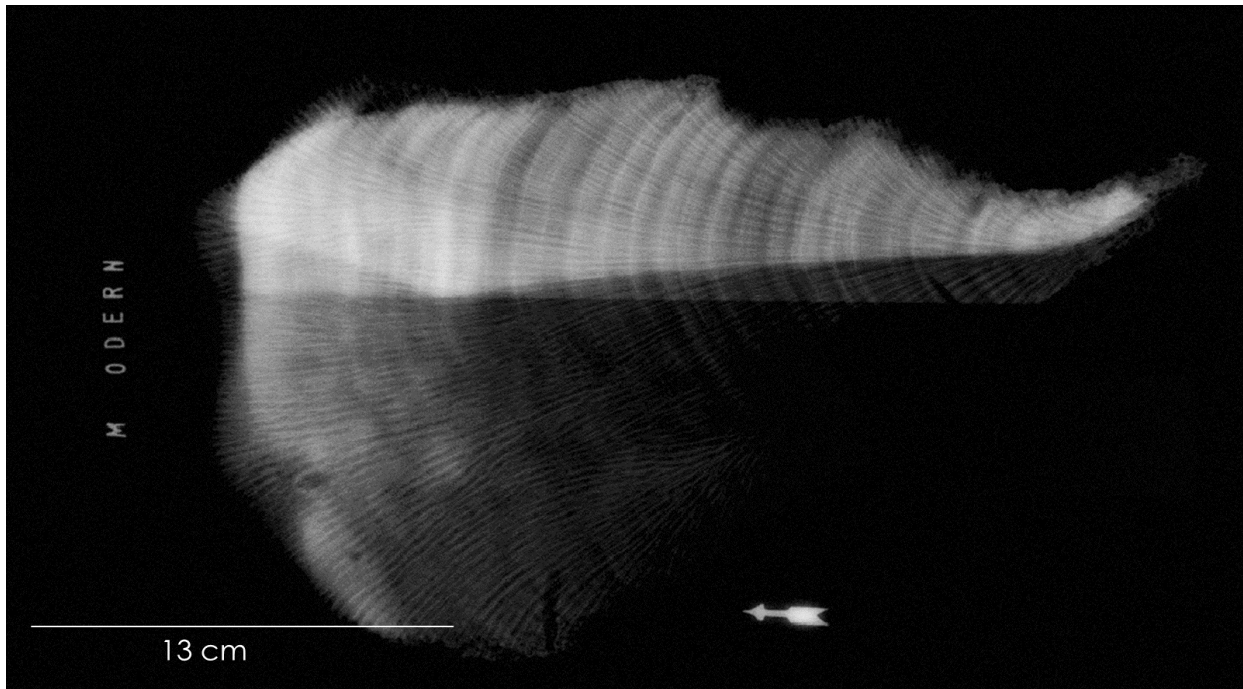


Figure 7. Radiograph of the modern *Orbicella complex* coral skeleton collected in Barahona Bay, Dominican Republic. Image illustrates high and low-density banding.

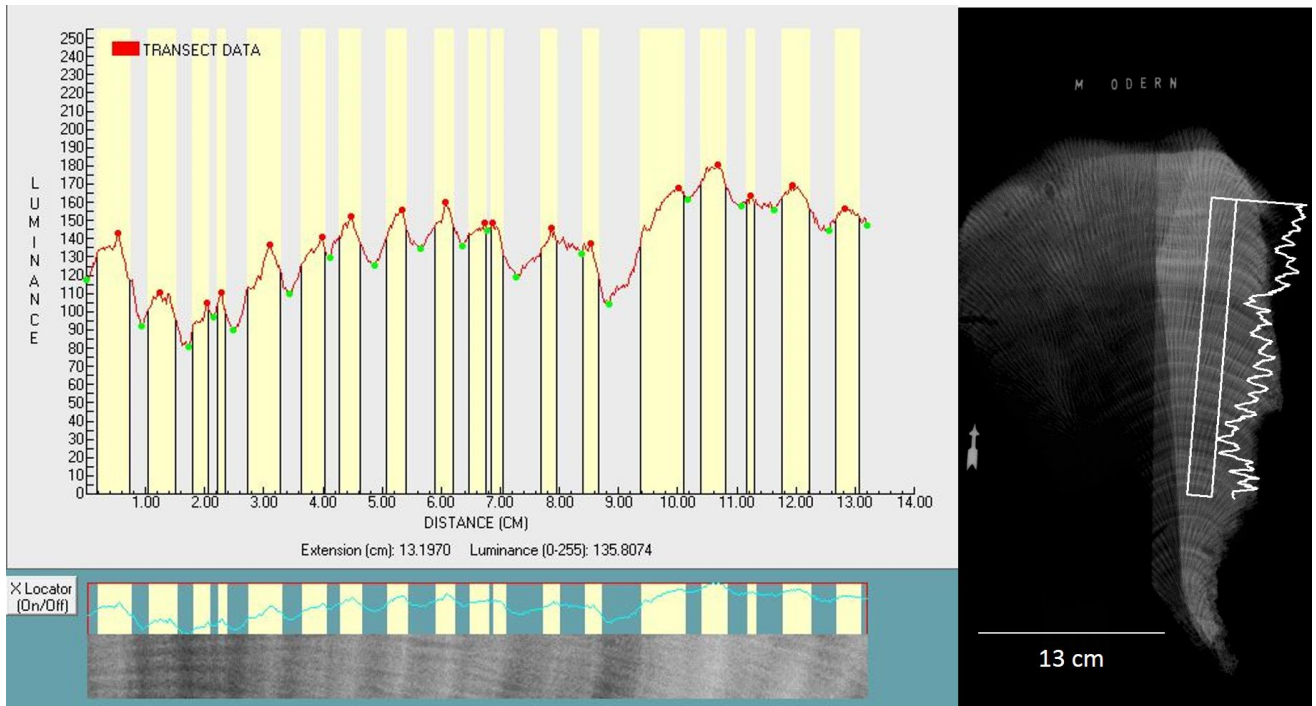


Figure 8. Luminance analysis of modern coral. Radiographs analyzed with “Coral XDS” program (Helmle et al., 2002).

3.2.2 Determine Coral Preservation State

3.2.2.1 XRD

X-Ray Diffraction (XRD) analyses were made to detect alteration in the mineralogy of the coral skeletons. This analysis shows if the composition of the fossil coral skeletons is still aragonite or if it has changed to calcite (Figure 9). This alteration process is very common in Holocene corals (Sayani et al., 2011). For this analysis, samples from the coral skeleton were ground with a mortar and pestle to produce a 0.1 g powder sample. This analysis carried out with a Siemens XRD Diffraktometer D5000 at the Earth X-ray Analysis Center of the Geology Department at the University of Puerto Rico Mayagüez Campus.

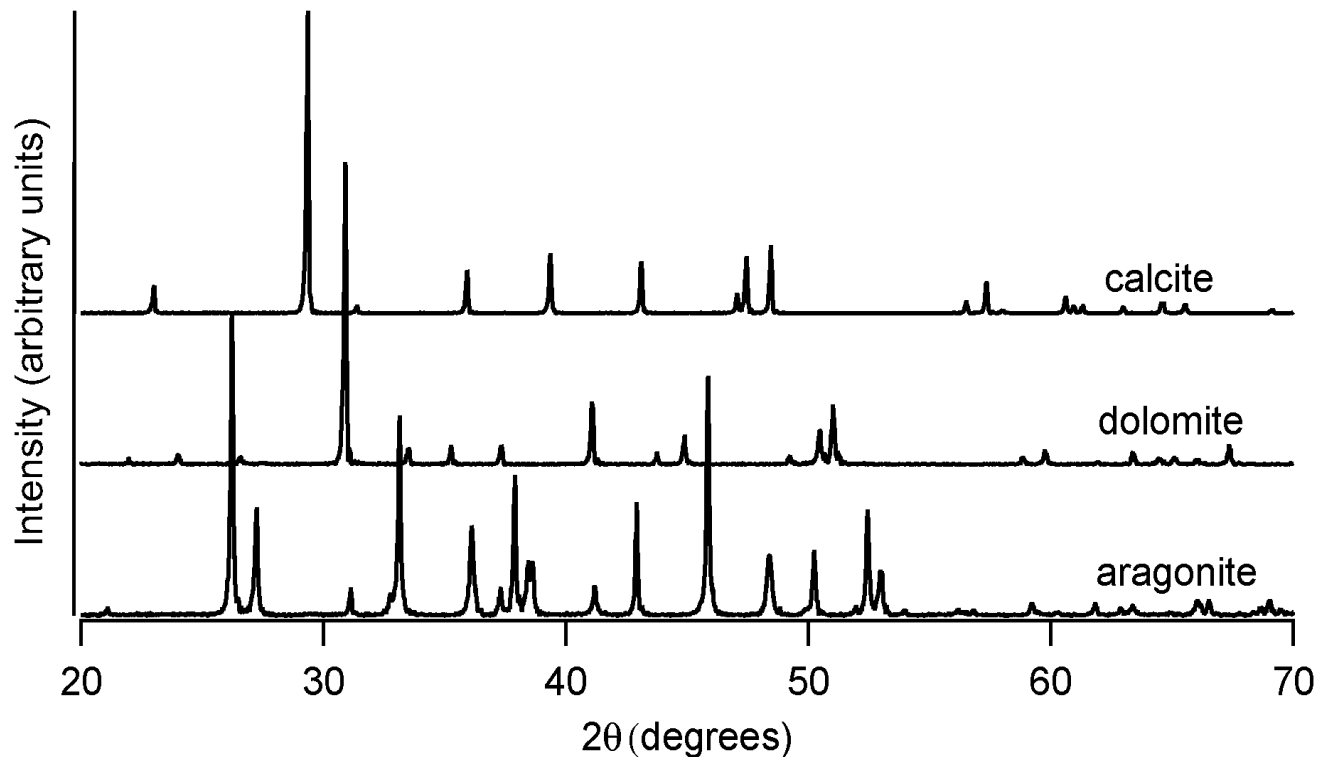


Figure 9. Diffractogram showing the 2θ location of the intensity peaks for the minerals calcite, dolomite and aragonite (from Xu et al., 2014).

3.2.3 Paleoenvironmental Analysis

3.2.3.1 Fossil Coral Dating

The coral skeletons were dated using Uranium-Thorium (U/Th) analysis. A fragment was collected from the basal section of each coral slab and then ground with a mortar and pestle to yield a 0.2 g sample powder. Corals and/or sections of the corals containing sedimentary particles and/or signs of bio-erosion from organisms like *Lithophaga sp.* were avoided. A Multi-Collector Inductively Coupled Plasma Mass Spectrometer (MC-ICP-MS) was used for the Uranium-Thorium (U/Th) radiogenic dating the Rosenstiel School of Marine and Atmospheric Science (RSMAS) in Miami, FL.

3.2.3.2 Sr/Ca analysis

The coral skeleton slabs were micro-sampled at the United States Geological Survey (USGS) laboratory at St. Petersburg, Florida, using a computer driven triaxial micro-milling machine. The coral skeleton was drilled with a 0.5mm diamond drill bit in a traverse line along the thecal wall of the same coralite at continuous 0.5 mm sampling intervals and parallel to the axis of primary growth. Sr/Ca and trace elemental ratios were measured with an Inductively Couple Plasma Optimal Emission Spectrometer (ICP-OES). The ICP-OES available at the USGS St. Petersburg requires at least 80 micrograms of aragonite powder from the coral skeleton. The Sr/Ca information obtained from the analysis was used to calculate Sea Surface Temperature (SST) in the fossil corals. Because Sr/Ca-T relationship is inversely proportional, a higher Sr/Ca value indicates a relatively lower water temperature (interpreted as winter) and a lower Sr/Ca signal indicates a relatively higher water temperature (interpreted as summer) (Smith et al. 1979).

4.0 Results

4.1 Growth rates for *Orbicella* complex.

Growth rate averages from fossil coral skeletons measured in this study are summarized in table 3. The coral estimated to have been deposited at the greatest depth, ~12 to 20 meters below paleo-sea level at about 9.0k (± 200) ybp.

Table 3: Growth Rate measurements of coral samples measured in this study.

Coral Sample	Years measured (n)	Extension (mm)	Growth rate (mm/year)	Depth Estimate (m)
M2-135	28	52.66	1.95	12-15
M2-146	19	37.72	1.98	9
MZ-172	25	33.17	1.32	8-10
M3-1	24	46.52	1.93	3-4
M3-4	21	38.42	1.82	3-4
Modern Coral	17	124.87	7.34	10

4.2 Coral skeleton preservation state

XRD analyses indicate that all five fossil coral samples, are aragonitic in composition; an example is shown in Figure 10. The other diffractograms are in Appendix 6 to 11. The XRD for calcite and aragonite detection limits are 0.90% and 2.90%, respectively (Kontoyannis, 2015). Although a minimal amount of calcite could be present in the coral samples less than (0.9%), the analysis is effective to establish these millennial corals have not suffered neomorphism. Sample M3-1 shows a discontinuity along the coral growth bands (Figure 11). This feature is probably the result of disruption that affected the normal growth of the coral. Coral M3-1 was sampled in three locations, one below the discontinuity band, one in the middle of the discontinuity band and one

on top of the discontinuity band, to assess if minerals other than aragonite could be detected along it. All three samples showed aragonitic composition indicating that no other minerals were present above the XRD detection limit (2.0%). Downs (2006) and Xu (2014) aragonite standard calibration diffractograms were used to characterize the position of the aragonite peaks (see Appendix 6 to 11).

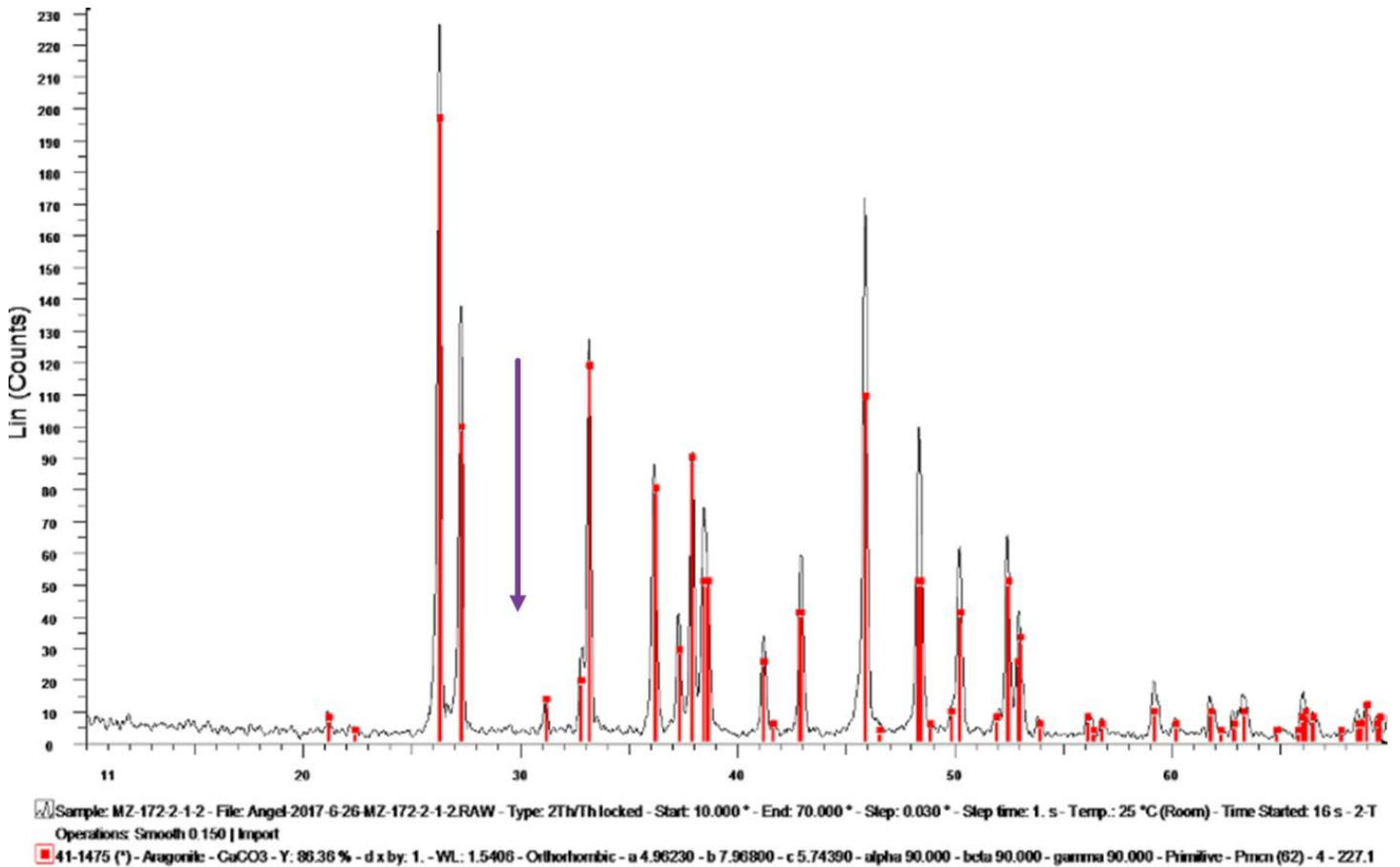


Figure 10. XRD results for the MZ fossil coral sample indicating a 100% aragonitic composition. Purple arrow indicates the location of the signal peak of calcite and the absence of detection of calcite (No Lin counts). The detection limit for calcite is 0.90% (Kontoyannis et al., 2015). The other diffractograms are in Appendix 6 to 11.

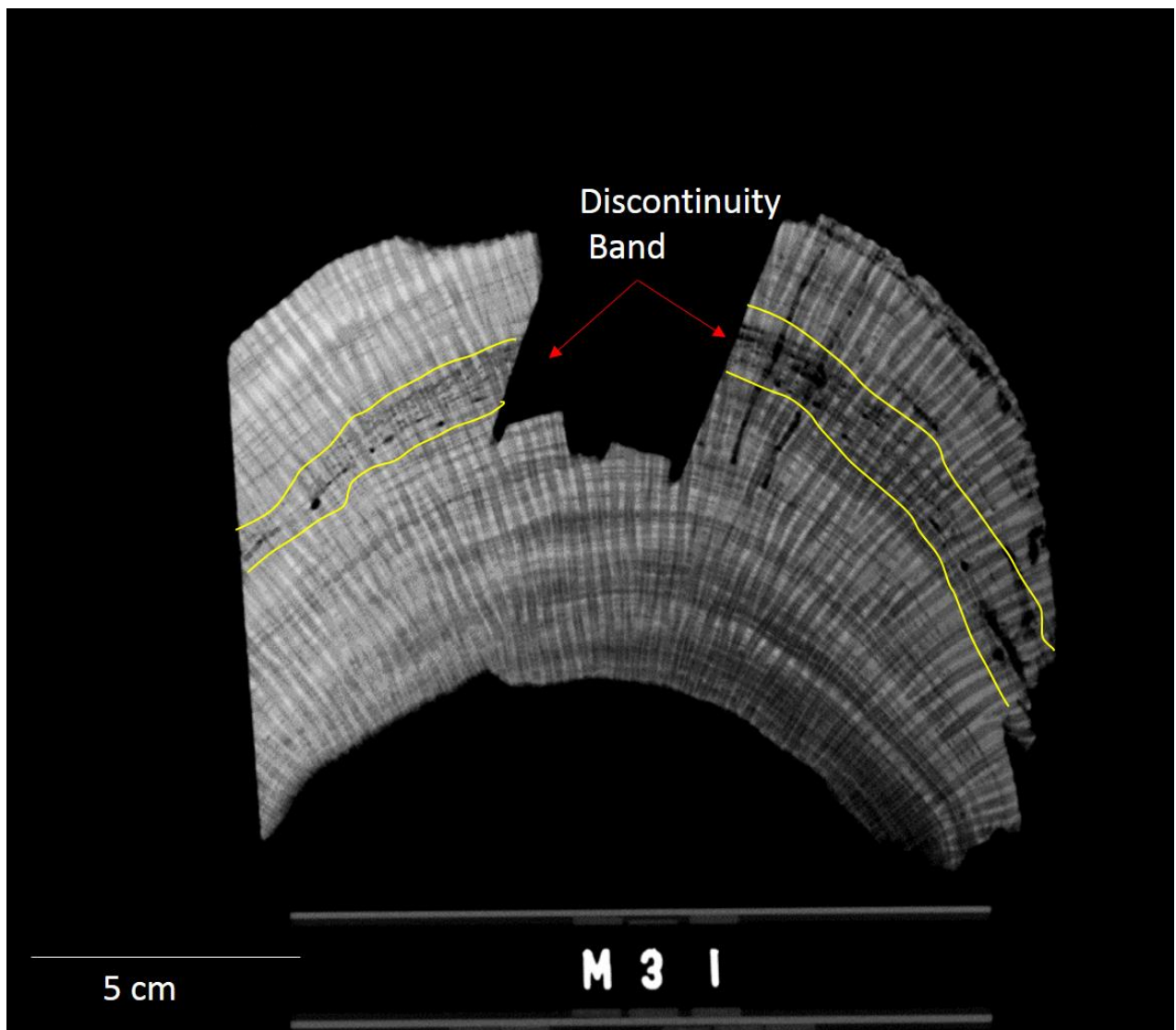


Figure 11. Discontinuity Band Observed in fossil coral M3-1. Samples were taken below, on the band and on top of the band. No other mineralogy in this coral aside aragonite was detected (3 samples).

4.3 Fossil coral radiogenic dates

U/Th dates were obtained from samples M2-146.7, MZ-157.3, MZ-172, M3-4 and M3-1.

These indicate the Cañada Honda reef started its accretion during the mid-early Holocene and continued its development until the mid-late Holocene epoch (see Table 4). Morales (2014) dated corals from the base of the reef in facies M1 and these showed ages from $8,910 \pm 28$ ybp $8,036 \pm 26$. Based on the dates obtained by this study as well as the dates obtained by Morales (2014), the

Cañada Honda reef was accreting from approximately 8.9 Kybp to 5.6 Kybp or for a time interval of about 3.3 K years. No radiometric date was acquired for M2-135 coral sample.

Table 4: U/Th fossil coral ages. Results are within a 95% confidence interval (C.I.)

Sample Name	M2-146.7	MZ-157.3	MZ-172.2	M-3-4	M3-1
Age CORRECTED	8166	6694	6521	5702	5690
\pm (95% C.I. = (Q97.5- Q2.5)/2 from MC var.)	35	48	32	30	29
Activity ratio $^{234}\text{U}/^{238}\text{U}$ initial	1.132	1.154	1.152	1.152	1.148
\pm (95% CI = (Q97.5- Q2.5)/2 from MC var.)	0.003	0.003	0.004	0.003	0.003

4.4 Sr/Ca analysis modern & fossil coral samples

Sr/Ca ratios from the modern *Orbicella complex* coral (sample B-20 from Barahona Bay) and fossil coral skeletons (samples M2-135, M2-146, MZ-172, M3-1, M3-4, from Cañada Honda) can be observed in figures 12 through 19. On the modern, coral several analytic replicates or paths were made to produce a dense and continuous Sr/Ca record (Figure 12 and 13). The Sr/Ca values were plotted relative to the location they were sampled in 0.5 mm increments from the top of the coral (Flannery et al., 2013).

In coral sample MZ-172, it was not possible to follow the same coralite line during the sampling, therefore, the analysis consists of short segments instead of a long interval of Sr/Ca values (Figure 14). Furthermore, the annual cyclicity of this sample was difficult to evaluate because the drilling was done on several thecal walls. Duplicate analytic replicates or paths were made (“Paths Re-drilled”, Figure 15). Re-drilled paths were the ones selected for SST calculations. Sample M2-135, illustrated in figure 16, provided a long continuous coralite and no re-drilled paths were necessary during the analysis of this coral. For sample M3-1 only a short segment was drilled

because this sample also did not provide a long coralite line through the coral slab (Figure 17). Sr/Ca values for sample M3-4 are shown on figure 18. This coral slab provided a few, long and separated coralites so no re-drilled paths were necessary during the sampling. Sr/Ca values for the oldest coral skeleton sample, M2-146, are shown on figure 19. In this coral slab, extensive *Lithophaga sp.* bioturbation (boring) was observed and therefore only a short segment was drilled. Due to this problem, the powdered samples collected from coral MZ-157 were not processed for trace element analysis.

The Sr/Ca obtained from fossil corals samples produced higher values relative to the modern coral, hence, a lower SST value was obtained for the Cañada Honda fossil corals relative to the Barahona Bay modern coral.

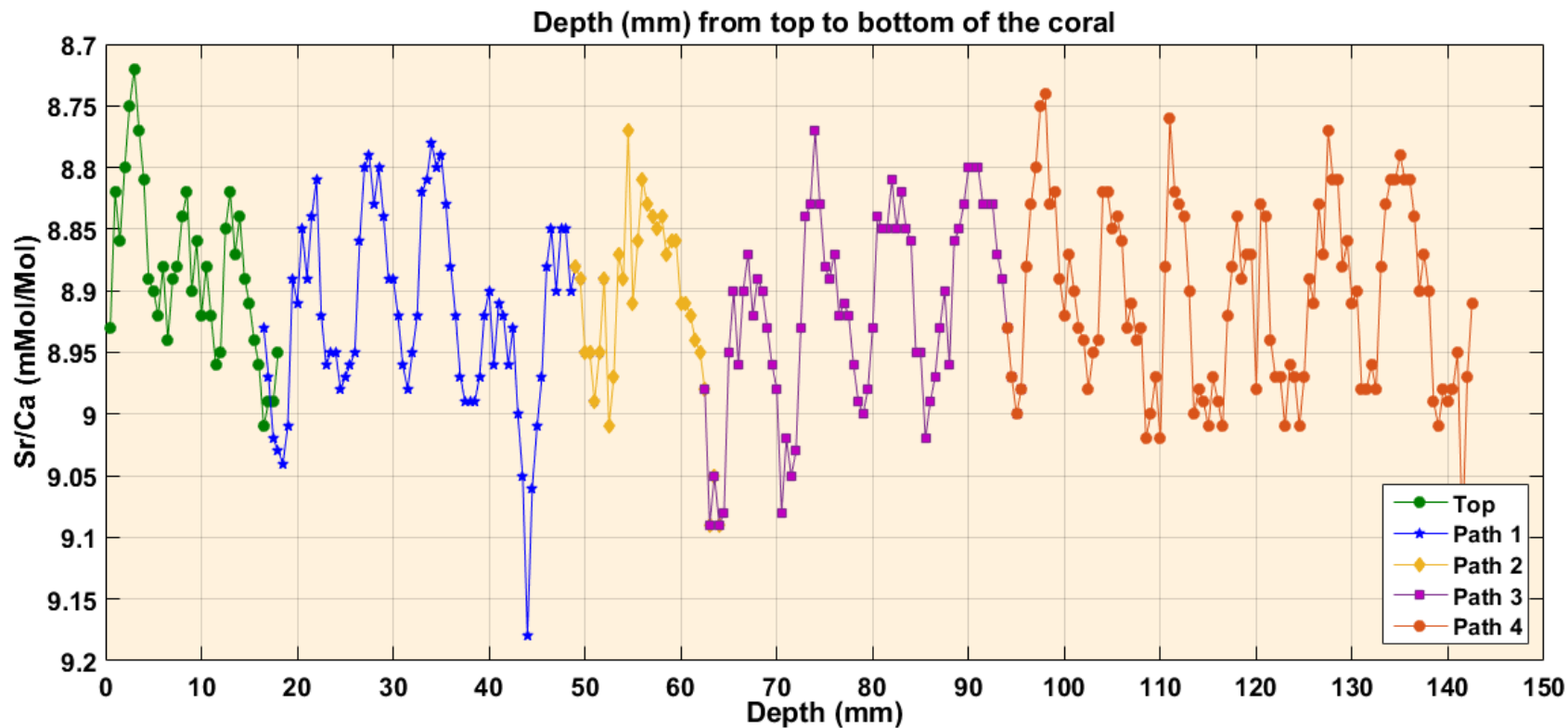


Figure 12. Sr/Ca ratios from the modern coral sample (B-20) collected in Barahona, Dominican Republic. This is a composite of several analytical paths sampled along the coral. Depth in mm, zero, represent the surface of the coral.

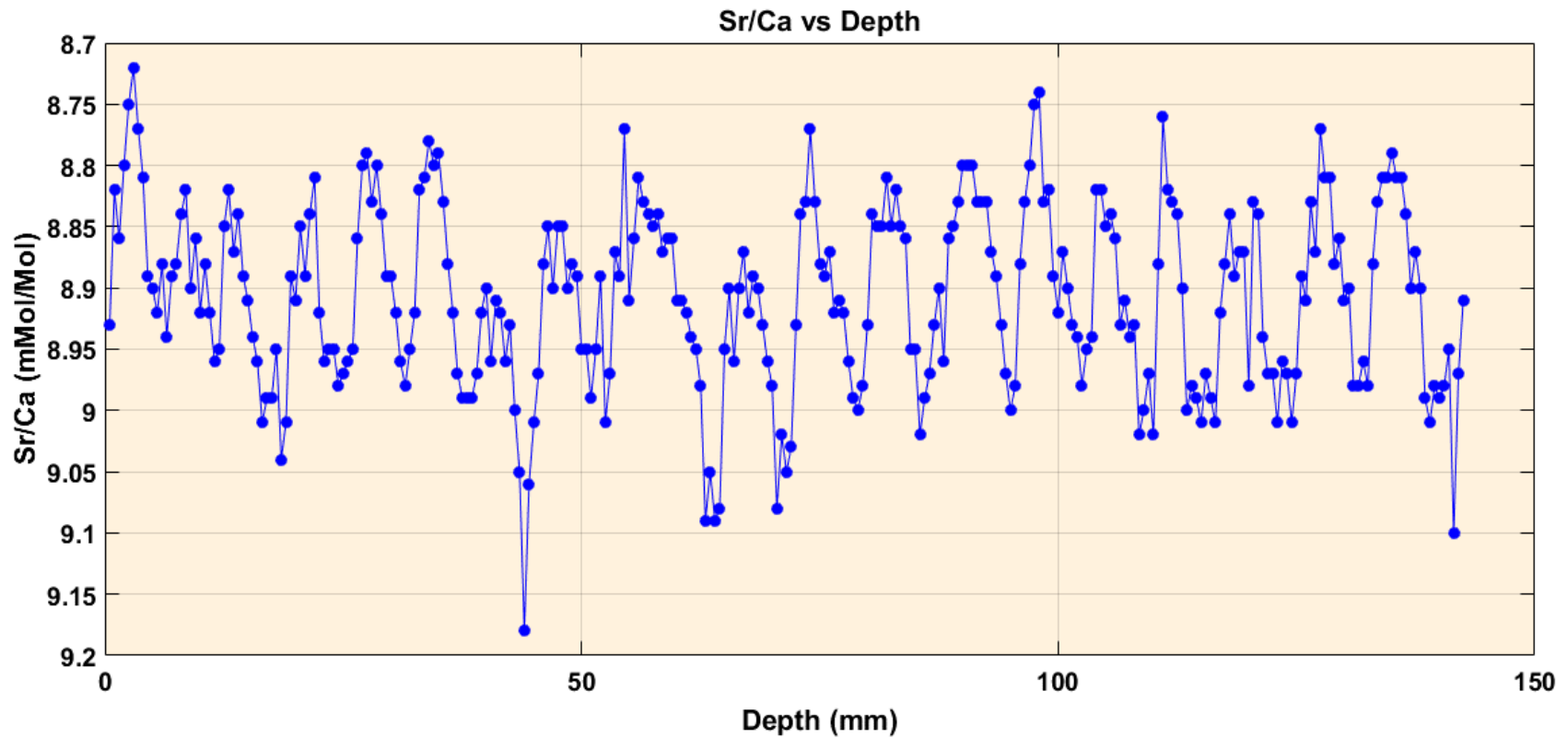


Figure 13. Composite of different analytical transects or paths made from the modern coral sample (B-20) collected in Barahona, Dominican Republic. Depth in mm, zero, represent the surface of the coral.

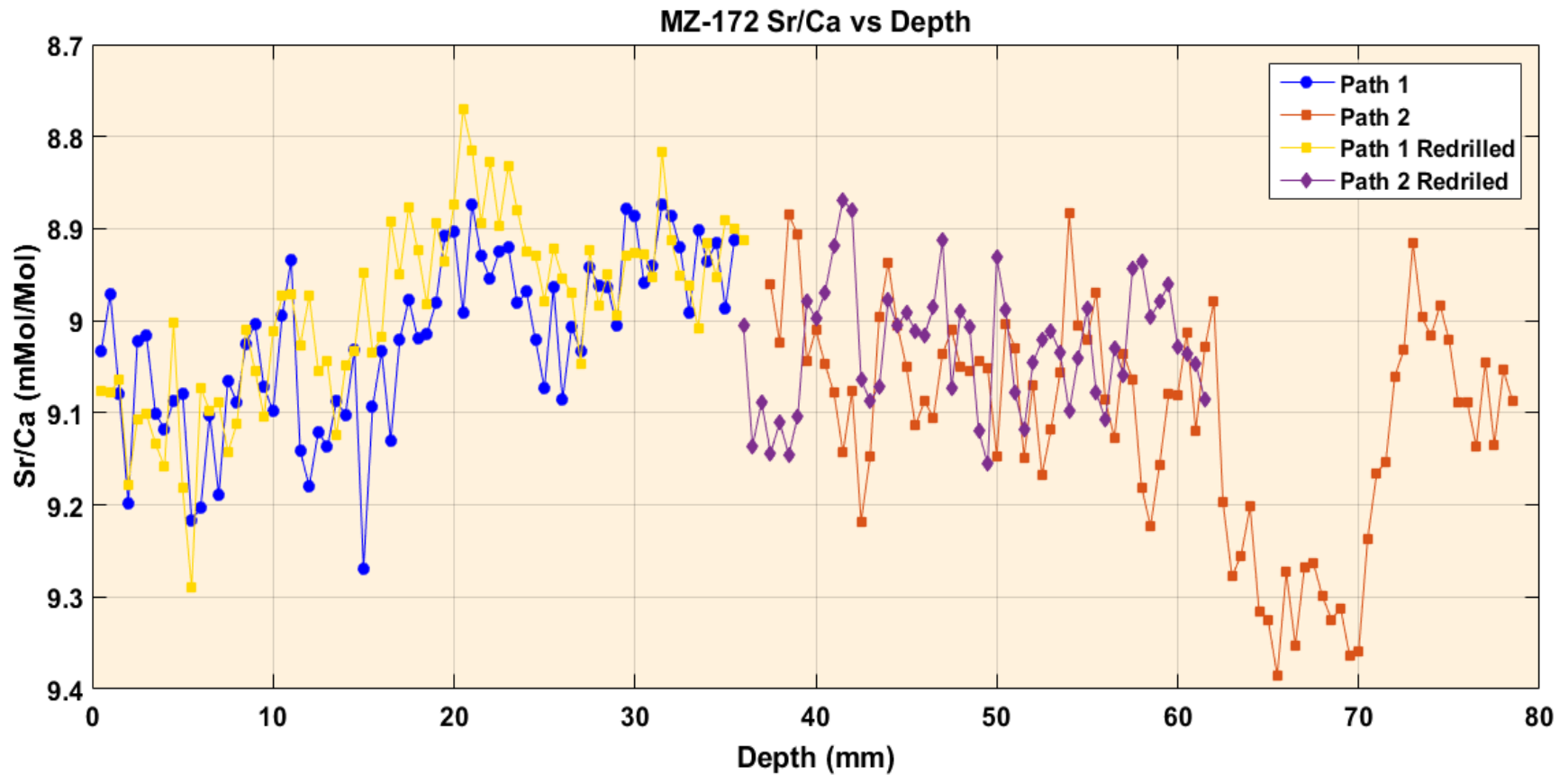


Figure 14. Analytical replicates or paths made on fossil coral sample MZ-172. Re-drilling paths were made to confirm that the drilling was made along the same thecal wall. If the Sr/Ca values are reliable the analytical replicates of every path should be reproduced within analytical error. Depth in mm, zero, represent the surface of the coral.

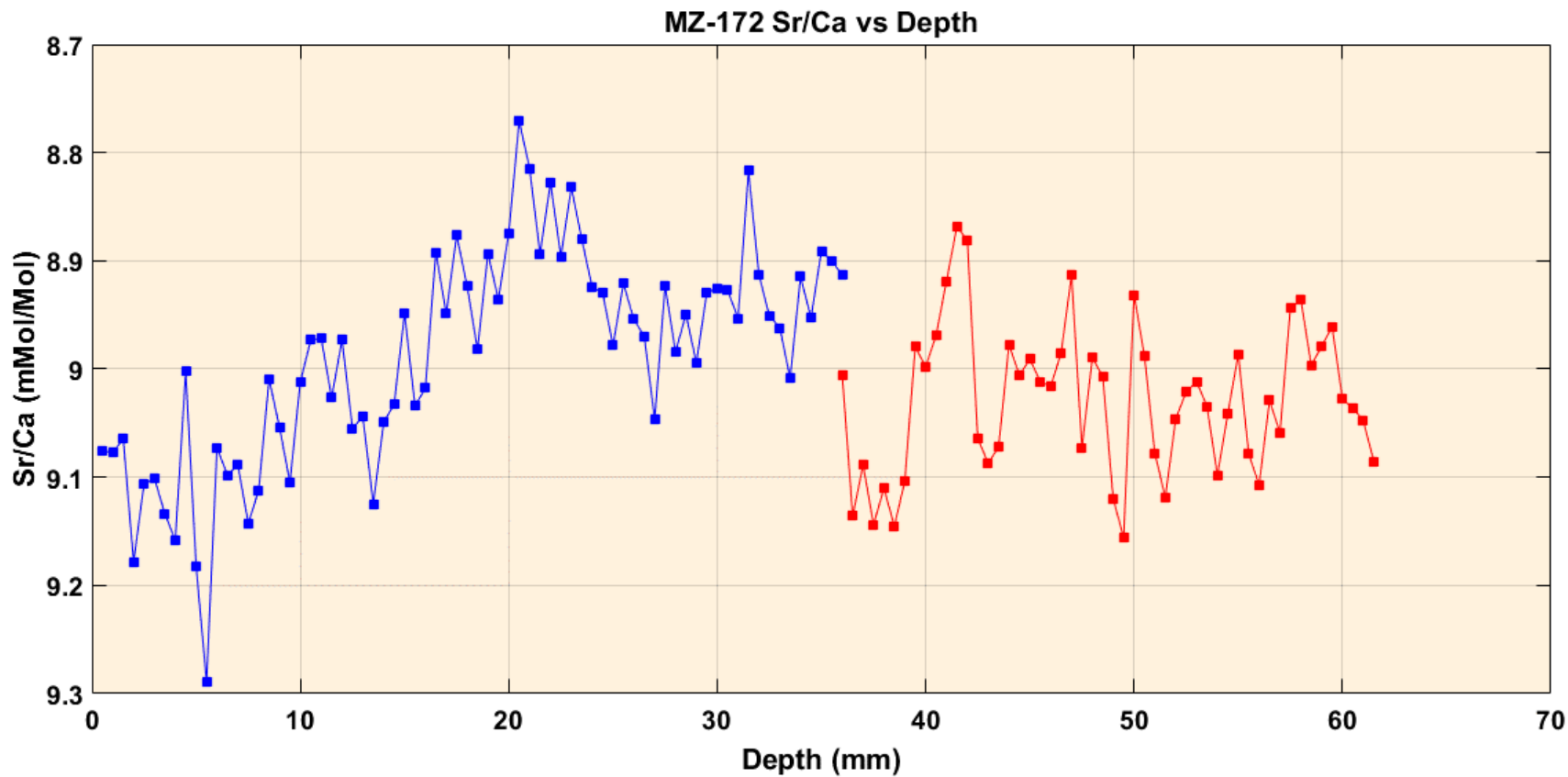


Figure 15. Sr/Ca values combined from several analytical paths and replicates for coral sample MZ-172. Depth in mm, zero, represent the surface of the coral.

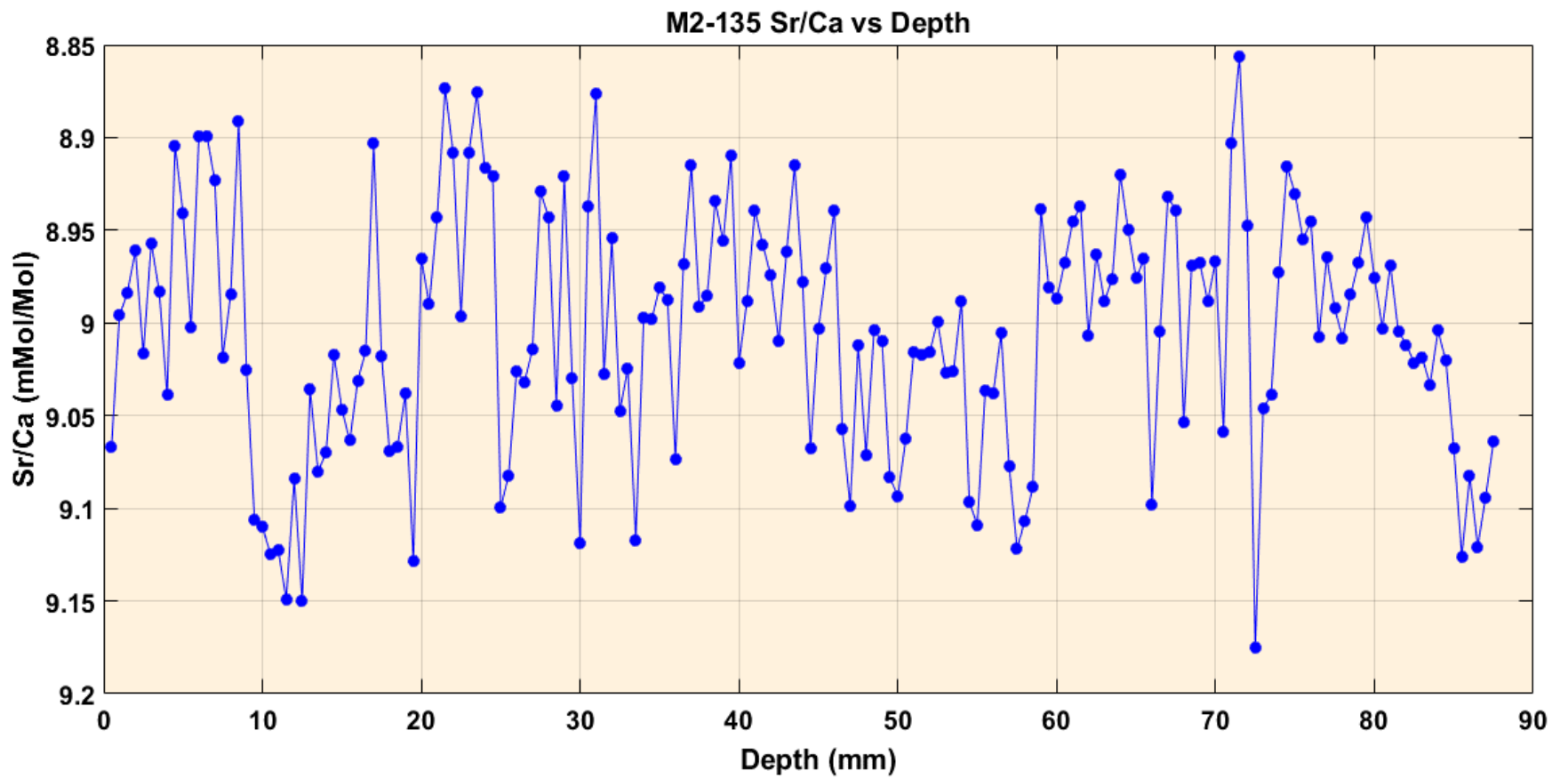


Figure 16. Sr/Ca values from fossil coral sample M2-135. Depth in mm, zero, represent the surface of the coral.

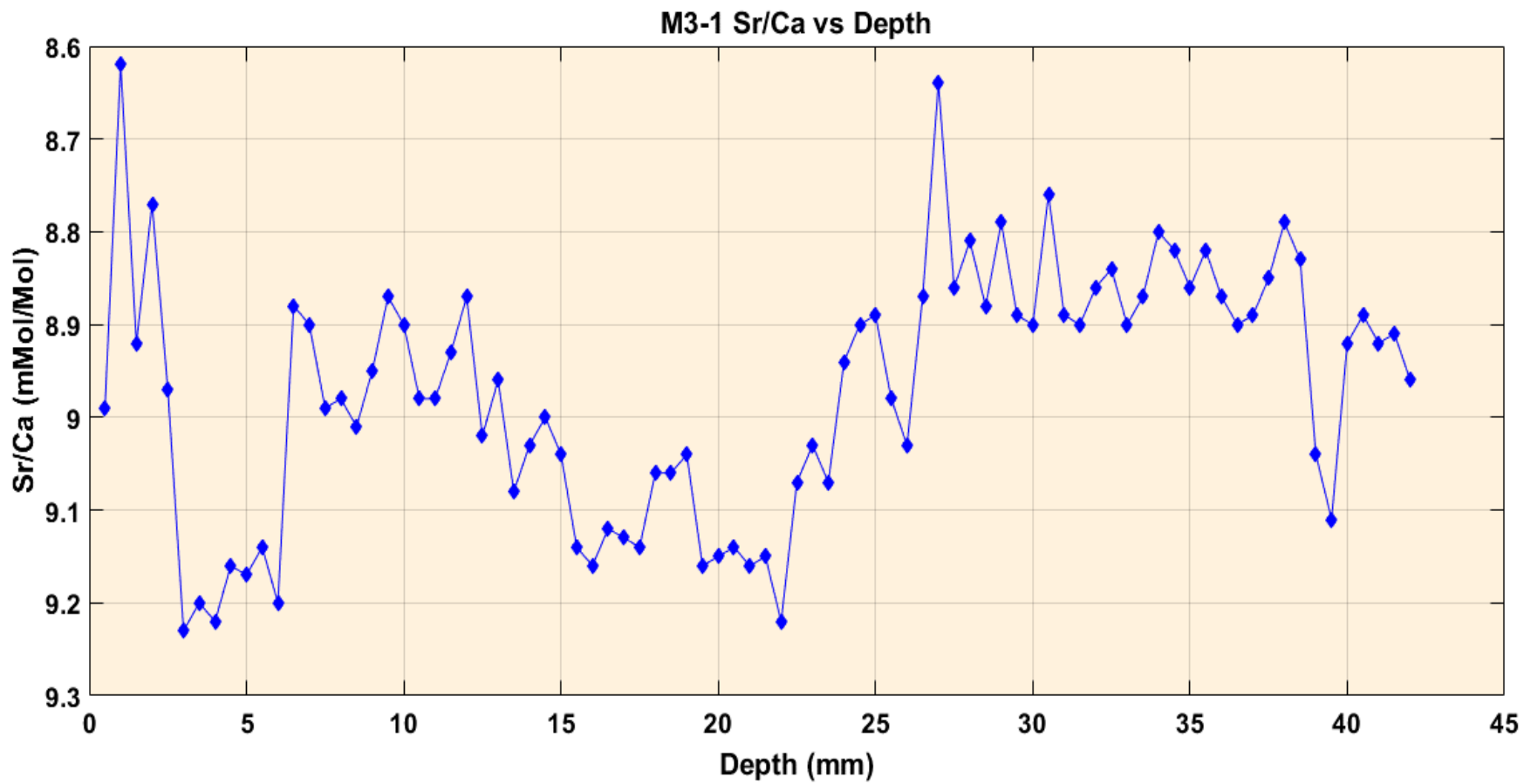


Figure 17. Sr/Ca values obtained from M3-1 coral sample. Depth in mm, zero, represent the surface of the coral.

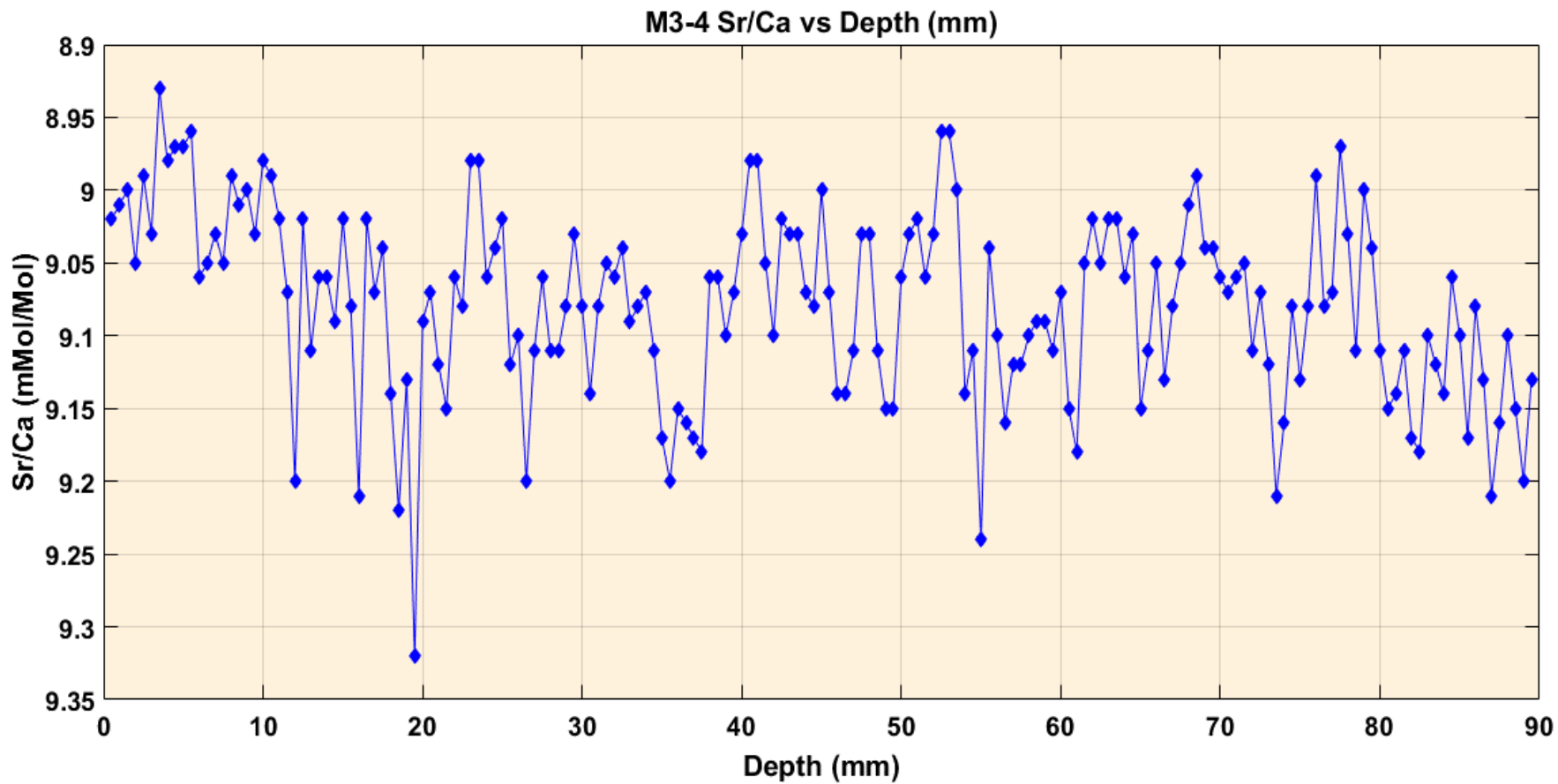


Figure 18. Sr/Ca ratios obtained from M3-4. Depth in mm, zero, represent the surface of the coral.

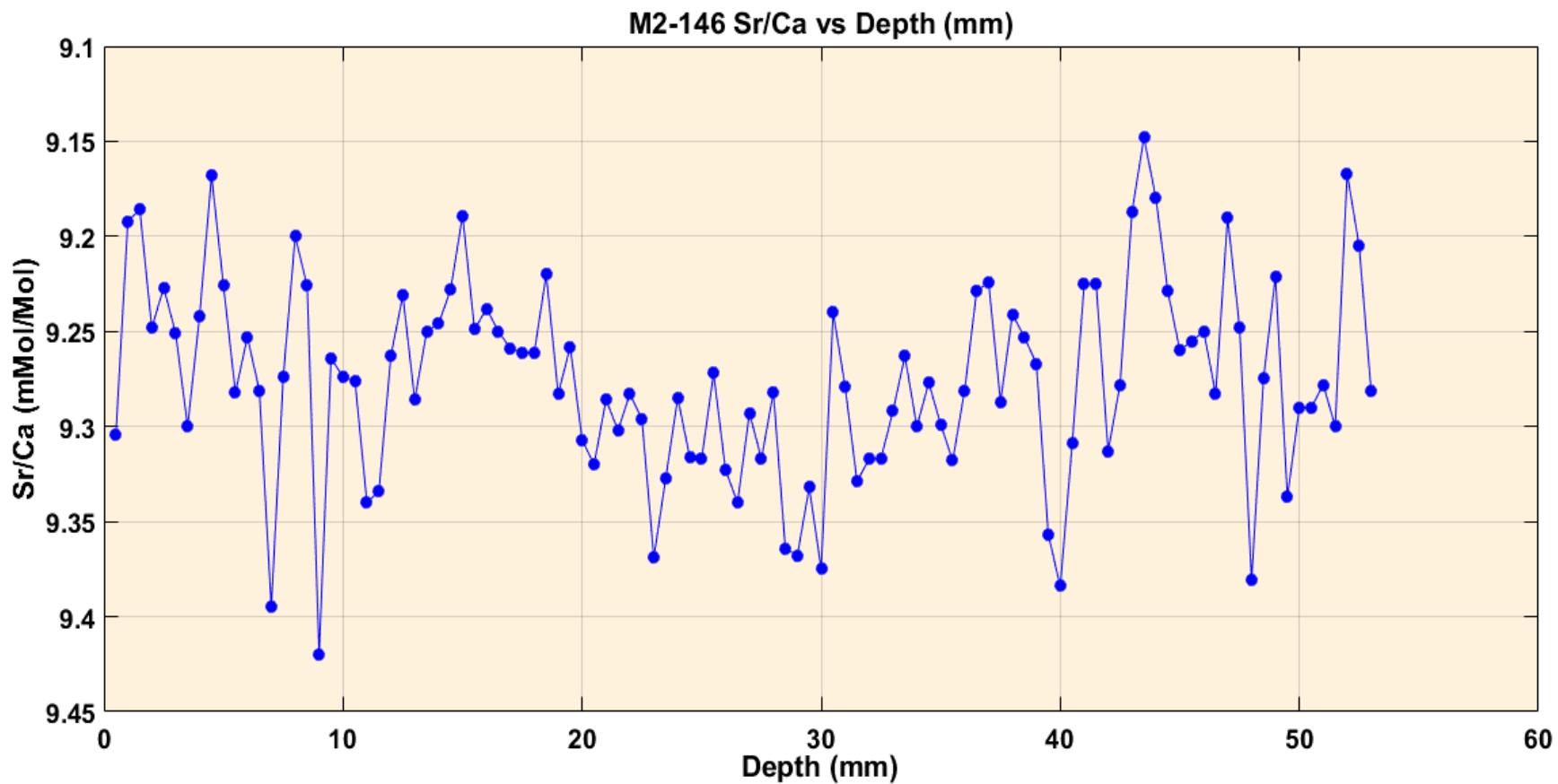


Figure 19. Sr/Ca ratios Obtained from M2-146 fossil coral sample plotted vs. Depth (from top of the coral slab). Depth in mm, zero, represent the surface of the coral.

4.5 SST Calculations from modern coral & fossil corals

Sr/Ca-T calibration equations have been produced by many studies from different locations and using different species of corals. One of the major problems reported in Sr/Ca-T calculations is that the temperatures obtained are strongly dependent on the location or site specific factors (Saenger et al. 2008). Based on these assessments Morales (2014) used Felis et al. (2004) (Eq.2) and Giry et al. (2011) (Eq. 3) Sr/Ca-T equations from the Red Sea and Bonaire using *Porites sp.* and *Diploria strigosa* respectively, alleging the corals used lived in similar environments to the ones he studied in Cañada Honda. Morales (2014) made this assumption because it is not possible to create Sr/Ca-T calibrations for living corals from the Holocene paleo-Enriquillo Bay since the area is not an open marine embayment anymore and no living corals are available from the Cañada Honda site. Flannery (2013) produced a calibration equation using *Orbicella faveolata* coral skeletons from the Dry Tortuga National Park (Eq. 4) and Swart et al., (2002) (Eq. 5) produced an equation using *Orbicella annularis* from Biscayne National Park, Fl. Neither location resemble the environmental conditions of the paleo-Enriquillo Bay. Nevertheless, Felis (2004) and Giry (2011) equations were used in Morales (2014) to calculate SST; Swart (2002) and Flannery (2013) were examined in this study.

Equation 2: $\text{Sr/Ca} = -0.0597 * \text{SST} + 10.781$

Equation 3: $\text{Sr/Ca} = -0.05 * \text{SST} + 10.6$

Equation 4: $\text{Sr/Ca} = -0.0392 * \text{SST} + 10.205$

Equation 5: $\text{Sr/Ca} = -0.0377 * \text{SST} + 9.94$

One of the goals of this study was to solve this problem as best as possible by creating a more appropriate Sr/Ca-T calibration equation to calculate SST for the paleo-Enriquillo Bay based on Cañada Honda corals. To attain this objective a modern coral was collected by Wilson R.

Ramirez-Martínez off the coast of Barahona, Dominican Republic at coordinates 18°14'4.88" N; -71°5'8.68"W. This location is the closest feasible site to the Cañada Honda exposure location and is in an embayment that has similar riverine influences (and from the same river) as the Cañada Honda reef had during its accretion. Modern SST data for the area were acquired from different database sources such as: Hadley Centre Sea Ice and Sea Surface Temperature (HADISST), National Buoy Data, Extended Reconstructed Sea Surface Temperature (ERSST) and Optimum Interpolation Sea Surface Temperature (OISST) (NOAA, 2011a; Boyin et al., 2015). A comparison between these four sources suggested that HADISST (Figure 20) is the more accurate data source to make the calibration equation since National Buoy Data does not provide a continuous times series, ERSST seems to underestimate winter intervals, and OISST seems to overestimate summer intervals. Once the Sr/Ca ratios from the modern coral and the SST HADISST data set were obtained, an age correlation model was applied using a program called “AnalySeries”. This software produces a lineage rescaling of the Sr/Ca using the HADISST data as reference (Figure 21). Once the data lineage was performed, a scatter plot was made (Figure 22). Flannery (2013) used maximum and minimum values from Sr/Ca-SST in a linear regression (95% confidence interval) to create a calibration equation of Sr/Ca dependent from Temperature using *Montastrea faveolata*. For the present study the calibration equation was made by a reduced major axis linear regression using a data set of 285 analyses. The resulting equation is $Sr/Ca = -0.0676 * SST + 10.7867$. The equation was then applied to the modern coral (B 20) to calculate monthly SST values from 2015 back to 1997 (Figure 23). In addition, Swart (2002) and Flannery (2013) equations were applied to the modern coral (B-20) Sr/Ca values to compare their SST calibration results to the ones obtained in this study. Flannery’s equation (Eq. 3) resulted with an (R= -0.97), Swart’s equation (Eq. 5) resulted with an (R= -0.94), while this study’s equation

resulted with a ($R = -0.83$). It should be noted that calculations of SST using the Flannery's (2013) equation produce much higher temperatures (about 4 to 6 degrees warmer) than the other equations. When using Swart's (2002) equation, similar average SST's are produced but with higher amplitudes (warmer summers and colder winters) suggesting that the new calibration presented here produce more accurate SST values (Figure 24).

The calibration equation to produce SST from Sr/Ca created in this study was applied then to the Cañada Honda corals sampled (Table 1; Figure 25-29) and the Cañada Honda corals processed by Morales (2014) (Table 2 Figure 30 through 33). Growth rates for fossil corals measured in this study average ~ 2 mm/year ($n=5$). The sampling procedure consisted on drilling the coral at increments of 0.5 mm producing about 4 samples per year (Cobb et al., 2003). The SST results from fossil corals were plotted in the Y axis vs. the internal coral chronology (nominal years) in the X axis.

A composite of all the Sea Surface Temperature calculations vs. the Th/U age of the corals is presented in figure 34. These data provide snapshots of SST through the Holocene epoch. Sr/Ca-SST calculations show that between $8.365 (\pm .024)$ and $8.166 (\pm .035)$ K ybp, the SST was at 20-25 °C, relatively colder than modern day conditions. The Temperature range in which *Orbicella complex* can live in modern day conditions is between 18-30 °C, and the temperature range for optimum living conditions is between 25-29 °C (Budd et al., 1994; Medina et al., 1999; Cruz-Piñón et al., 2003; Voolstra et al., 2009).

In modern day conditions in the Caribbean Region, the SST ranges between 25-30 °C (approximately 0-10 °C warmer than the early Holocene) (Beck et al., 1992; Haase-Schramm et al., 2003). In addition, a warming trend can be observed in the data. This trend has also been documented by Alley (2005), Thomas et al. (2007), and Lachniet (2009). From $8.166 (\pm .035)$ to

8.036 ($\pm .026$) K ybp, a SST drop of ~ 4 to $\sim 6^\circ\text{C}$ can be observed in the data. Fensterer et al. (2013) proposed a drop in SST of ~ 6 to $\sim 7^\circ\text{C}$ for the Caribbean between 8.2-8.0 K ybp, using speleothem collected in Cuba. Both this study and Fensterer et al. (2013) agree on this temperature drop. There is a gap in our data between ~ 8.0 to ~ 6.7 K ybp and also between ~ 6.7 and ~ 5.7 K ybp.

The Sr/Ca-SST values obtained from the modern coral collected in Barahona Bay (B20) are also plotted on the composite data graph (Figure 34). The modern SST values provided by the coral are warmer than all the SST values obtained from Cañada Honda corals. This is consistent with the SST expected values for the Holocene.

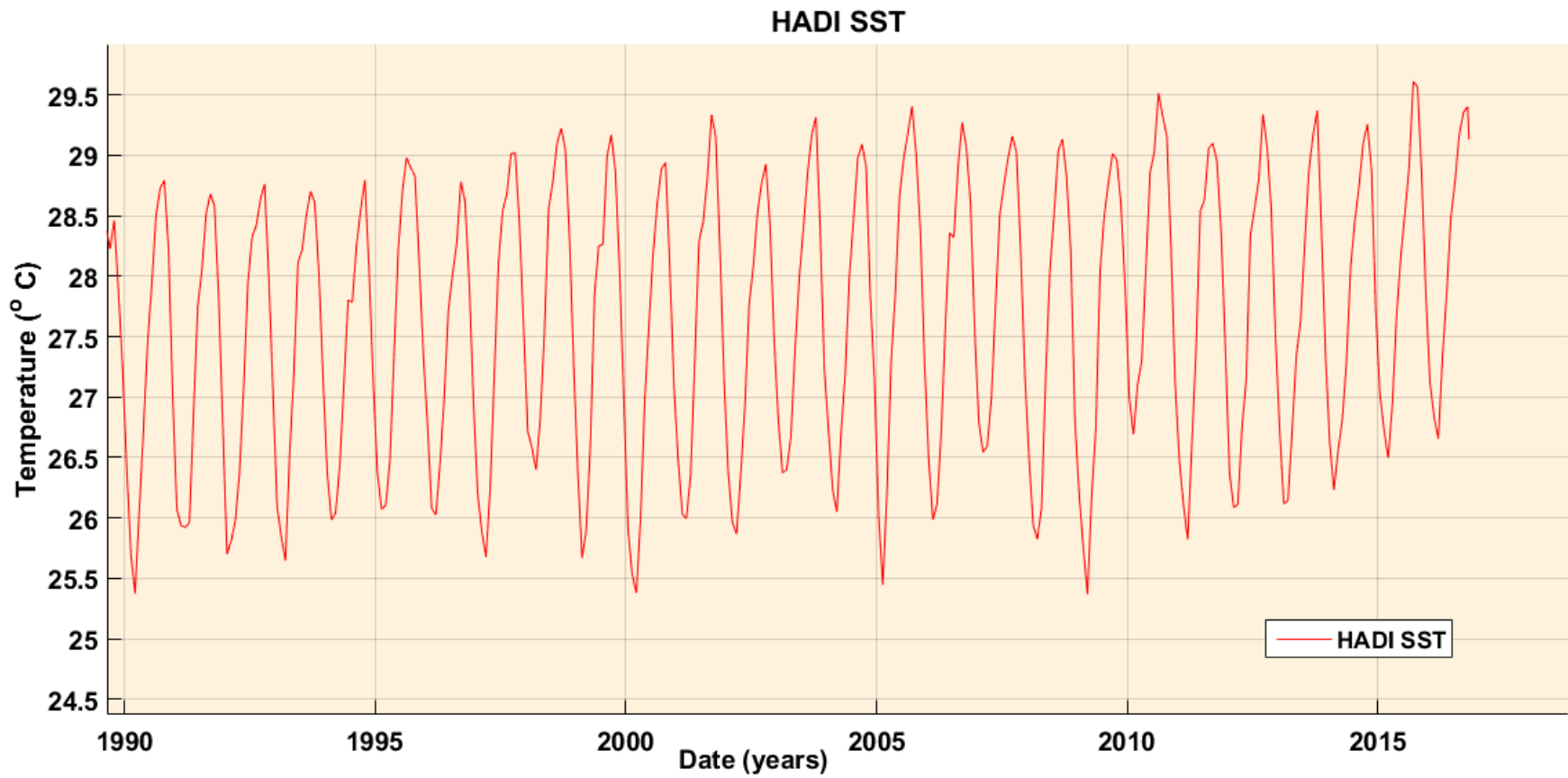


Figure 20. HADISST data set from Rayner et al. (2003). Measured for Barahona Bay, Dominican Republic.

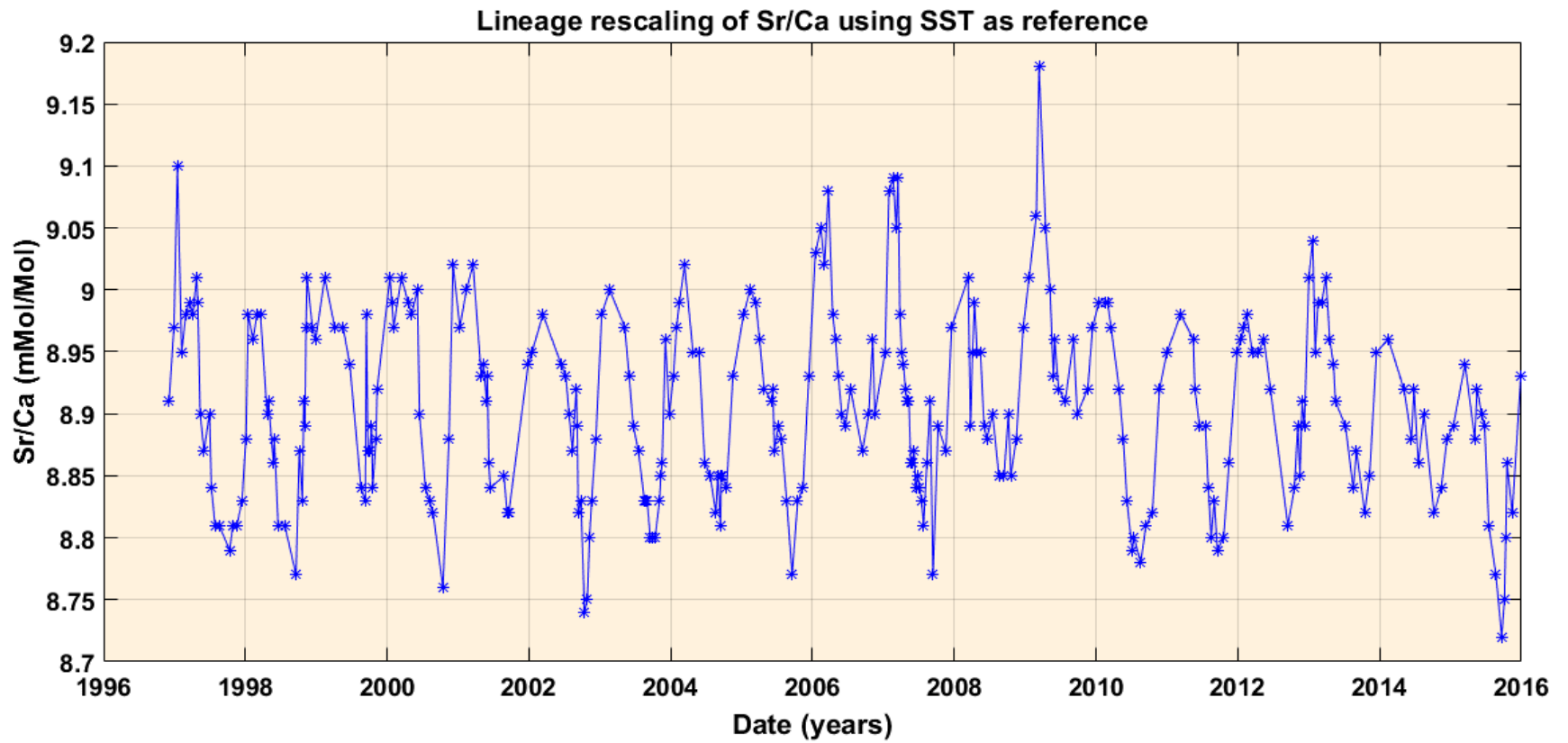


Figure 21. Lineage rescaling of Sr/Ca using HADI SST as reference.

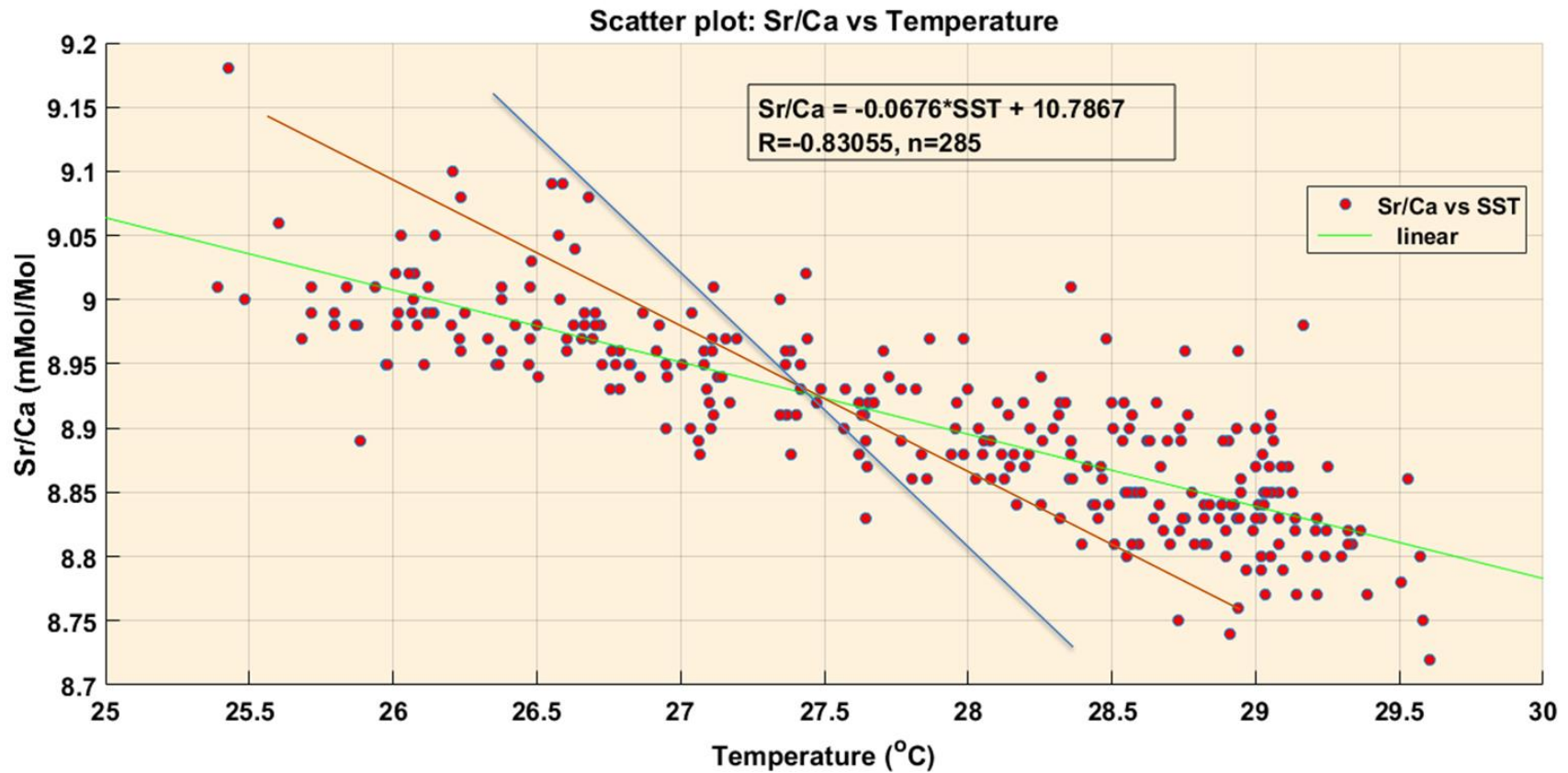


Figure 22. Scatter plot and linear regression Sr/Ca (mmol/Mol) vs. temperature (°C) obtained from the modern coral (B-20) collected alive from the Barahona Bay, Dominican Republic. The graph also shows the calibration equations obtained from the linear regression and the correlation for the equation ($R^2 = -0.83$). Flannery 2013 equation (blue), Swart 2002 equation (orange)

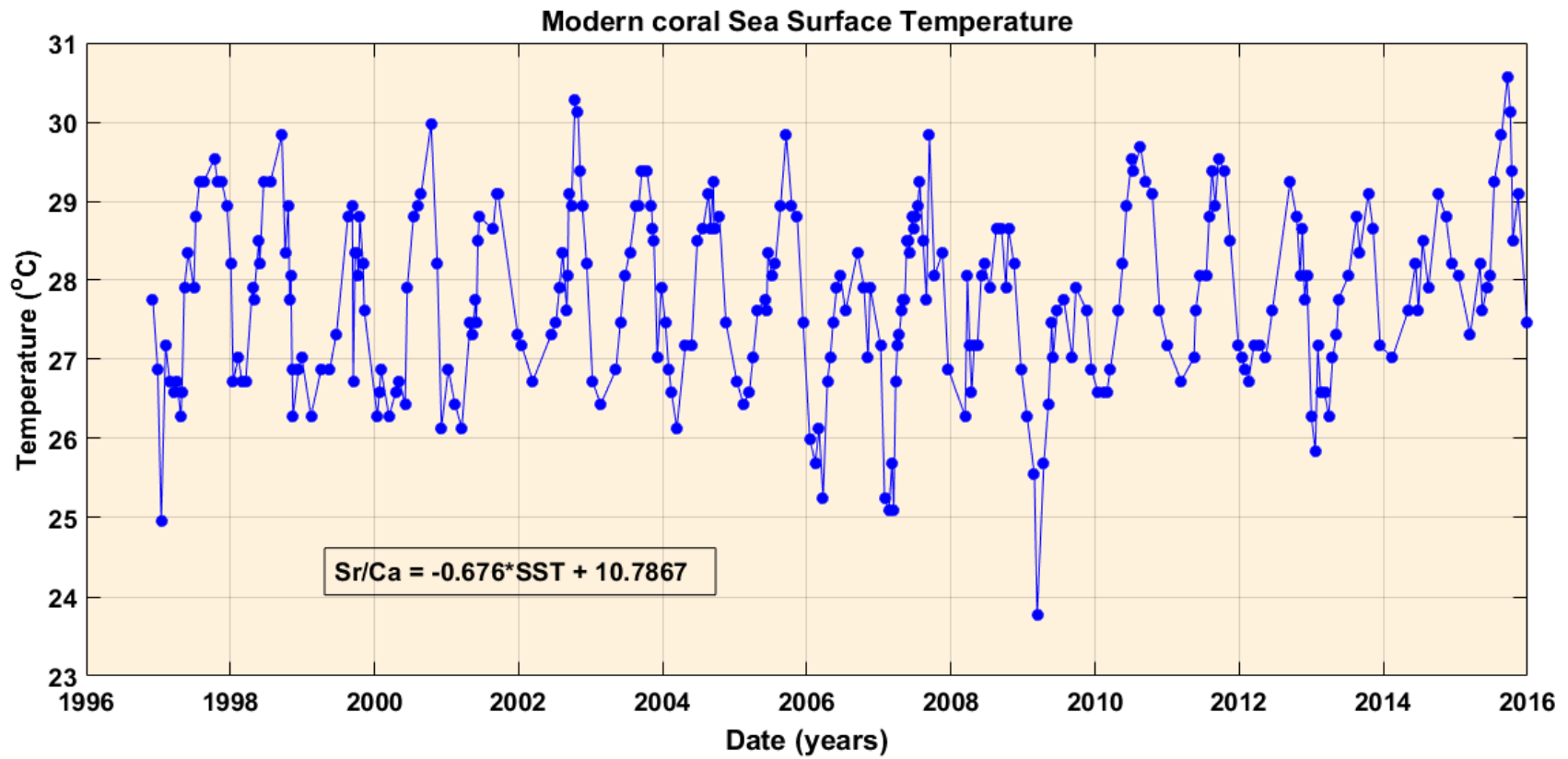


Figure 23. SST calculations for Sr/Ca obtained from the modern coral (B-20) collected alive in Barahona Bay, Dominican Republic. The equation used for the SST calculations is the one developed by this study.

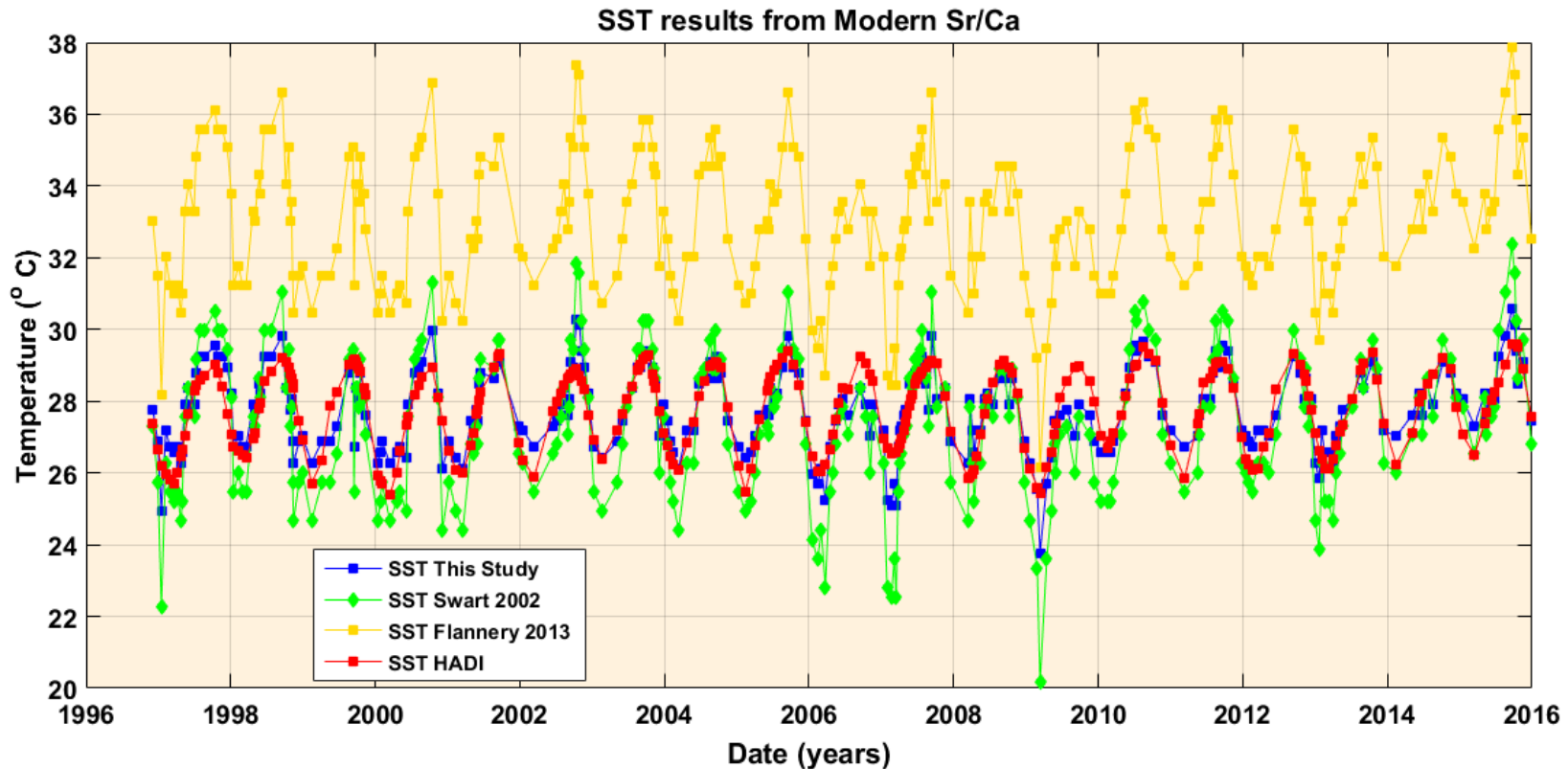


Figure 24. Comparisons of the SST (°C) vs. time (years) for the modern coral (B-20) calculated from Sr/Ca, using different equations (Swart 2002 (green); Flannery 2013 (gold); this study (blue)) and also measured SST obtained from HADI (red). When all the results are compared Flannery (2013) SST is about 3 degrees warmer in average and Swart (2002) shows a similar average with higher high and low values. SST from the equation produced in this study is the most compatible with the measured HADI values. The equation obtained on this study exhibits a temperature average of 27.8 ± 1.1 , with maximum, minimum temperatures values of 30.5 ± 1.1 and 23.7 ± 1.1 , respectively. Using Flannery's (2013) equation on the modern coral shows an average, maximum and minimum temperature values of 33.8 ± 1.5 , 37.6 ± 1.5 and 28.4 ± 1.5 , respectively. Using Swart's (2002) equation on the modern coral exhibits a temperature average of 27.4 ± 1.9 , with maximum and minimum temperature values of 32.3 ± 1.9 and 20.15 ± 1.9 respectively.

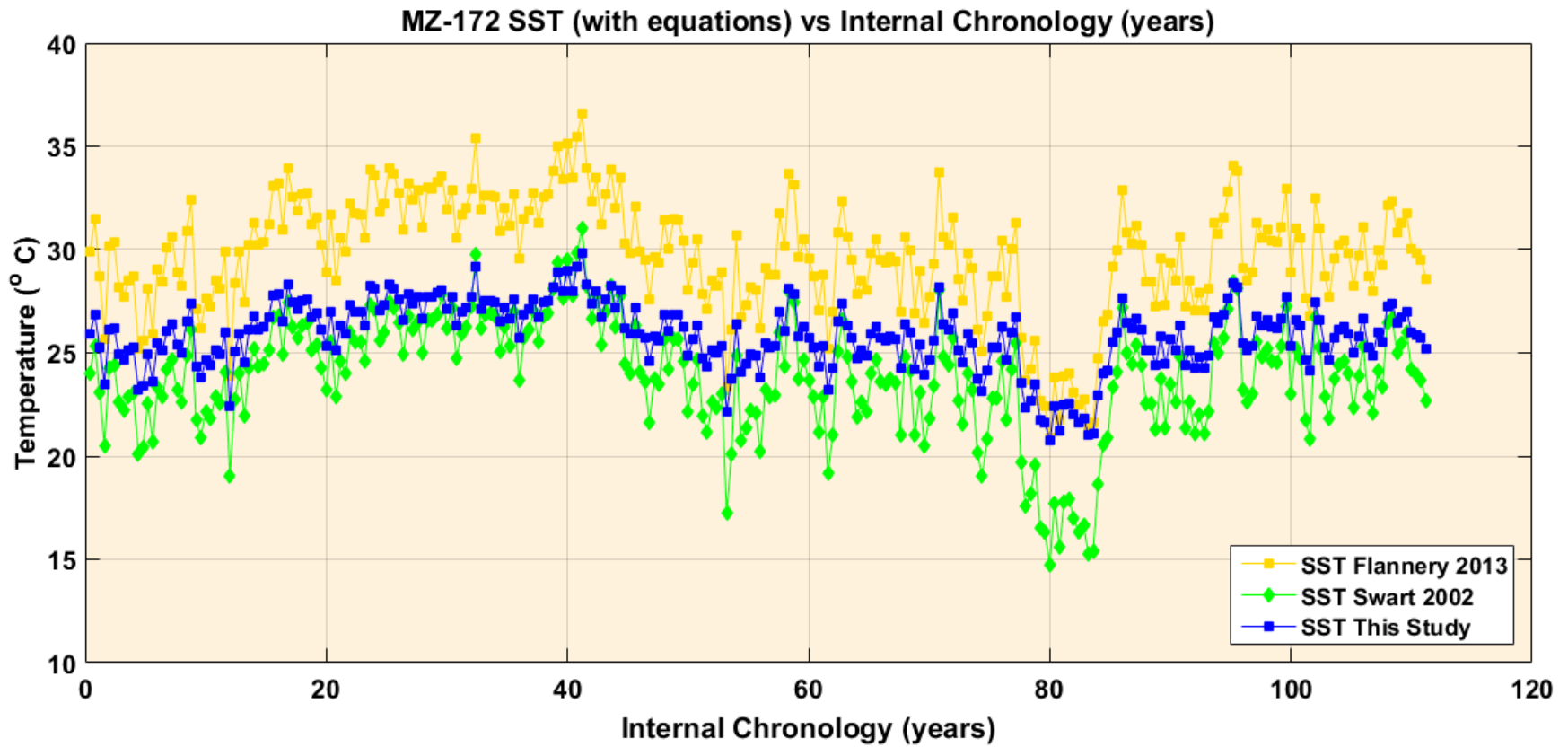


Figure 25. Sea Surface Temperature calculations for fossil coral sample MZ-172 using equations from Swart (2002), Flannery (2013), and this study. Flannery (2013) resulted in a warmer temperature while Swart (2002) resulted in a colder temperature relative to our equation. The temperature values obtained by this study’s equation are more similar to Swart (2002).

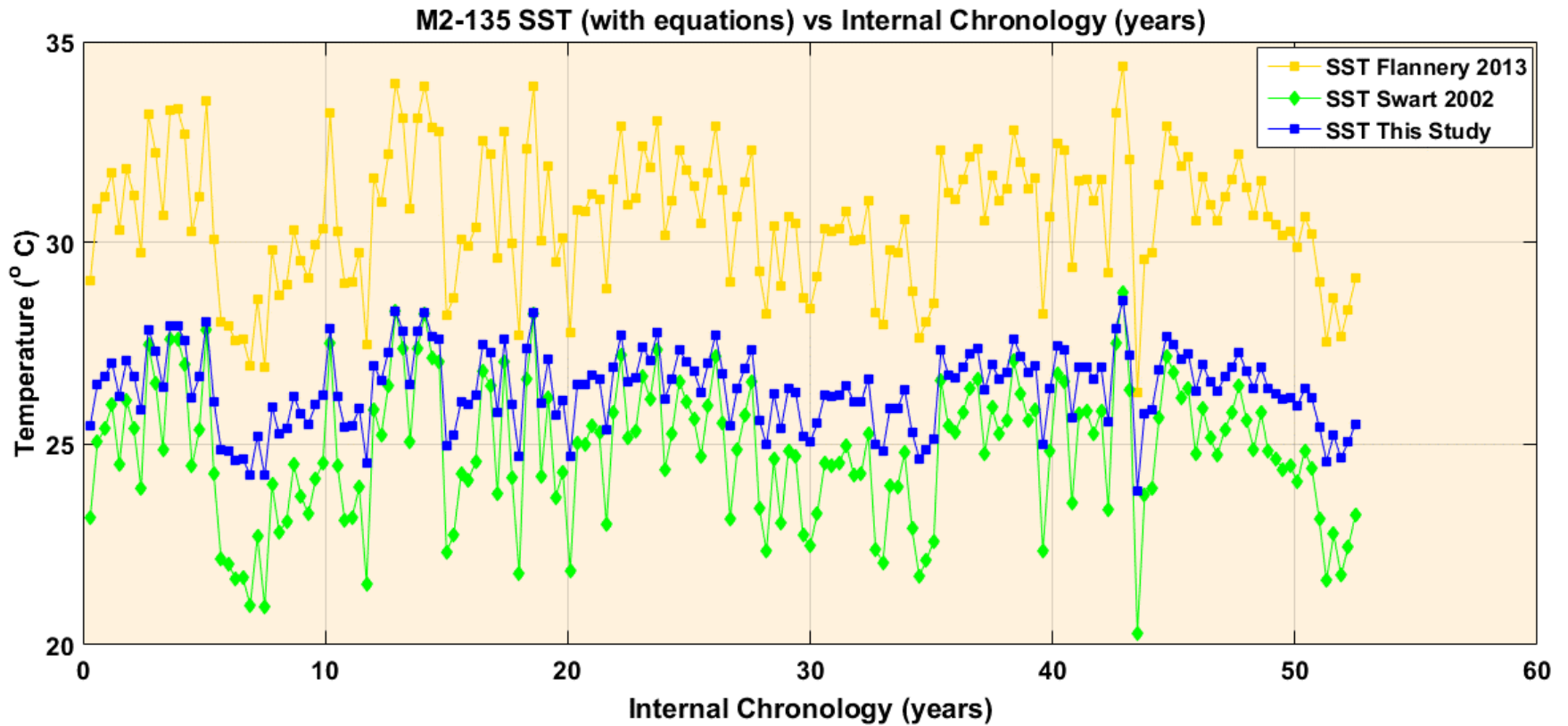


Figure 26. Sea Surface Temperature calculations for fossil coral sample M2-135 using equations from Swart (2002), Flannery (2013), and this study. Flannery (2013) and Swart (2002) resulted in warmer and colder SST values respectively. The temperature values obtained by this study's equation for fossil coral MZ-172 are similar to Swart (2002) SST values.

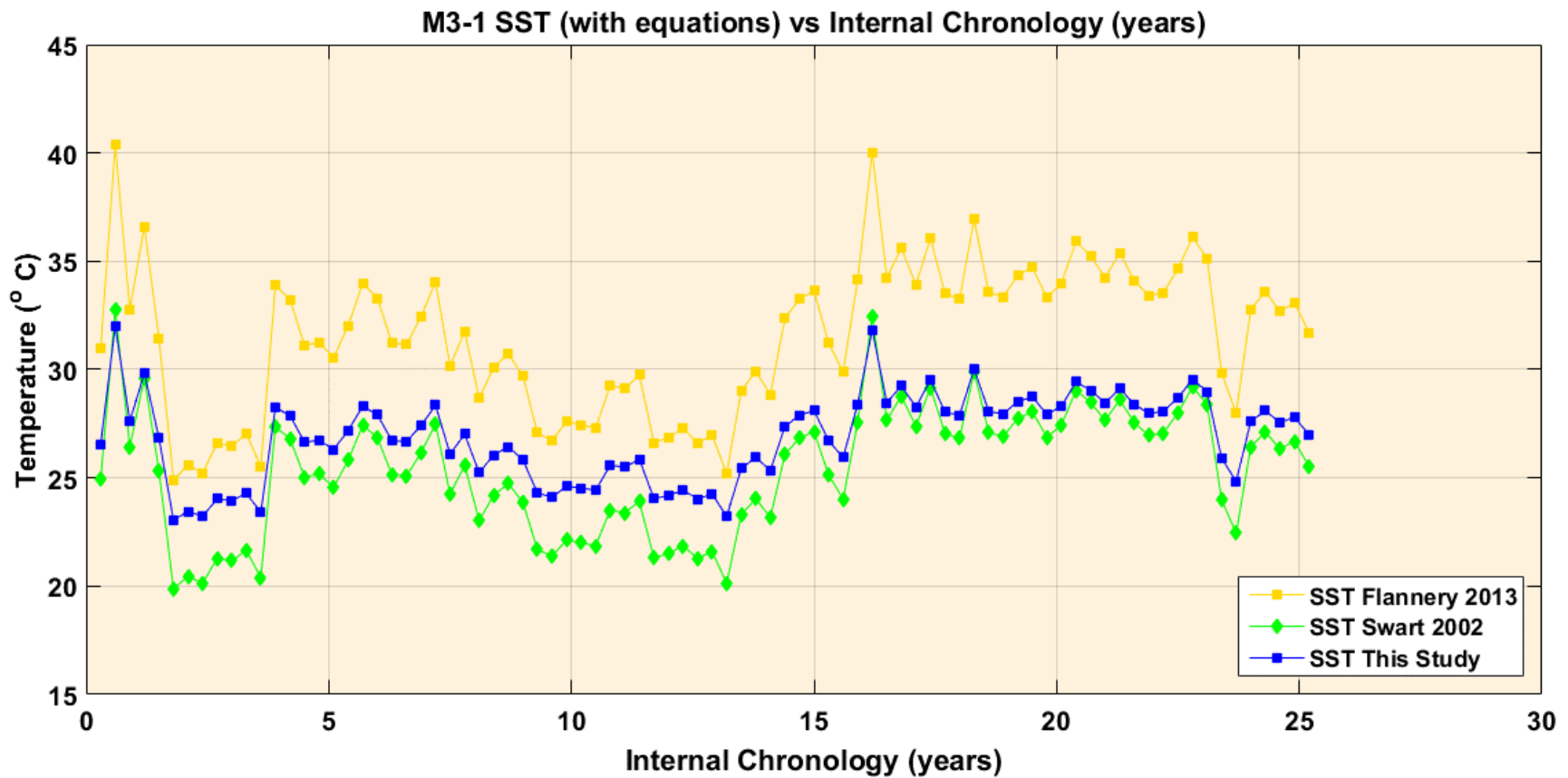


Figure 27. Sea Surface Temperature calculations for fossil coral sample M3-1 using equations from Swart (2002), Flannery (2013), and this study. Flannery (2013) and Swart (2002) resulted in warmer and colder SST values respectively. The temperature values obtained by this study's equation for fossil corals are more similar to Swart (2002).

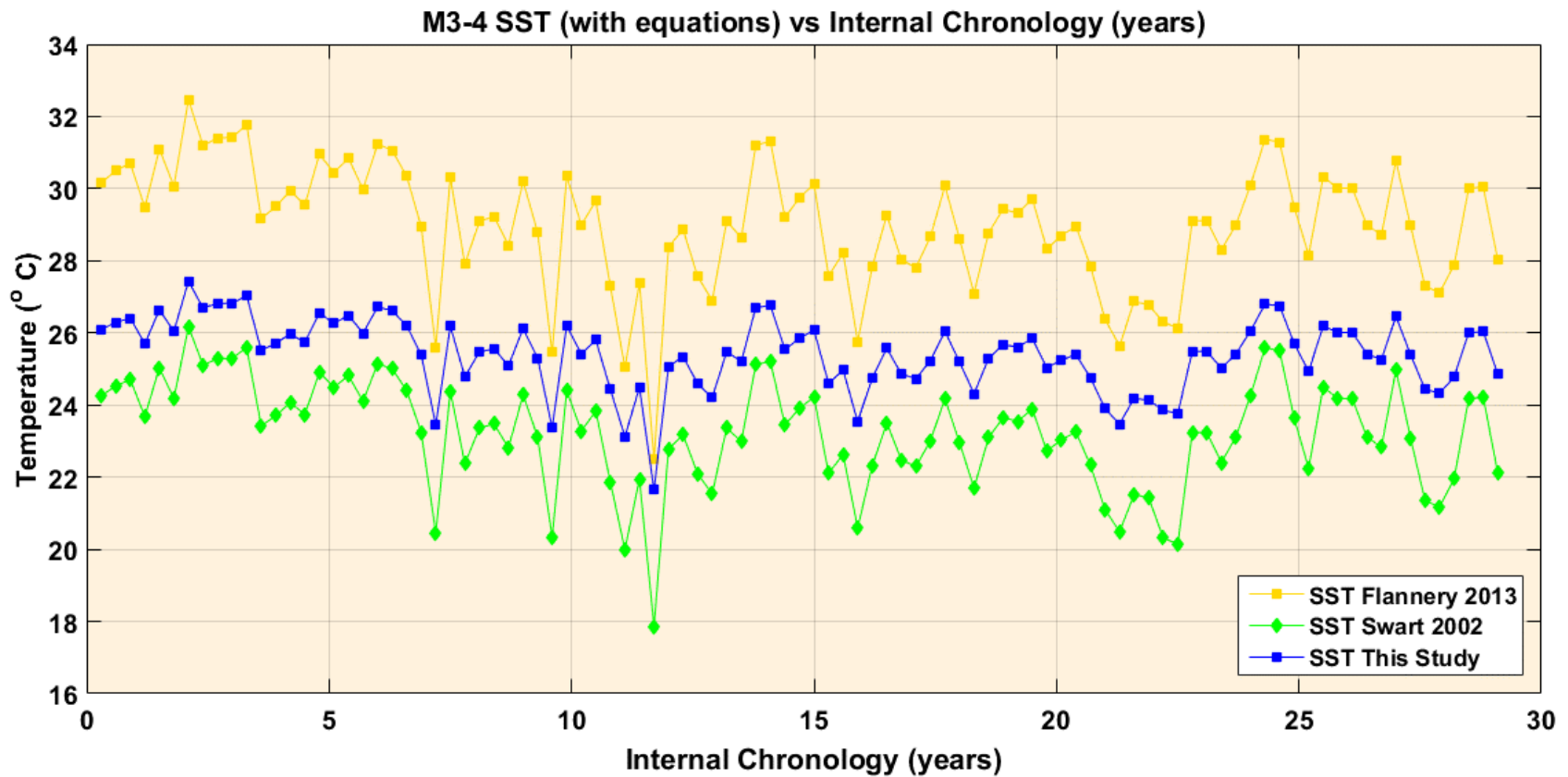


Figure 28. Sea Surface Temperature calculations for fossil coral sample M3-4 using equations from Swart (2002), Flannery (2013), and this study. Flannery (2013) and Swart (2002) resulted in warmer and colder SST values respectively. The temperature values obtained by this study's equation for fossil coral M3-4 resulted in similarities with Swart (2002).

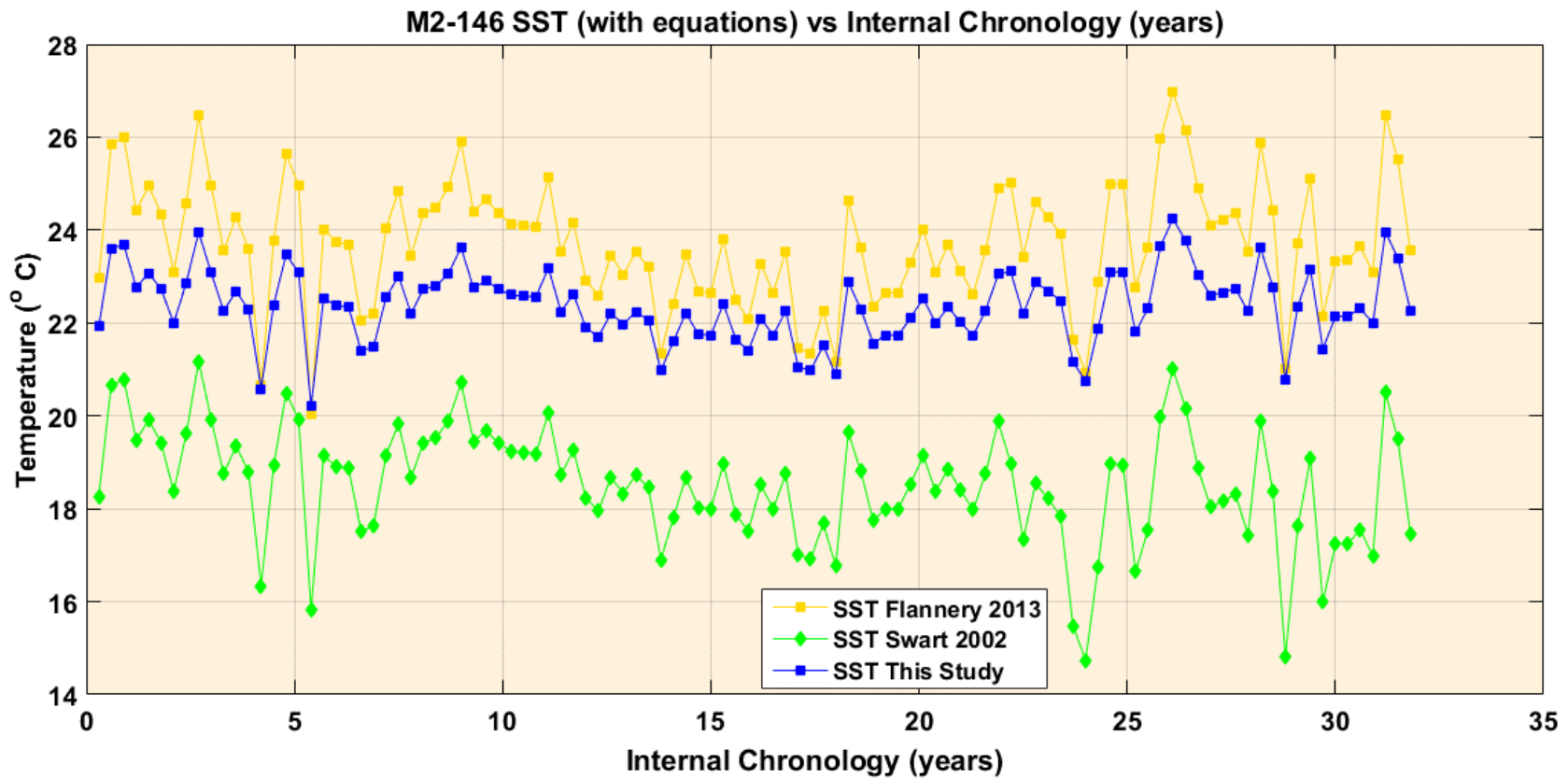


Figure 29. Sea Surface Temperature calculations for fossil coral sample M2-146 using equations from Swart (2002), Giry (2011), and this study. Flannery (2013) and Swart (2002) resulted in warmer and colder SST values respectively. The temperature values obtained by this study’s equation for fossil coral M2-146 are colder than Flannery (2013)

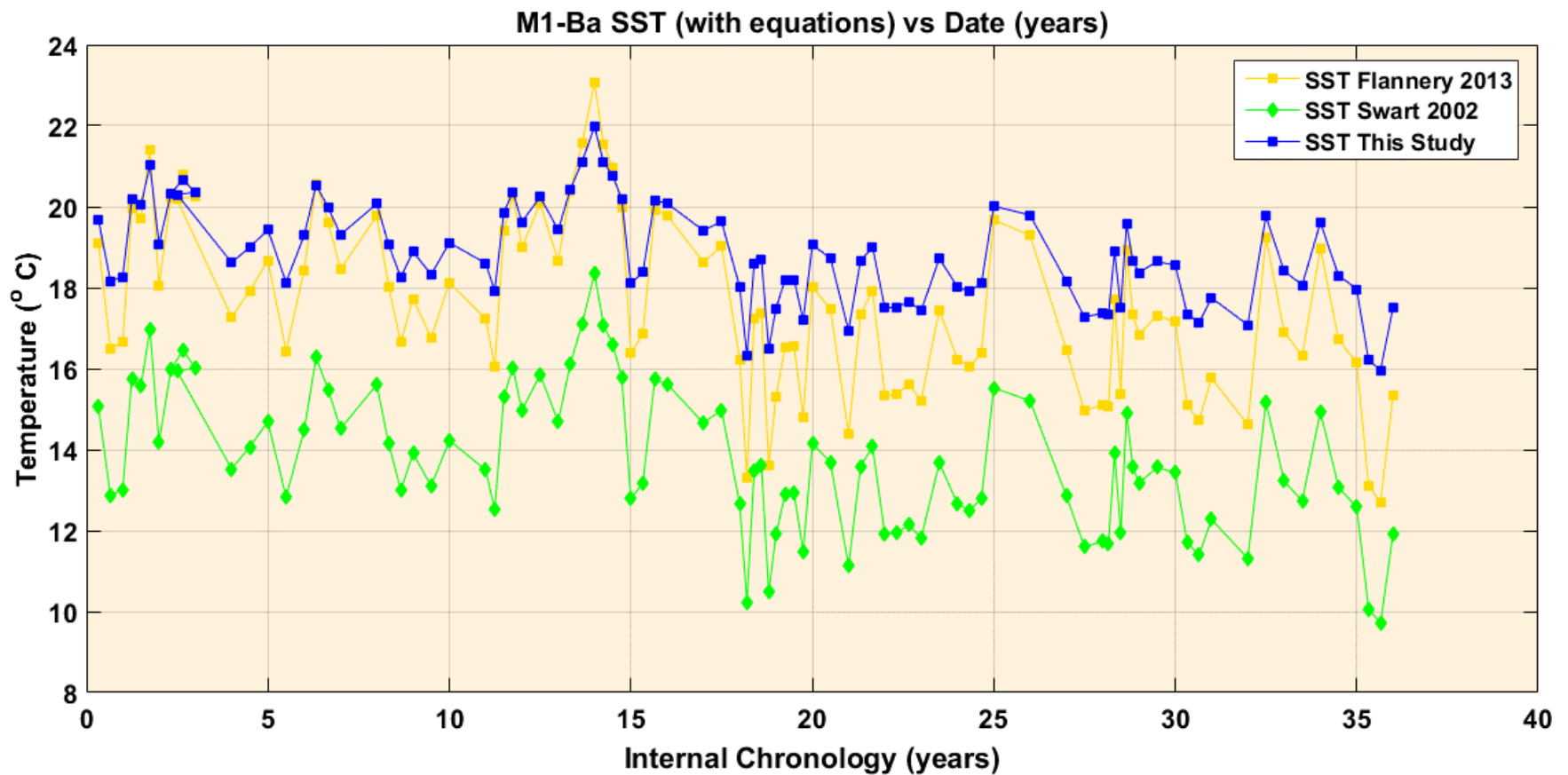


Figure 30. Sea Surface Temperature calculations for fossil coral sample M1-Ba using equations from Swart (2002), Giry (2011), and this study. Flannery (2013) and Swart (2002) resulted in slightly colder and colder SST values respectively. It should be noted that SST calculations using this study's equation resulted in similarities with Flannery (2013).

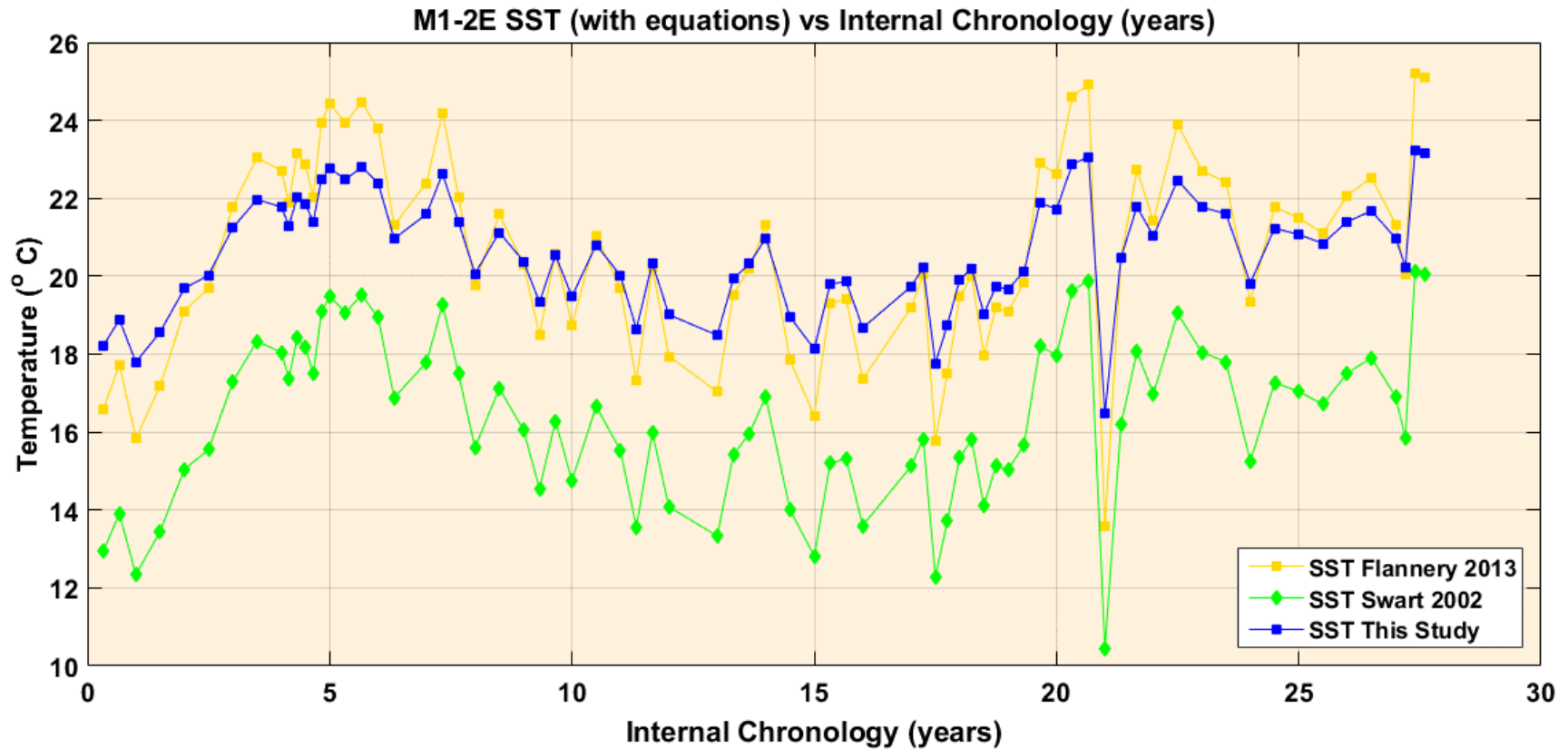


Figure 31. Sea Surface Temperature calculations for fossil coral sample M1-2E analyzed by Morales (2014) using equations from Swart (2002), Flannery (2013), and this study. Swart (2002) resulted in colder temperatures. M1-2E with Flannery (2013) resulted in slightly colder SST values. With this study's equation M1-2E resulted in similarities with Flannery (2013).

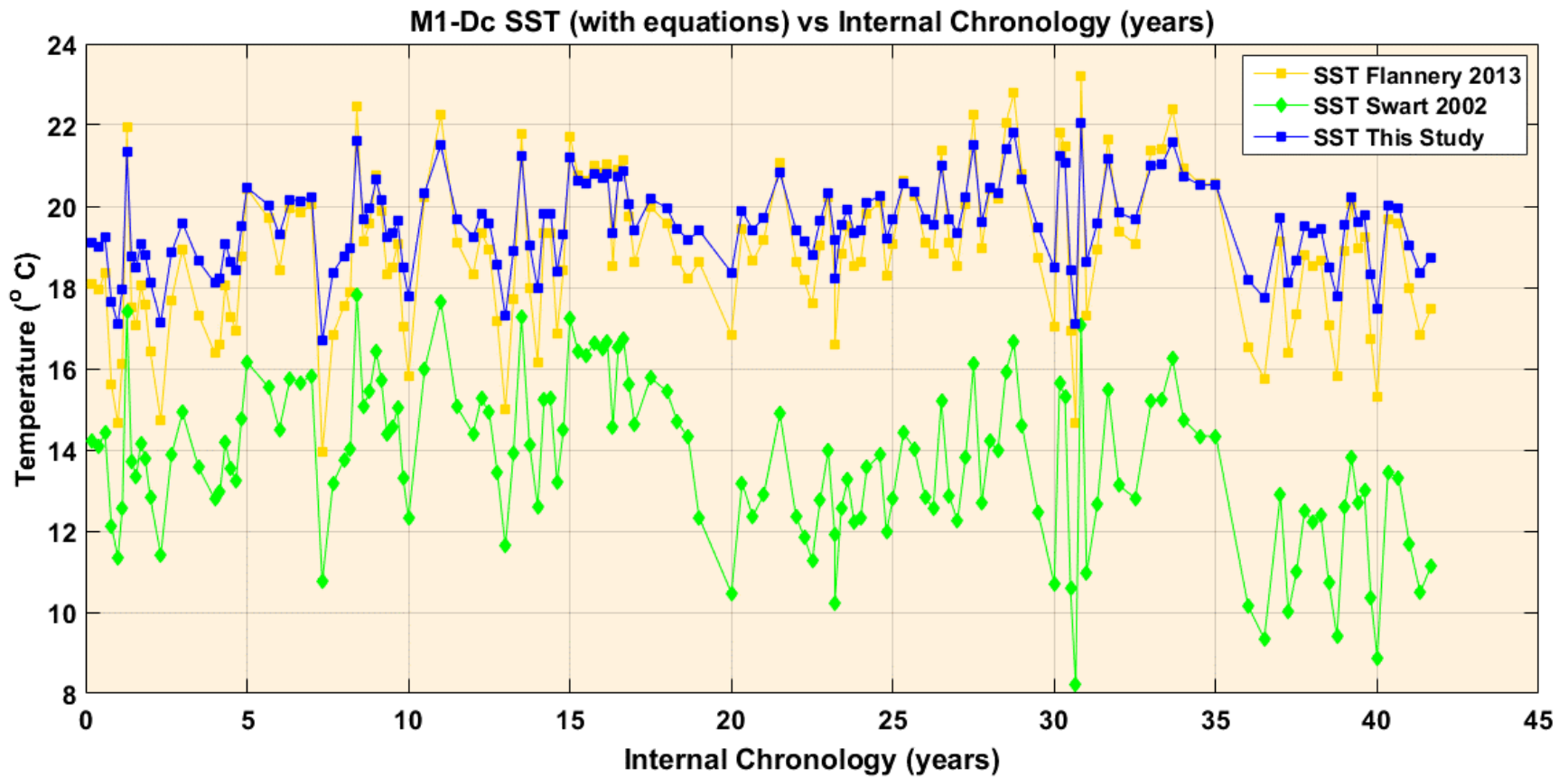


Figure 32. Sea Surface Temperature calculations for fossil coral sample M1-Dc processed by Morales (2014) using equations from Swart (2002), Flannery (2013), and this study. Flannery (2013) resulted in slightly colder SST values and Swart (2002) resulted in colder SST values. The SST values produced by this study’s equation resulted in similarities with Flannery (2013).

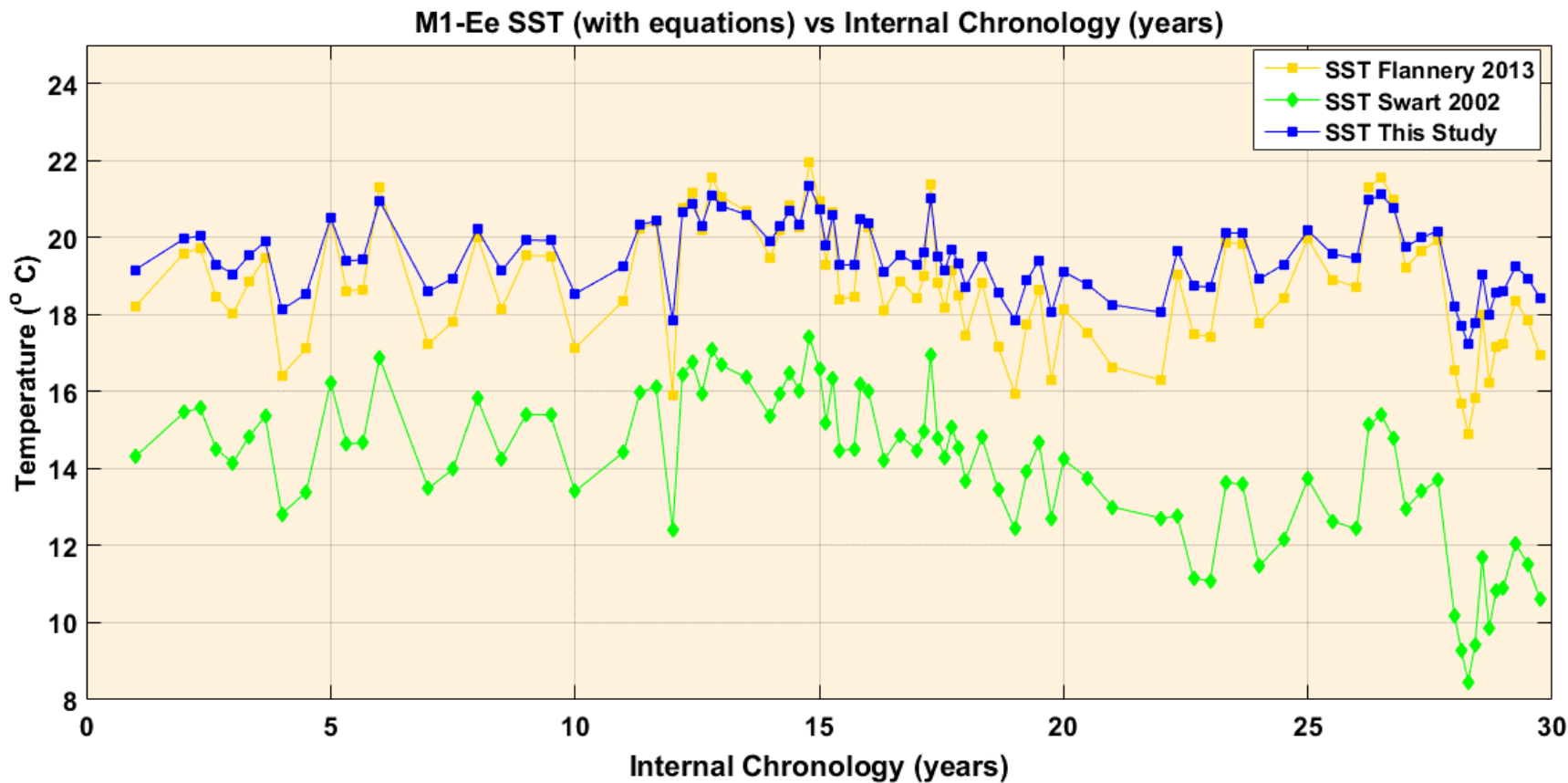


Figure 33. Sea Surface Temperature calculations for fossil coral sample M1-Ee processed by Morales (2014) using equations from Swart (2002), Flannery (2013), and this study. Flannery (2013) resulted slightly colder SST values, while Swart (2002) resulted in colder SST values. The SST values produced by this study's equation resulted with similarities with Flannery (2013).

Holocene Sea Surface Temperature Calculations

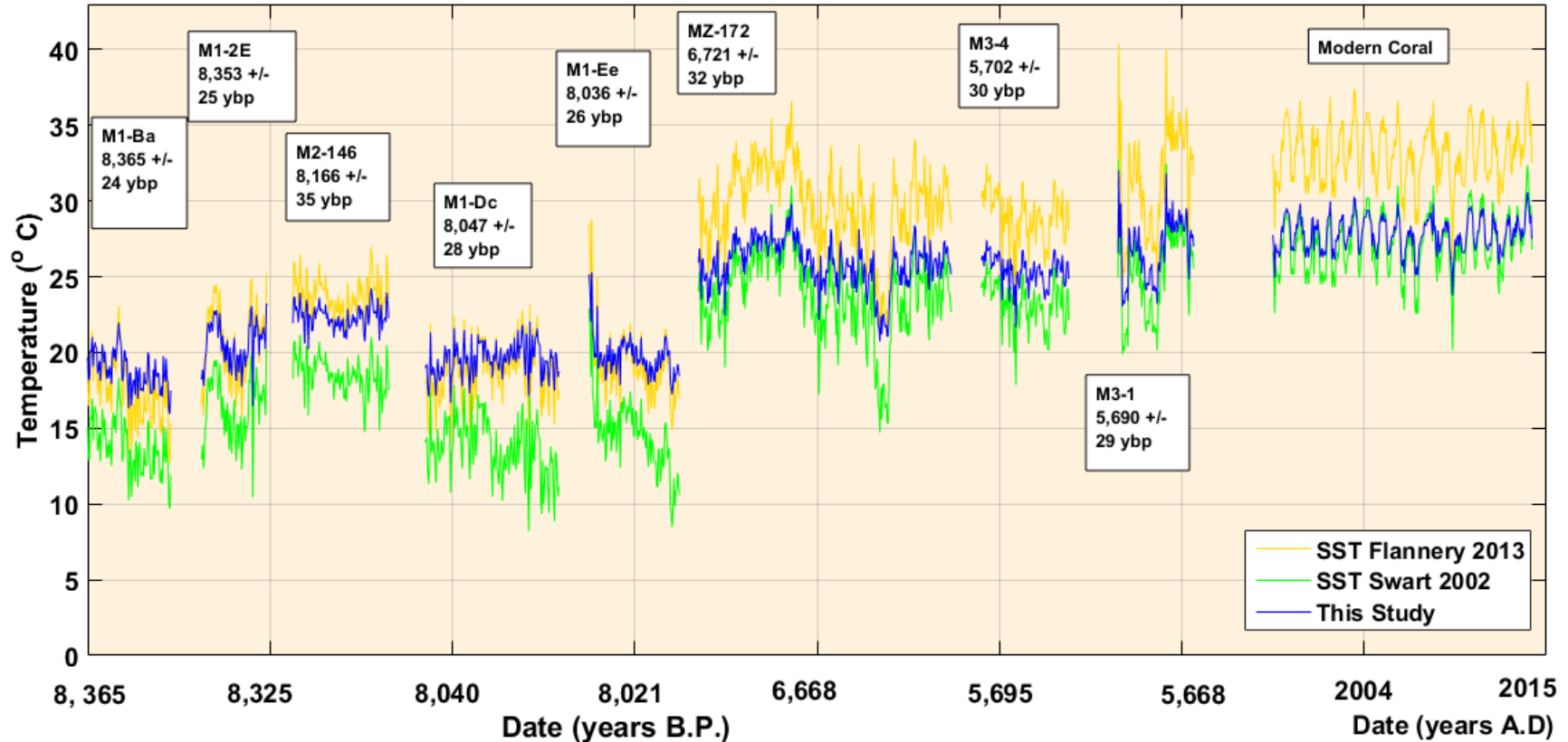


Figure 34. Composite graph of all SST calculated from Sr/Ca using equations by Flannery (2013) (gold), Swart (2002) (light green), and this study (royal blue). Sr/Ca data set of Massive Coral 1 (M1) was sampled and analyzed by from Morales 2014. Samples M2, MZ, M3-1 and M3-4 were sampled and analyzed for Sr/Ca in this study. The graph also includes Sr/Ca -SST values from the modern coral B-20 collected in Barahona Bay and processed by this study.

5.0 Discussion

Table 5 shows the names of the seven coral skeleton samples utilized and the analysis performed for each one of the samples. Economic limitations and sample problems associated with diagenetic alterations and intense boring did not permit for all coral skeletons to be analyzed with all the techniques applied.

5.1 Growth Rates

In this study, growth rate measurements obtained from *Orbicella sp.* complex skeletons produced in this study were 1.95 mm/year (n=28) and 1.98 mm/year (n=19) for M2 corals M2-146 (8,166 ± 35) and M2-135 (no age acquired) that grew at a water depth of approximately 8 meters below sea level; 1.32 mm/year (n=25) for the MZ coral MZ-172 (6.521 ± 32 K ybp) that grew at a water depth of approximately 6 meters below sea level; 1.93 mm/year (n=17) and 1.82 mm/year (n=21) for M3 corals M3-1 (5690 ± 29) and M3-4 (5702 ± 30 k ybp) that grew at a water depth of approximately 3 meters below sea level; and 7.34 mm/year (n=17 years) for the Modern Coral (collected in 2015) that grew at a water depth of approximately 10 meters below sea level. M2 corals have about 0.6 mm/year (n=29 and 28, years) higher growth rate relative to MZ and M3 corals. Cuevas (2005) reported *Orbicella sp.* growth rates for Cañada Honda corals from 1.30 to 4.50 mm/year for M2 facies; a growth rate range of 2.40 to 3.70 mm/year for MZ facies and 1.70 mm/year for M3 facies. Our results are within the range presented by Cuevas (2005) for M2 facies corals; lower for MZ facies corals (1.08 mm/year); and slightly lower for M3 facies corals (0.12 mm/year). Cuevas (2005) reported the M3 facies as the facies with the lowest growth rates in the Cañada Honda reef. The corals present in the M3 facies, as described by Hubbard (2004) and Cuevas (2005) and corroborated by this author, have distinctive and exaggerated foliated

morphology (Figure 35), which is abundant in waters of ~4 meters depth. In addition, this is the only facies as described by Hubbard (2004) and Cuevas (2005 & 2009) and corroborated by this author, that has *Orbicella franksi*, a coral that usually lives between 15 to 30 meters depth (Vize, 2006). Furthermore, the *Montastrea cavernosa* specimens present in these facies have an exaggerated columnar morphology relative to the other facies in the Cañada Honda reef, that has been observed at 20 meters depth (Figure 36, Parguera, P.R. Shelf edge) or high sedimentation areas (Mayagüez, P.R.) (Ramírez-Martínez, personal communication). These observations have been proposed to suggest that environmental conditions during the development of the M3 facies were the most challenging during all the Cañada Honda history of accession. In this study, the lowest growth rates were measured in coral MZ-172 1.32 mm/year, (6.521 ± 32 K ybp) of the MZ facies, facies that according to Hubbard (2004) and Cuevas (2005 & 2009) developed during a time of “better” environmental conditions.

It is difficult to establish meaningful comparisons between growth rates, even in the same species, because growth rate in corals are dependent on water depth also on environmental factors including water clarity (Hubbard et al., 1985; Morelock et al., 2000; Cruz-Piñón et la., 2003; Hubbard et al., 2008; Weinstein et al., 2016). However, the growth rates from the fossil (Holocene) corals of the *Orbicella sp.* complex (Cañada Honda) are significantly different from most measurements in modern corals of the same species. As examples, the modern *Orbicella sp.* coral collected for this study in Barahona Bay from a water depth of ~10 meters produced a growth rate of 7.34 mm/year, *Orbicella sp.* collected at ~12 meters water depth in the US Virgin Islands, 12 mm/year (Hubbard et al., 1985); and an *Orbicella sp.* coral collected at ~1 to 2 meters in Chinchorro and Mahahual, Mexico, 4.8 – 7.2 mm/year (Cruz-Piñón et la., 2003). These modern

Orbicella sp. coral growth rates from shallow waters are 5-10 mm/year higher than the growth rates obtained from Cañada Honda Corals.

A comparison with different modern corals collected in the Caribbean at different water depths together with the Barahona Bay modern coral, showed a similar average range ($\sim 6.6 \pm 1.77$ mm/year at a water depth less than 10 meters; 5.0 ± 3.0 mm/year at a water depth greater than 10 meters. (Figure 37)

Growth rate data set was acquired from previous studies for fossil corals from Cañada Honda reef is shown in Figure 38 for comparison. Fossil corals measured in this study resulted within the range of values relative to the growth rates acquired in previous studies. However, when values are compared to the growth average of the facies, resulted in ~ 1.12 mm/year lower for M2, 3.08 mm/year for MZ and M3 resulted very similar to the growth average calculated for these facies. When analyzing the whole Cañada Honda reef panorama (growth average per facies) it should be noted that M1 showed slow growth of 2.6 mm/year; M2 showed 3.13 mm/year; MZ resulted in 4.4 mm/year and M3 showed 1.91 mm/year. M1, been at the basal of the reef at a ~ 12 meters, turbidity and decrease on light penetration might had driven the slow development of the M1 corals. M2 at a water depth of ~ 8 meters resulted only 0.4 mm/year higher relative to M1, which suggest, that the same factor affecting growth on M1 was affecting M2 as well. Mz at a water the of ~ 5 meters resulted in the highest growth rate acquire (4.4 mm/year). Conditions by this facies/time were slightly favorable for corals. By this, we validate what Hubbard (2004) and Cuevas (2005 & 2009) proposed for corals from MZ, that were living under “better conditions” relative to the other facies. M3 resulted with the lowest growth average of all facies, showing an average of 1.91 mm/year. This suggests that conditions around this time were critical for corals to live. Because M3 has (1) slow growth, (2) characteristic and morphologies mentioned above

(foliated), (3) no other coral facies above it, and (4) corals no younger than 5.0 K ybp, it suggests that conditions were critical due to the gradually enclosure of the Bay around this time (Taylor et al., 1984; Mann et al., 1995).

Corals from Cañada Honda reef, when compared to modern analogs in terms of species and water depth, still suggest slow growing of corals. Cañada Honda was developed at no greater water depth than ~12 meters, in comparison with the modern analogs the growth rate collected lower than 10 meters, suggest a growth rate range from 5 to 8 mm/year. Based on this MZ in the only facies that can lie within closer within the range. (Figure 39) It should be noted that for the modern and fossil corals data set of growth, only *Orbicella complex* was considered.



Figure 35. Images that illustrate exaggerated foliated morphology on shallow water corals (~3 meters depth) in M3 facies.

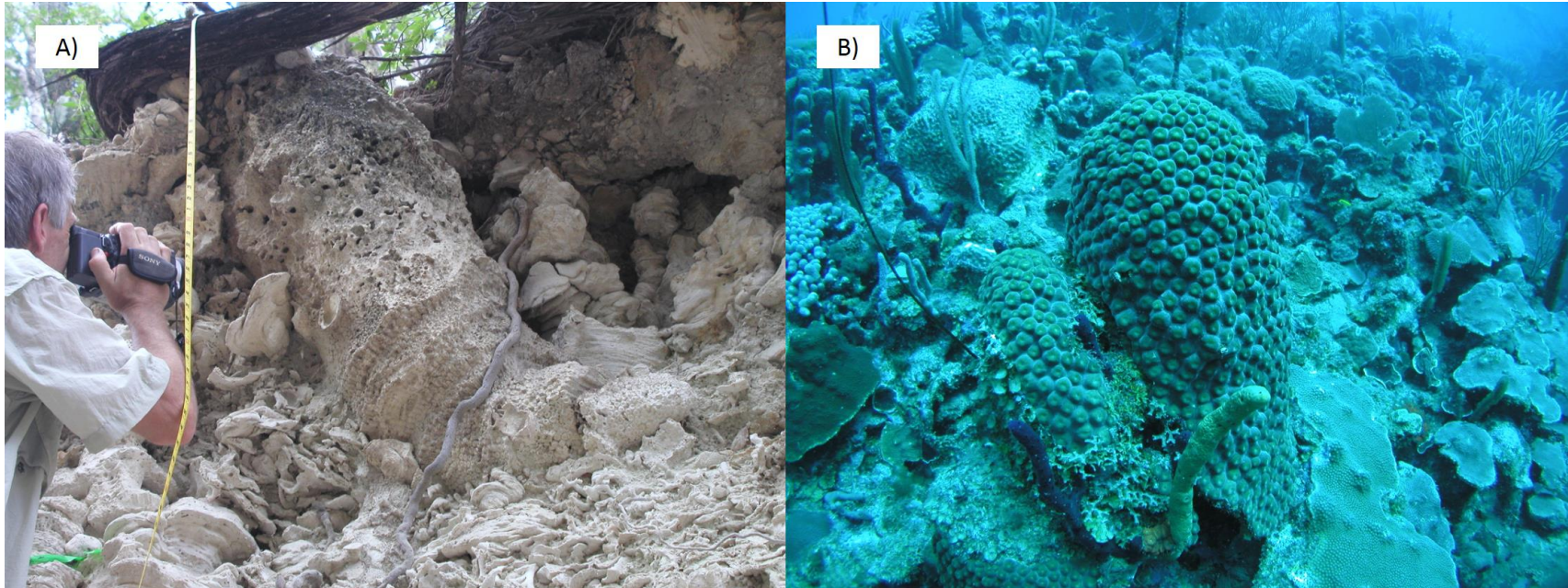


Figure 36. Modern (Parguera Shelf Edge, PR) vs. Fossil (Holocene Cañada Honda Reef RD) examples of similar morphologies in the coral *Montastrea cavernosa*. A) *Montastrea cavernosa* from the Cañada Honda reef assumed to have lived an estimated depth of ~3 meters water. B) *Montastrea cavernosa* from the Parguera Shelf Edge in Lajas, Puerto Rico observed at a water depth of ~30 meters. The exaggerated columnar morphology of the fossil coral colony's. The estimated depth where it grew suggests that environmental conditions in the Holocene Cañada Honda reef were not optimal at the time when coral facies M3 accreted (Wilson R. Ramírez - personal communication)

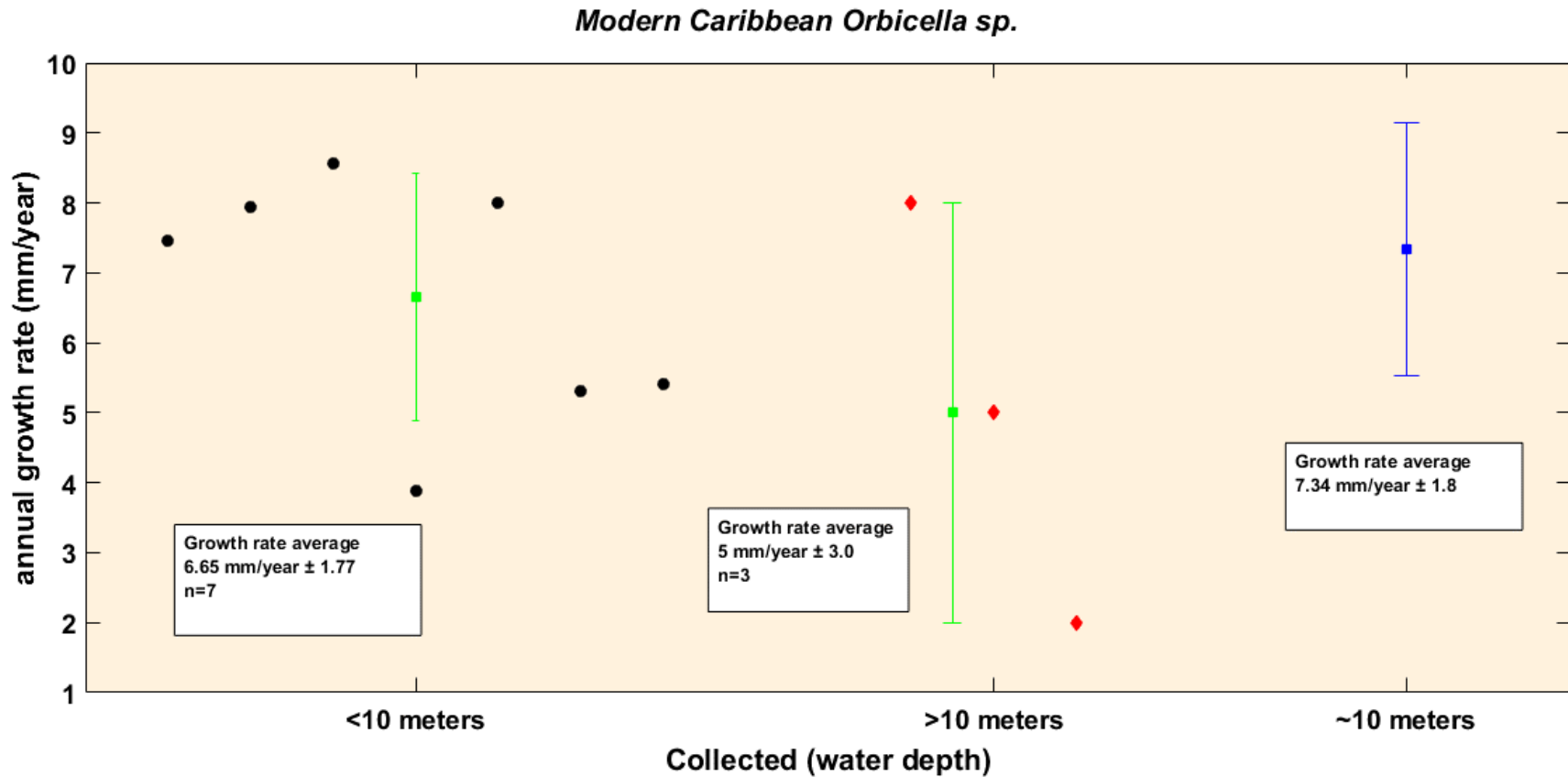


Figure 37. Modern Caribbean growth rates of *Orbicella* complex. A comparison between corals that were collected on previous studies at a water depth lesser than 10 meters in, St. Croix, USVI; Jamaica & Bermuda; Costa Rica; Puerto Rico; Mexico, ((black) (data from Gladfelter et al. 1978; Fairbanks and Dodge, 1979; Cortés and Risk, 1985; Torres and Morelock, 2002; Cruz-Piñón et al. 2003, respectively). Corals collected greater than 10 meters in St. Croix, USVI (red) (Hubbard et al., 1985) and this study at 10 meters water depth (Blue) (Barahona Bay). Average growth rate was calculated for data set and are represented as green. Error was calculated using standard deviation.

5.2 XRD analysis

XRD analyses made on M2-146, MZ-172, MZ-157, M3-4, M2-128, M3-1 band, M3-1 bottom, M3-1 top fossil coral indicates all samples are aragonitic in composition. Although the detection limit of the analysis is 2% (Kontoyannis et al., 2015), the visual inspection of the coral skeletons and the success of most of the diverse analytical procedures performed serve as independent assessments of the coral skeletons pristine preservation.

5.3 U/Th

Figure 39 summarizes the resulted ages for Cañada Honda fossil corals used in this study and in Morales (2014) using U/Th dating.

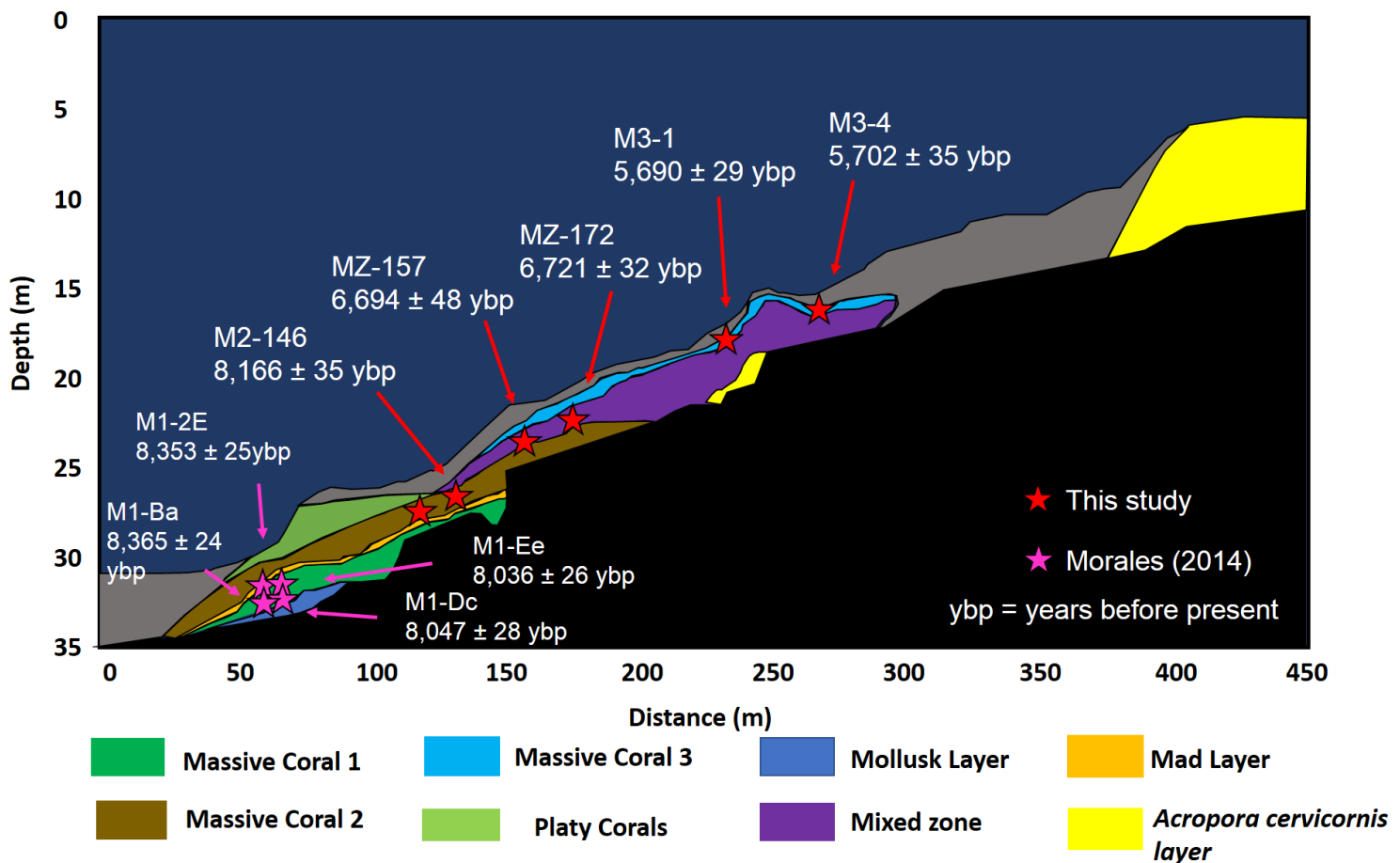


Figure 39. Cross sectional view of Cañada Honda reef showing the U-Th dates acquired from corals collected for this study and also corals studied by Morales (2014). U-Th dating for coral sample M2-135 was not determined (see Table 5).

5.4 Sr/Ca-T calculations

The Sr/Ca values obtained for fossil corals (M1-Ba, M1-2E, M2-146, M1-Dc, M1-Ee, Mz-172, M3-4, M3-1) range between 9.0 – 9.50 mmol/mol (n=5) and are 0.4 mmol/mol higher in average than the ones obtained from the modern coral *Orbicella sp. complex* collected in Barahona Bay that ranged between 8.85 -9.0 mmol/mol (Figure 40). If SST is calculated from Sr/Ca (with the new equation presented here: $Sr/Ca = -0.0676 * SST + 10.7867$), this 0.4 mmol/mol value is equivalent to a difference in SST of -0.4 °C. Holocene SST are expected to be colder than modern day conditions, which can support having higher Sr/Ca ratios throughout the Holocene (Beck et al., 1992; Haase-Schramm et al., 2003).

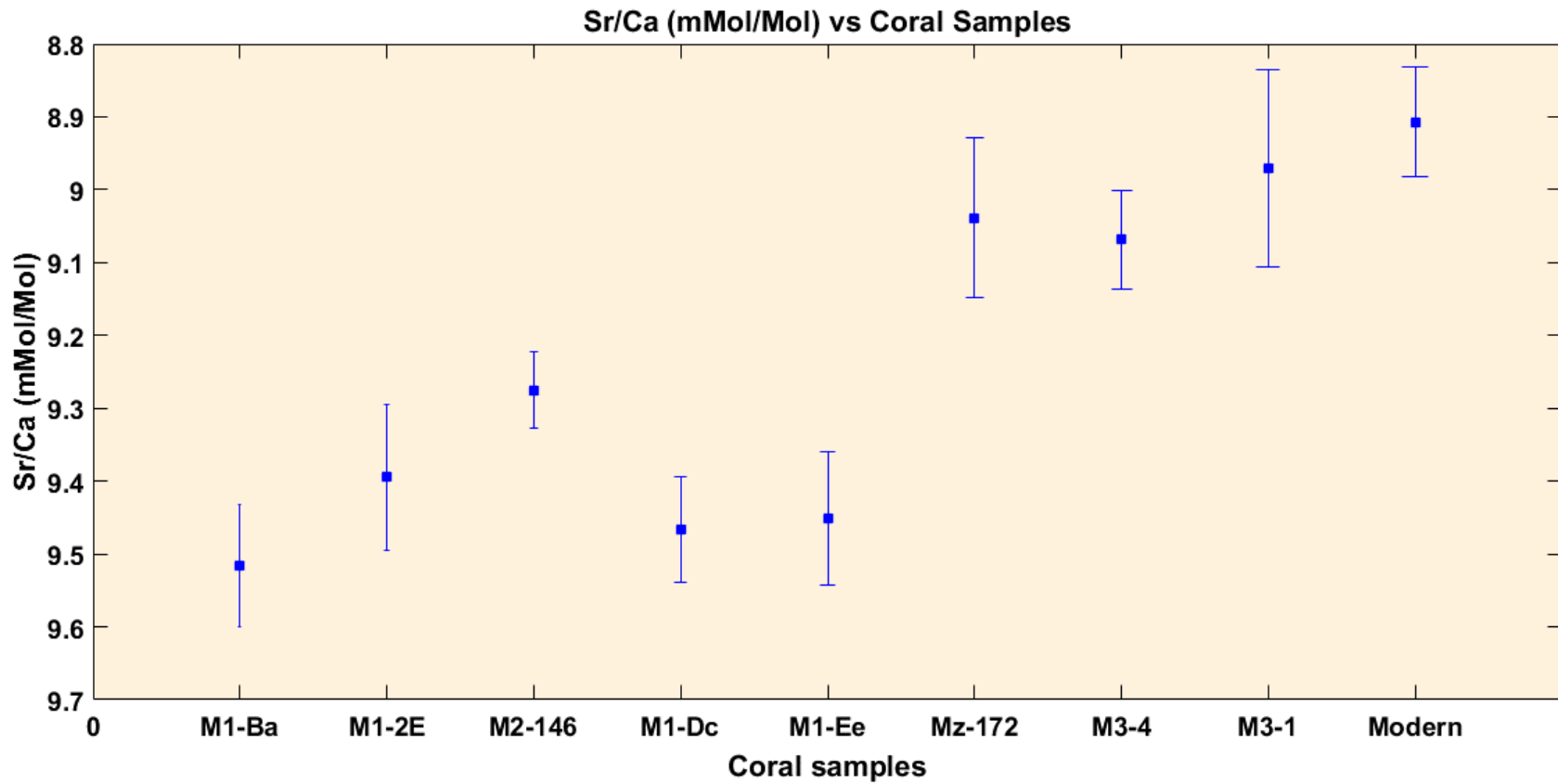


Figure 40. Figure shows the distributions of Sr/Ca ratios acquired for fossil collected from Cañada Honda. M1-Ba, M1-2E, M1-Dc, M1-Ee coral sample were acquired by Morales (2014), while M2-146, Mz-172, M3-4, M3-1 and Modern coral were acquired by author. Data set was arranged based on the U/Th ages acquired from each coral (oldest to youngest) (see Table 4 & Figure 34).

Secondary aragonite contamination is not expected to be a problem present in our samples because the samples were inspected for the presence of secondary aragonite and they showed pristine samples (Enmar et al., 2006; Sayani et al., 2011). Based on results SEM Results acquired by Arana (2018), Herrera (2018), and Rodríguez (2018) (MZ, M2, and M3 respectively), no secondary aragonite is present in Cañada Honda samples.

Another source of uncertainty could be the input of Strontium into the marine paleo-Enriquillo Bay environment from terrestrial sources that could have raised the Strontium concentration above the expected marine values imprinting them in the Sr/Ca of the skeletons. These influences are expected to have come into the bay continuously or episodically from either the Río Yaque del Sur and/or underground water springs that discharge into the Lake today and are assumed to have discharged into the paleo-Enriquillo Bay during the early Holocene (Taylor et al., 1985; Mann et al., 1991; Buck et al., 2005; Mendez et al., 2016; Delanoy et al., 2017). Hydrological studies in the area have reported the water level of Enriquillo Lake was 42 m below sea level before 2014 rising to 29 m below sea level after 2014 (Mendez et al., 2016; Delanoy et al., 2017). According to Buck et al. (2005), Mendez et al. (2016) and Delanoy et al. (2017), the increase in the lake level was produced by inputs of abundant fresh ground water coming out from springs that are recharged in the Sierra de Neiba and Sierra Batoruco mountain ranges (Limestone rocks). However, modern Sr/Ca-SST relation might not have been remained constant throughout the Holocene.

Sea Surface Temperature (SST) calculated for Sr/Ca obtained from modern *Orbicella sp. complex* corals using Flannery's (2013) and Swart's (2002) equations as well as this study's equation resulted on average temperature values of 33.11 ± 1.9 °C, 27.4 ± 1.9 °C, and 27.8 ± 1.1

°C, respectively. Maximum and minimum temperature ranges calculated with all 3 equations, and this study, on the modern coral from Barahona Bay resulted in; 37.88 ± 1.9 °C, 26.14 ± 1.9 °C, 32.3 ± 1.9 °C, 20.1 ± 1.9 °C, 30.5 ± 1.1 °C, respectively (Figure 41). The average temperature (Sr/Ca-T) of 33.11 ± 1.9 °C by Flannery's (2013) equation is significantly higher than 25 to 29 °C, the temperatures were *Orbicella sp. complex* corals can live (Budd et al., 1994; Medina et al., 1999; Cruz-Piñón et al., 2003; Voolstra et al., 2009). Swart's (2002) equation produced an average temperature (Sr/Ca-T) of 27.4 ± 1.9 °C which is within the range of living conditions for *Orbicella sp. complex* corals. Satellite measurements (HADISST) (see Figure 24) for the south of Dominican Republic (Caribbean) reported average SST values of 27.79 ± 1.1 °C which are well within the range of living conditions for this coral and other coral species.

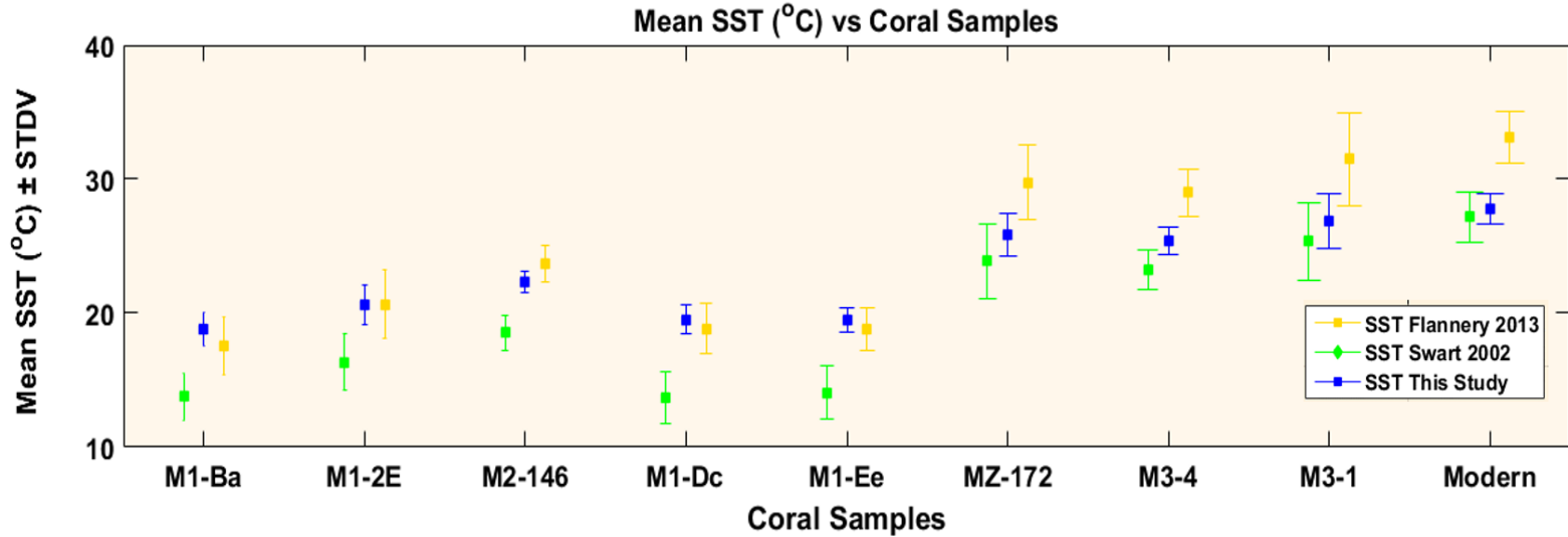


Figure 41. SST's mean of Flannery (2013) (gold), Swart (2002) (green), and this study (blue) equations calculated for each fossil coral along with the modern coral (\pm stdv). Fossil corals SST calculations using our equation resulted with similarities with Flannery (2013) while the modern coral resulted with similarities with Swart (2002). A warming trend still can be observed going from ~ 20 °C (8365 \pm 24 K ybp) to ~ 27 °C (modern corals, collected in 2015).

5.5 Cañada Honda SST Record from corals vs. the Holocene SST record

According to the data obtained from the Sr/Ca-T in this study the SST during the early Holocene in the paleo-Enriquillo Bay was cooler than modern day conditions. This is expected base on paleoclimate information from other studies that include other proxies (Beck et al., 1992). The Sr/Ca-T calculations produced by the equation derived in this study range from 19-27 °C (see figures 24 to 33). The equation developed in this study (from the modern Barahona Bay coral) produced intermediate SST values consistently when compared with the SST living range for corals. Our equation also provides less variability on peaks and valleys (winters and summers).

The temperature fall of ~ 4°C, from 22-19 °C recorded in fossil corals M2-146 and M1-Dc, if produced by SST changes, can be associated with a documented 8.2 K ybp global cooling event (Alley et al., 1997; Alley et al., 2005; Thomas et al., 2007; Wiersma, 2008; Daley et al., 2011; Fensterer et al., 2013; Winter et al., 2013, Boyd 2015; Vieten, 2017). This 8.2 K ybp cooling event has been well documented in different parts of the world by assessing the $\delta^{18}\text{O}$ from lake sediments (Mississippi Delta), ice cores (Greenland), and speleothems (Brazil, Oman, China, Puerto Rico, Venezuela Cuba and Trinidad). $\delta^{18}\text{O}$ from Greenland ice cores demonstrate the North Atlantic and European regions experienced a temperature drop of ~3 to ~6 °C at 8.2 K ybp. Speleothems collected from southern China, Oman, and in Brazil revealed an abrupt change in $\delta^{18}\text{O}$, interpreted as the 8.2 K ybp cooling event that lasted ~150 years (Chend et al., 2009). In the Caribbean, speleothems from western Cuba, Trinidad, Venezuela, and Puerto Rico have shown a temperature drop of ~3 to ~7°C around 8.2 K ybp that extended for approximately 100 to 160 years (Wiersma, 2008; Li et al., 2012; Fensterer et al., 2013; Winter et al., 2013; Vieten, 2017). The detection of this 8.2 K ybp cooling event in our SST data using coral fossil skeletons as a proxy

confirms the success of our technique to produce reliable Holocene SST data from Cañada Honda Corals in the Caribbean. This study cannot refine the duration of this event in the study area because our sampling and analytical strategy created a gap of ~100 years (from 8.166 (\pm .035) to 8.036 (\pm .026) K ybp) produced by the difference in ages between the two corals analyzed.

Table 5: Coral skeleton samples analyzed and analysis performed on each one of the sample.

Corals Collected	Analysis			
	Growth Rates	XRD	U-Th	Sr/Ca-SST
M2-146	x	x	x	x
M2-135	x	n/a	n/a	x
MZ-172	x	x	x	x
MZ-157	n/a	x	x	n/a
M3-1	x	x	x	x
M3-4	x	x	x	x
Modern coral	x	n/a	n/a	x

6.0 Conclusions

The conclusions of the study are listed below.

1. This study demonstrated the preservation of the Cañada Honda Holocene reef and its corals from early to mid-Holocene ($9.0 \text{ K} \pm 200$ to $5.6 \text{ K} \pm 29$ ybp) is suitable to gather SST records from that age in the Caribbean.
2. Growth rates acquired in this study from fossil *Orbicella sp. complex* corals (1.95 mm/year, 1.98 mm/year, 1.32 mm/year, 1.93 mm/year, 1.82 mm/year) are 5.38 to 6.02 mm/year in average lower than its modern counterparts (7.34 mm/year) at similar depths (10 meters) and suggest that the Cañada Honda paleo-reef environment was not a favorable one for the growth of the corals. Measurement of growth rates from modern coral suggest normal conditions for modern *Orbicella complex* on Barahona Bay. (Cuevas 2005; Greer et al., 2006). The slow of growth rate in M2, MZ and M3 facies at shallow water depth (< 12 meters), when compared to modern corals collected around the same depth <10 meters, fossil corals had suffered detrimental environmental conditions during this time. Two significant factors are proposed for to affect the calcification rates of the corals in Cañada Honda; (1) the high turbid waters produced by the input of sediments due to the high relief of Sierra Bahoruco and Sierra de Neiba mountain ranges and influx from Río Yaque del Sur into the paleo-embayment, which control the light penetration that reached the corals and therefore limit the efficiency of the symbiotic organism (*Zooxanthella*) within the coral (Hubbard et al., 1985) and (2) the influx of fresh water into the system from Río Yaque del Sur and abundant springs causing estuarine extreme changes in salinity.
3. XRD analyses indicate all samples used are aragonitic in composition. Although the detection limit of the analysis is 2% (Kontoyannis et al., 2015), the visual inspection of the coral skeletons and the success of most of the diverse analytical procedures performed serve as independent

assessments of the coral skeletons pristine preservation. Therefore, we conclude that no alteration is present in the coral skeletons studied and that the elemental values obtained from the corals represent the composition of the original components of the waters where the corals precipitated the calcium carbonate in its aragonitic composition.

4. U-Th dating acquired in this study were consistent with results from Taylor (1985) and Hubbard (2004), which suggests that Cañada Honda's longevity was from early through mid-Holocene.

5. A calibration equation to calculate SST from Sr/Ca ($Sr/Ca = -0.0676 * SST + 10.7867$) was produced in this study from a modern coral located close to the fossil coral exposure. This Sr/Ca-T equation provided better SST predictions for the corals in this area than the Flannery (2013) and Swart (2002) equations when compared with HADI SST measurements as reference. Flannery's (2013) SST from Sr/Ca in Cañada Honda corals resulted in slightly warmer SST values (see figures 24 to 33) relative to the SST values produced by our equation and by Swart (2002). Swart's (2002) SST from Sr/Ca in Cañada Honda corals resulted in cooler temperatures (see figures 24 to 33) relative to the SST values produced by our equation. Swart (2002) SST from Sr/Ca in Cañada Honda corals is outside the range (too cold) suitable for corals to survive (18 to 30 (°C), with optimum living conditions between 25 to 29 (°C)) (Budd et al., 1994; Medina et al., 1999; Cruz-Piñón et al., 2003; Woolstra et al., 2009). Calculations using the equation developed in this study produced values that are consistent with the living temperature conditions required for *Orbicella complex* corals. SST calculated using the equation developed in this study resulted in SST more similar to the SST produced by Flannery's (2013) equation

6. Additional Sr/Ca-SST data should be acquired in order to fill gaps obtained in this study, therefore, a more detailed Holocene SST from Cañada Honda Reef will be resulted.

References

- Alley, R. B., Mayewski, P. A., Sowers, T., Stuiver, M., Taylor, K. C., & Clark, P. U., 1997, Holocene climatic instability: A prominent, widespread event 8200 yr ago. *Geology*, 25, 483–486.
- Alley, R.B. and Ágústsdóttir, A.M., 2005. The 8k event: cause and consequences of a major Holocene abrupt climate change. *Quaternary Science Reviews*, 24(10-11), pp.1123-1149.
- Barnes, D. J., and M. J. Devereux. 1984, Productivity and calcification on a coral reef: a survey using pH and oxygen electrode techniques. *Journal of Experimental Marine Biology and Ecology* 79.3: 213-231.
- Barnes, D. J., and J. M. Lough. 1993, On the nature and causes of density banding in massive coral skeletons. *Journal of Experimental Marine Biology and Ecology* 167.1: 91-108.
- Barnes, D. J., and J. M. Lough. 1992, Systematic variations in the depth of skeleton occupied by coral tissue in massive colonies of *Porites* from the Great Barrier Reef. *Journal of Experimental Marine Biology and Ecology* 159.1: 113-128.
- Beck, J.W., Edwards, L.R., Ito, E., Taylor, F.W., Recy, J., Rougerie, F., Joannot, P., Henin, C., 1992, Sea-surface temperature from coral skeletal strontium/calcium ratios, *Science*, 257, 644-647.
- Boyd, M., 2015. Speleothems from warm climates: Holocene records from the Caribbean and Mediterranean regions (Doctoral dissertation, Department of Physical Geography, Stockholm University).
- Boyin Huang, Viva F. Banzon, Eric Freeman, Jay Lawrimore, Wei Liu, Thomas C. Peterson, Thomas M. Smith, Peter W. Thorne, Scott D. Woodruff, and Huai-Min Zhang, 2015: Extended Reconstructed Sea Surface Temperature Version 4 (ERSST.v4). Part I: Upgrades and Intercomparisons. *J. Climate*, 28, 911–930.
- Brachert, T. C., M. Reuter, K. F. Kroeger, and J. M. Lough, 2006, Coral growth bands: A new and easy to use paleothermometer in paleoenvironment analysis and paleoceanography (late Miocene, Greece), *Paleoceanography*, 21, PA4217, doi:10.1029/2006PA001288.
- Buck, D.G., Brenner, M., Hodell, D.A., Curtis, J.H., Martin, J.B., Pagani, M., 2005, Physical and chemical properties of hypersaline Lago Enriquillo, Dominican Republic, *Verh. Internat. Verein. Limnol.*, 29, 7p.
- Budd, A., Stemann, T., & Johnson, K. 1994, Stratigraphic distributions of genera and species of Neogene to Recent Caribbean reef corals. *Journal of Paleontology*, 68(5), 951-977. <https://doi:10.1017/S0022336000026585>

- Chend, H., Fleitmann, D., Edwards, R.L., Wang, X., Cruz, F.W., Auler, A.S., Mangini, A., Wang, Y., Kong, X., Burns, S.J., Matter, A., 2009, Timing and structure of the 8.2kyr B.P. event inferred from $\delta^{18}\text{O}$ records of stalagmites from China, Oman and Brazil.
- Cobb, K.M., Charles, C.D., Cheng, H., Kastner, M., Edwards, R.L., 2003, U/Th-dating living and young fossil corals from the central tropical Pacific, *Earth and Planetary Science Letters*, 210, 91-103.
- Corrège, Thierry. 2006, Sea surface temperature and salinity reconstruction from coral geochemical tracers. *Palaeogeography, Palaeoclimatology, Palaeoecology* 232.2 (20): 408-428.
- Cortés, J., and M. J Risk. 1985. A reef under siltation stress: Cahuita, Costa Rica. *Bulletin of Marine Science* 36: 339-356.
- Cruz-Piñón, G., J. P., Carricart-Ganivet, and J. Espinoza-Avalos 2003, Monthly skeletal extension rates of the hermatypic corals *Montastrea annularis* and *Montastrea faveolata*: biological and environmental controls. *Marine Biology* 143.3: 491-500.
- Cuevas, D., Sherman, C.E., Ramirez, W., Díaz, V., Hubbard, D.K., 2005 Development of Mid-Holocene Cañada Honda fossil reef, Dominican Republic: Preliminary results and implications to modern trends of reef degradation in high sedimentation environments, 17th Caribbean Geological Conference in San Juan, Puerto Rico
- Cuevas, D. N., Sherman, C. E., Ramírez, W., & Hubbard, D. K., 2009, Coral growth rates from the Holocene Cañada Honda fossil reef, Southwestern Dominican Republic: Comparisons with modern counterparts in high sedimentation settings. *Caribbean journal of science*, 45(1), 94-109.
- Daley, T. J., Thomas, E. R., Holmes, J. a., Street-Perrott, F. A., Chapman, M. R., Tindall, J. C., ... Roberts, C. N. 2011, The 8200yr BP cold event in stable isotope records from the North Atlantic region. *Global and Planetary Change*, 79, 288–302.
- Delanoy, R. A., & Méndez-Tejeda, R. 2017, Hydrodynamic Study of Lake Enriquillo in Dominican Republic. *Journal of Geoscience and Environment Protection*, 5(05), 115
- Downs, R.T., 2006, The RRUFF Project: an integrated study of the chemistry, crystallography, Raman and infrared spectroscopy of minerals. Program and Abstracts of the 19th General Meeting of the International Mineralogical Association in Kobe, Japan, O03-13.
- Ellis J, Solander DC., 1786, *The natural history of many curious and common zoophytes*. London: Benjamin White & Son. 208 pp., 63 pls.
- Enmar R., Stein, M., Bar-Matthews, M., Sass, E., Katz, A., Lazar, B., 2000, Diagenesis in live corals from the Gulf of Aqaba: I. The effect on paleo-oceanography tracers, *Geochim. Cosmochim. Acta*, 64, 3123–3132.

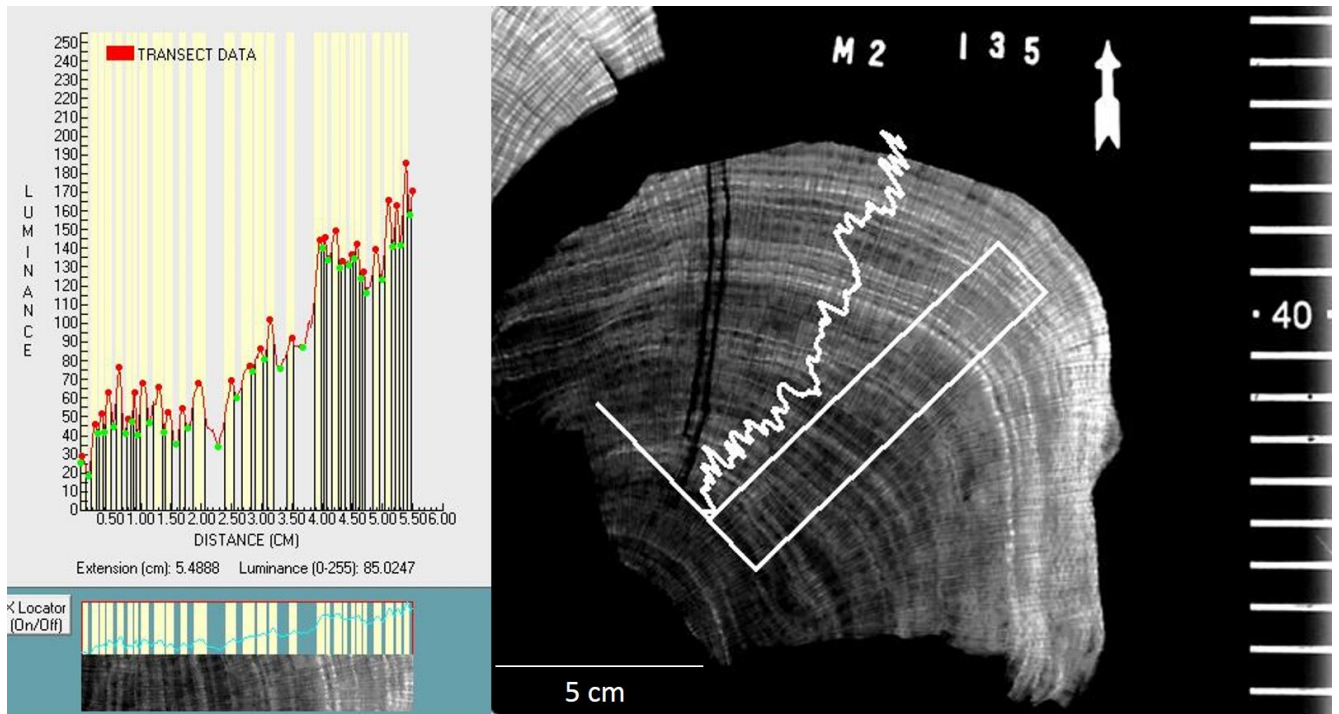
- Fairbanks, R. G., and R. E. Dodge. 1979. Annual periodicity of the 18 O/ 16 O and 13 C/ 12 C ratios in the coral *Montastraea annularis*. *Geochimica et Cosmochimica Acta* 43:1009-1020.
- Felis, T. and Pätzold, J., 2004, Climate reconstructions from annually banded corals. *Global environmental change in the ocean and on land*, pp.205-227.
- Fensterer, C., Scholz, D., Hoffman, D.L., Spötl, C., Schröder-Ritzrau, A., Horn, C., Pajón, J.M., Mangini, A., 2013, Millennial-scale climate variability during the last 12.5 ka recorded in a Caribbean speleothem, *Earth and Planetary Science Letters*, 361, 143-151.
- Flannery, J.A., Poore, R.Z., 2013, Sr/Ca proxy sea-surface temperature reconstructions from modern and Holocene *Montastrea faveolata* specimens from the Dry Tortugas National Park, Florida, U.S.A., *Journal of Coastal Research*, 63, 20-31. Karl, Thomas R., and Kevin E. Trenberth. "Modern global climate change." *science* 302.5651 (2003): 1719-1723.
- Jennifer, A., Julie, N., Richard, Z. and Kristine, L., 2016. Multi-species coral Sr/Ca based sea-surface temperature reconstruction using *Orbicella faveolata* and *Siderastrea siderea* from the Florida Straits. *Palaeogeography, palaeoclimatology, palaeoecology*.
- Gaetani G. A., Cohen A.L., Wang Z., Crucius J., 2011, Rayleigh-based, multi-element coral thermometry: A biomineralization approach to developing climate proxies. *Geochimica et Cosmochimica Acta*, Vol. 75, p. 1920-1932.
- Giry, C., Felis, T., Kölling, M., Scholz, D., Wei, W., Lohmann, G., Scheffers, S., 2012, Mid-to late Holocene changes in tropical Atlantic temperature seasonality and interannual to multidecadal variability documented in southern Caribbean corals, *Earth and Planetary Science Letters*, 331-332, 187-200.
- Gladfelter, E. H., Monahan, R. K. and Gladfelter W. B., 1978, Growth rates of five reef-building corals in the Northeastern Caribbean. *Bulletin of Marine Science* 28(4): 728-734.
- Greer, L. and Swart, P.K., 2006, Decadal cyclicity of regional mid-Holocene precipitation: Evidence from Dominican coral proxies. *Paleoceanography*. Vol. 21.
- Grottoli, A.G, 2001, Climate: Past Climate from Corals, in: *Encyclopedia of Ocean Sciences* [eds. Steele, J., Thorpe, S., Turekian, K.], Academic Press, London p. 2098-2107.
- Haase-Schramm, A., Boehm, F., Eisenhauer, A., Joachimski, M.M., Reitner, J. and Dullo, W.C., 2001, December. Sr/Ca ratios and oxygen isotopes from sclerosponges: Temperature and salinity records from the Caribbean mixed layer and thermocline. In *AGU Fall Meeting Abstracts*
- Helmle, K.P., K.E. Kohler, and R.E. Dodge 2002 "Relative Optical Densitometry and The Coral X-radiograph Densitometry System: CoralXDS" Presented Poster (omitted from

- abstract book, but included in program), Int. Soc. Reef Studies 2002 European Meeting. Cambridge, England. Sept. 4-7.
- Hubbard, D. K., & Scaturro, D. 1985. Growth rates of seven species of scleractinean corals from Cane Bay and Salt River, St. Croix, USVI. *Bulletin of Marine Science*, 36(2), 325-338.
- Hubbard, D.K., Ramirez, W., Cuevas, D., 2004. A preliminary model of Holocene coral-reef development in the Enriquillo Valley, SW Dominican Republic. Abstract. *GSA Abstracts with Programs*, Vol. 36, No. 5, p. 291.
- Hubbard, D.K., Ramirez, W., Cuevas D., Erickson, T., Estep, A., 2008, Holocene reef accretion along the north side of Bahia Enriquillo (western Dominican Republic): unique insights into patterns of reef development in response to sea-level rise, *Proceedings of the 11th International Coral Reef Symposium*, Ft. Lauderdale, Florida, 43-47.
- Kontoyannis, C. G. (2015). Calcium Carbonate Phase Analysis Using XRD and FT – Raman Spectroscopy spectroscopy, (January 2000). <https://doi.org/10.1039/a908609i>
- Lachniet, M. S. (2009). Climatic and environmental controls on speleothem oxygen-isotope values. *Quaternary Science Reviews*, 28(5–6), 412–432. <https://doi.org/10.1016/j.quascirev.2008.10.021>
- Leder, J.J., Swart, P.K., Szmant, A., Dodge, R.E., 1996, The origin of variations in the isotopic record of Scleractinian corals; I Oxygen, *Geochim. Cosmochim. Acta*, 60, 2857-2870.
- Li, W.-X., Lundberg, J., Dickin, A. P., Ford, D. C., Schwarcz, H. P., McNutt, R., & Williams, D. (1989). High-precision mass-spectrometric uranium-series dating of cave deposits and implications for palaeoclimate studies. *Nature*, 339, 534–536.
- Mann, P., Lawrence, S., 1991, Petroleum potential of Southern Hispaniola: *Journal of Petroleum Geology*, 14, No. 3, 291-308.
- Mann, P., Taylor, F. W., Burke, K., & Kulstad, R., 1984, Subaerially exposed Holocene coral reef, Enriquillo Valley, Dominican Republic. *Geological Society of America Bulletin*, 95(9), 1084-1092.
- Medina, M., Weil, E., & Szmant, A. M. (1999). Examination of the *Montastraea annularis* Species Complex (Cnidaria : Scleractinia) Using ITS and COI Sequences, 89–97.
- Mendez-Tejeda, R., Rosado, G., Rivas, D. V., & Infante, M. I. 2016. Physicochemical analysis of Lake Enriquillo in Dominican Republic. *Open Science Journal*, 1(4).
- Morelock, J., Capella, J., Garcia, J. R., & Barreto, M. 2000, PUERTO RICO-Seas at the Millennium. *Seas at the millennium*. Oxford University Press, London.

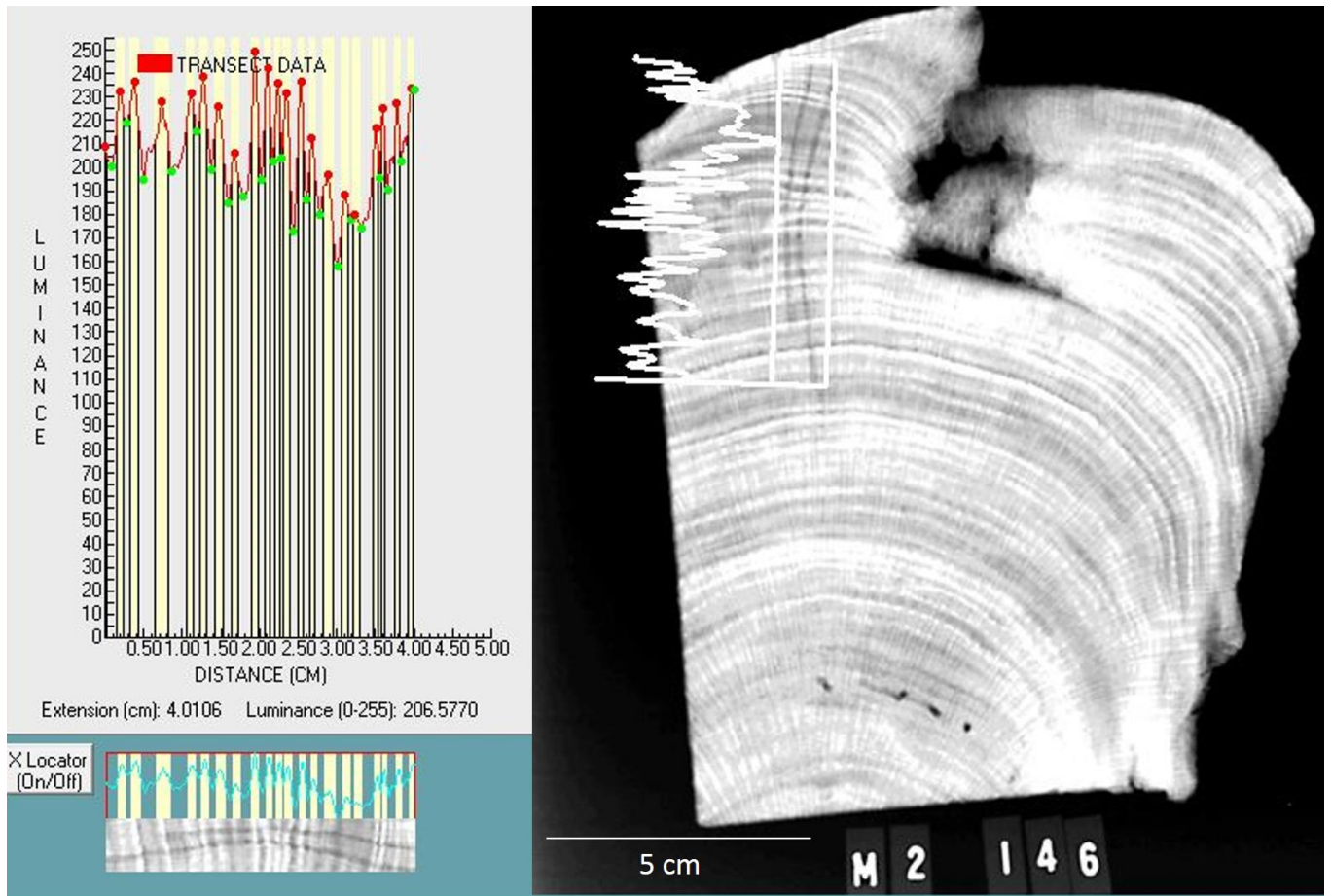
- Morales, J., 2014, Reconstructing Sea Surface Temperatures during the early-mid Holocene from a reef exposure in Cañada Honda, Enriquillo Valley, Dominican Republic. [MS Thesis], University of Puerto Rico, Mayaguez. 97p
- NOAA, 2011a. National Data Buoy Center. URL: <http://www.ndbc.noaa.gov>; accessed on June 18, 2017.
- Rayner, N. A., D. E. Parker, E. B. Horton, C. K. Folland, L. V. Alexander, D. P. Rowell, E. C. Kent, and A. Kaplan, 2003, Global analyses of sea surface temperature, sea ice, and night marine air temperature since the late nineteenth century *Journal of Geophysical Research*, 108.
- Rowan, R., & Knowlton, N., 1995, Intraspecific diversity and ecological zonation in coral-algal symbiosis. *Proceedings of the National Academy of Sciences*, 92(7), 2850-2853.
- Saenger, C., Cohen, A.L., Oppo D.W., Hubbard, D, 2008, Interpreting sea surface temperature from strontium/calcium ratios in *Montastraea* corals: Link with growth rate and implications for proxy reconstructions, *Paleoceanography*., Vol. 23
- Sayani, H.R., Cobb, K.M., Cohen, A.L., Crawford, E.W., Nurhati, I.S., Dunbar, D.B., Rose, K.A., Zaunbrecher, L.K., 2011, Effect of diagenesis on paleoclimate reconstructions from modern and young fossil corals, *Geochimica et Cosmochimica Acta*, 75, 6361-6373.
- Smith, S. V., Buddemeier, R. W., Redalje, R. C., & Houck, J. E., 1979. Strontium-calcium thermometry in coral skeletons. *Science*, 204(4391), 404-407.
- Swart, P.K., Elderfield, H., Greaves, M.J., 2002, A high-resolution calibration of Sr/Ca thermometry using the Caribbean coral *Montastraea annularis*, *Geochem. Geophys. Geosyst.*, 3, 11, 8402.
- Taylor, F.W., Mann, P., Valastro, S., Burke, K., 1985, Stratigraphy and radiocarbon chronology of a sub aerially exposed Holocene coral reef, Dominican Republic, *The Journal of Geology*, 93, No. 3, 311-332.
- Thomas, E.R., Wolff, E.W., Mulvaney, R., Steffensen, J.P., Johnsen J., Arrowsmith, C., White, J.W.C., Vaughn, B., Popp, T., 2007, The 8.2ka event from Greenland ice cores, *Quaternary Science Reviews*, 26, 70-81.
- Toller, W.W., Rowan, R., & Knowlton, N., 2001, Zooxanthellae of the *Montastraea annularis* species complex: patterns of distribution of four taxa of *Symbiodinium* on different reefs and across depths. *The Biological bulletin*, 201 3, 348-59.
- Torres, J., and Morelock, J., 2002, Effect of terrigenous sediment influx on coral cover and linear extension rates of three Caribbean massive coral species. *Caribbean Journal of Science*, 38(3-4): 222-229.

- Vaughan TW., 1918, Some shoal-water from Murray Island (Australia), Cocos-Keeling Islands, and Fanning Island. Papers Department of Marine Biology, Carnegie Institute of Washington, Publication No. 213 9: 49-234, pl. 20-90.
- Vieten, R., Warken, S., Winter, A., Scholz, D., Black, D., Zanchettin, D. and Miller, T.E., 2017, April. Abrupt drying events in the Caribbean related to large Laurentide meltwater pulses during the glacial-to-Holocene transition. In EGU General Assembly Conference Abstracts (Vol. 19, p. 1450).
- Vieten, R., 2017, ABRUPT CLIMATE EVENTS IN THE CARIBBEAN. [PhD Thesis], University of Puerto Rico, Mayaguez.
- Vize, P. D., 2006, Deepwater broadcast spawning by *Montastraea cavernosa*, *Montastraea franksi*, and *Diploria strigosa* at the Flower Garden Banks, Gulf of Mexico. *Coral Reefs*, 25(1), 169-171.
- Voolstra, C. R., Schnetzer, J., Peshkin, L., Randall, C. J., Szmant, A. M., & Medina, M. 2009, *Montastraea faveolata*, 9, 1–9. <https://doi.org/10.1186/1471-2164-10-627>
- Weinstein, D. K., Sharifi, A., Klaus, J. S., Smith, T. B., Giri, S. J., & Helmle, K. P., 2016, Coral growth, bioerosion, and secondary accretion of living orbicellid corals from mesophotic reefs in the US Virgin Islands. *Marine Ecology Progress Series*, 559, 45-63
- Wiersma, A.P., 2008, Character and causes of the 8.2ka climate event – Comparing coupled climate model results and palaeoclimate reconstructions, [Ph.D. thesis], Vrije Universiteit Amsterdam.
- Winsor, K., Curran, H.A., Greer, L., Glumac, B., 2006, Paleoenvironmental implications of mid-Holocene serpullid tube/tufa mounds and underlying coral colonies, Enriquillo Valley, Dominican Republic. 2006 Philadelphia Annual Meeting.
- Winter, A., Ishioroshi, H., Watanabe, T., Oba, T., Christy, J., 2000, Caribbean Sea surface temperatures: Two-to-three degrees cooler than present during the Little Ice Age. *Geophysical Research Letters* 27.20: 3365-3368.
- Winter, A., Vieten, R., Miller, T., Mangini, A., Scholz, D., 2013, 8.2ky event associated with high precipitation in the eastern Caribbean, American Geophysical Union, Fall Meeting 2013, abstract #PP31B-1870.
- Xu, B., Poduska, K., M., 2014, Linking crystal structure with temperature-sensitive vibrational modes in calcium carbonate minerals. *Physical Chemistry Chemical Physics*, 16(33), 17634-17639.

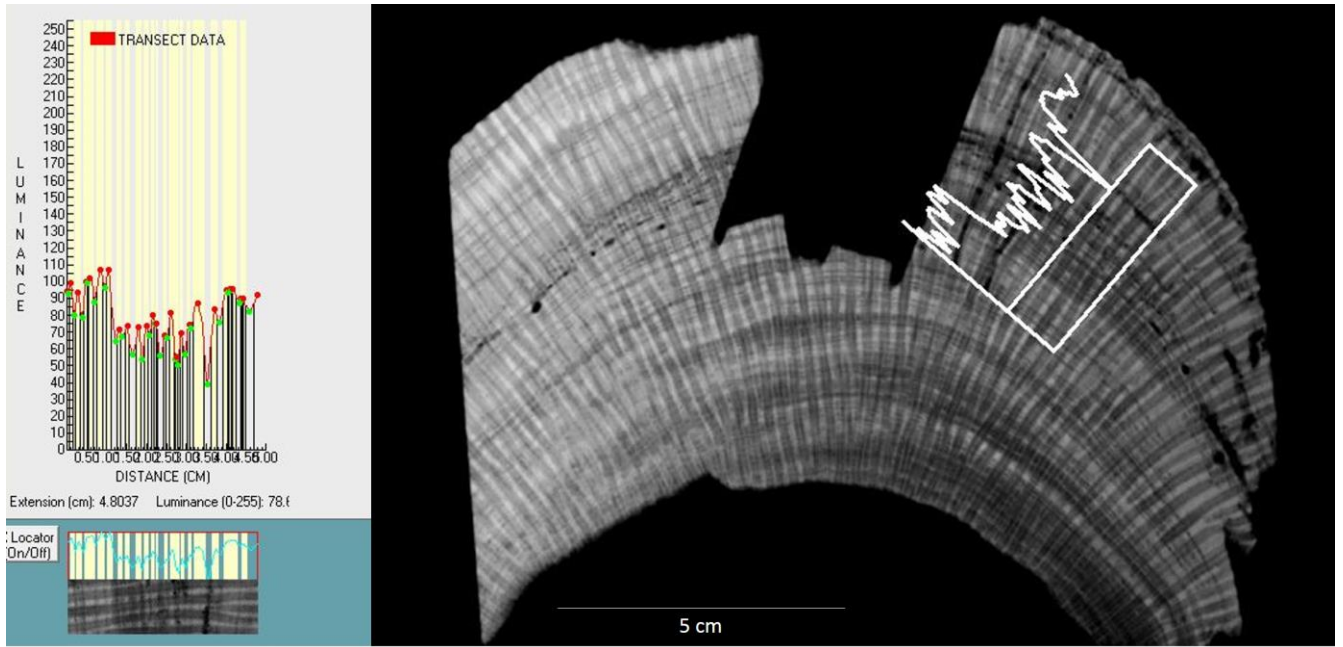
Appendix



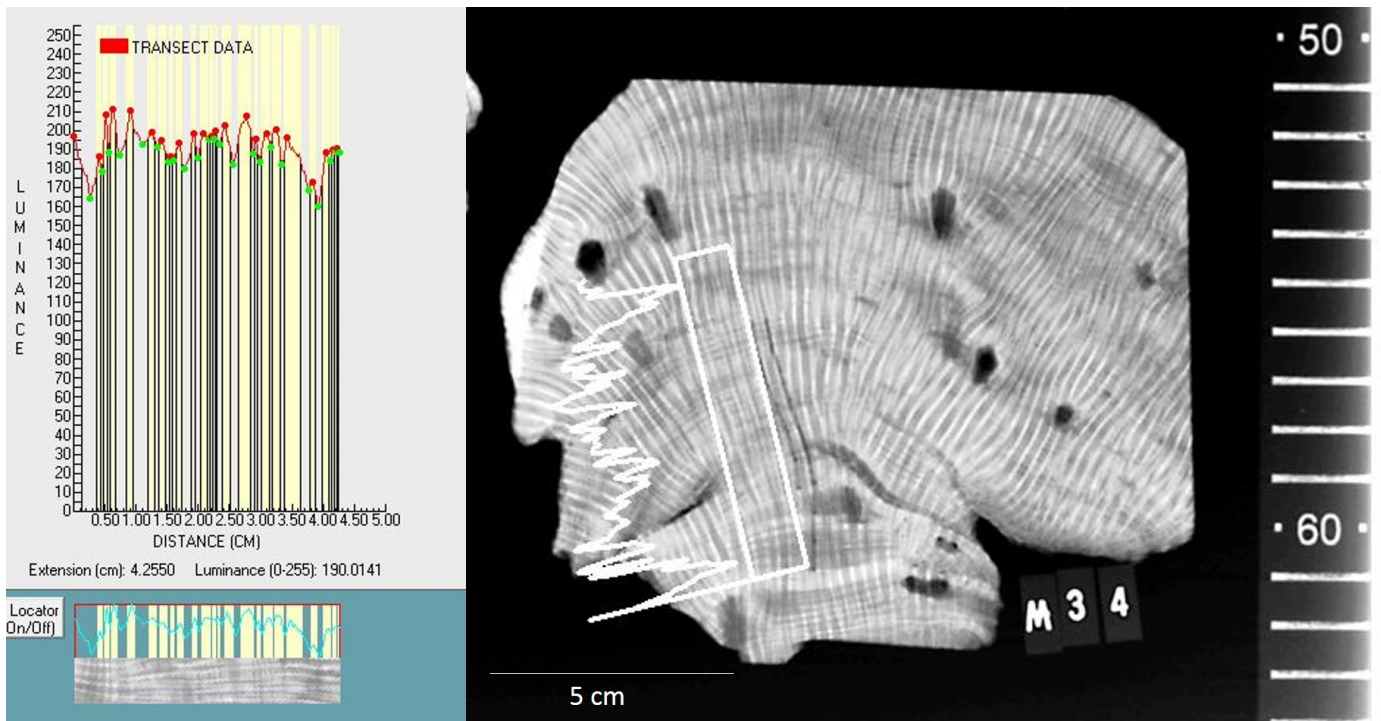
Appendix 1: Densitometry analysis of M2-135 fossil coral sample. This sample showed a growth rate of 1.95 mm/year.



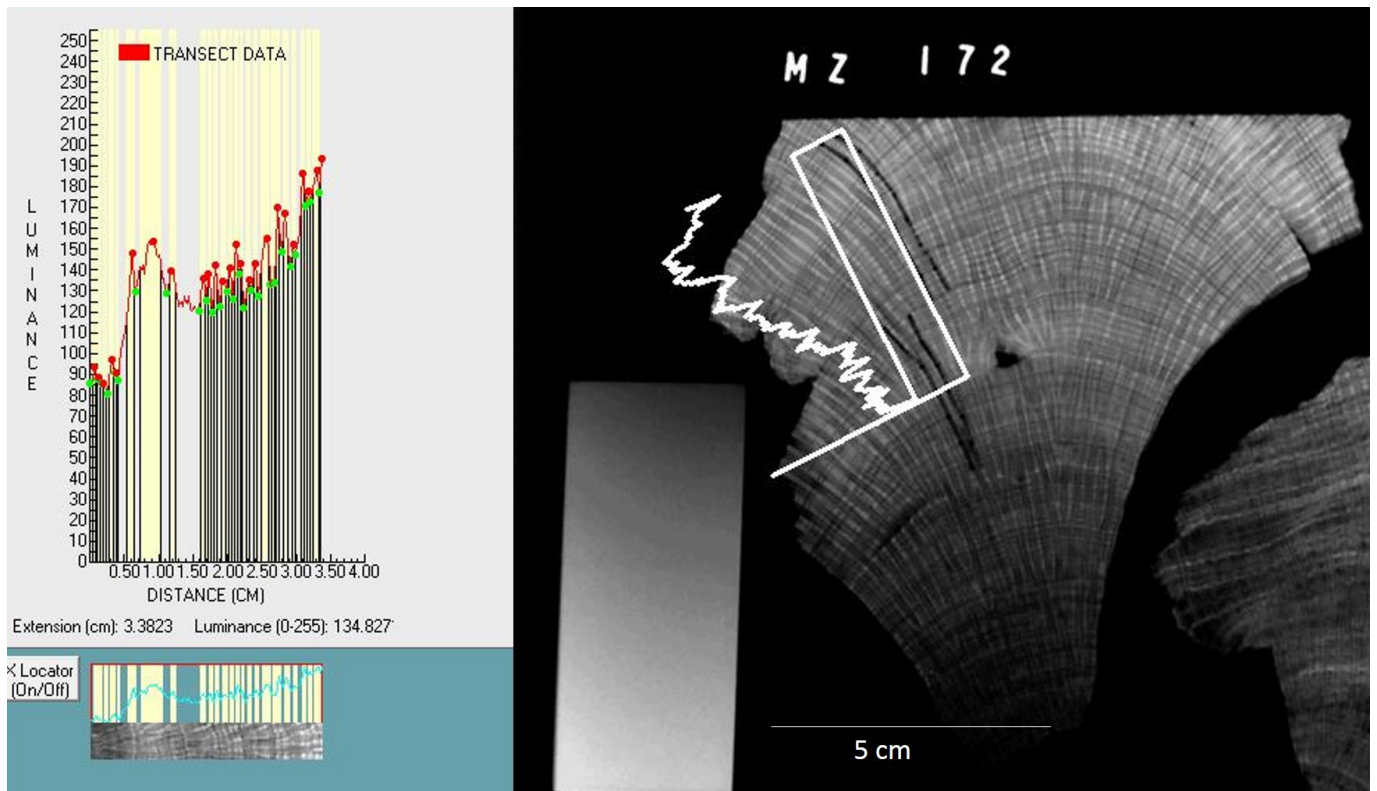
Appendix 2: Densitometry analysis of M2-146 coral sample. Growth rate acquired for this sample is 1.98 mm/year.



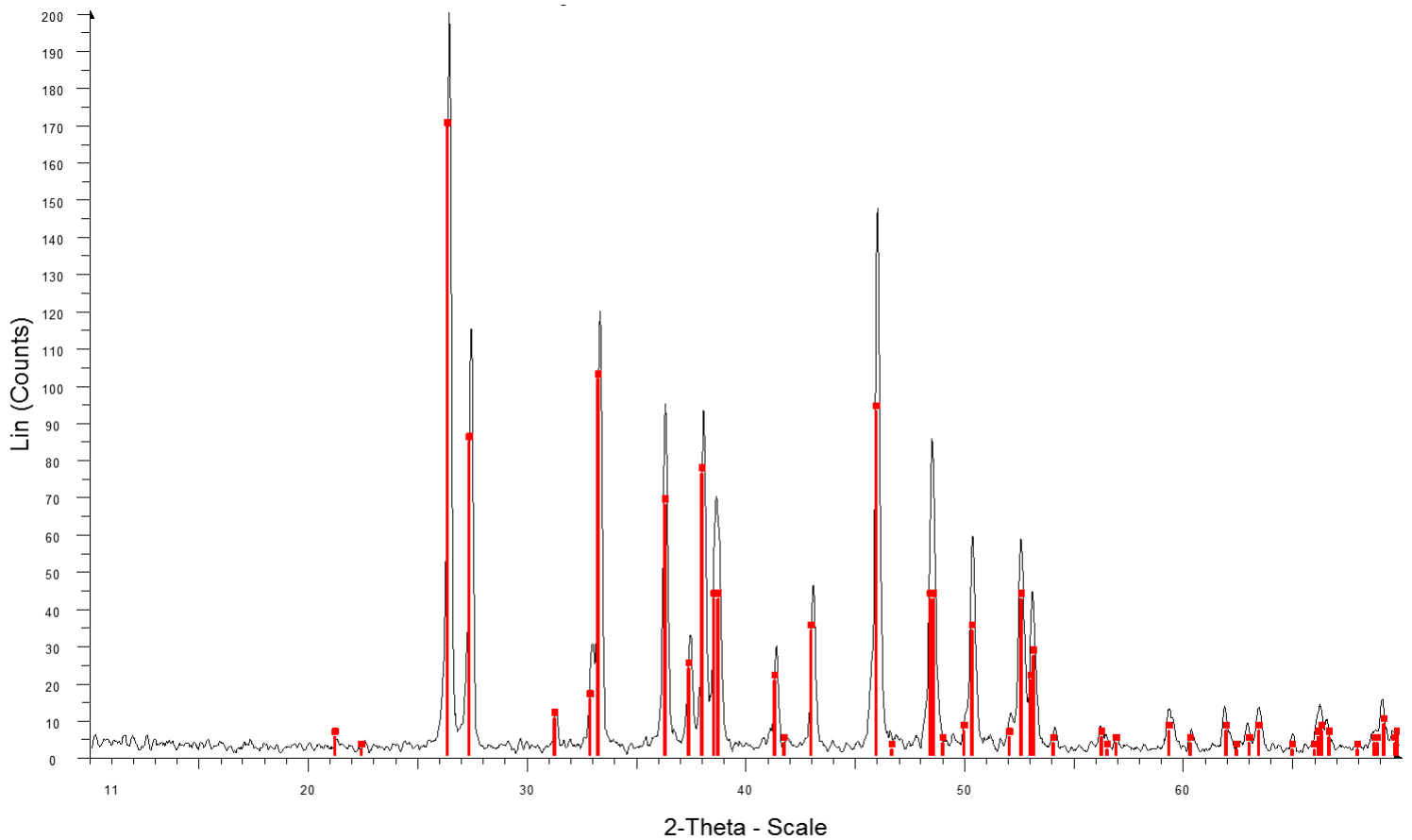
Appendix 3: Densitometry analysis of M3-1 coral sample. This coral exhibits a growth rate of 1.93 mm/year



Appendix 4: Densitometry analysis of M3-4 coral sample. This coral showed an average growth rate of 1.82mm/year.

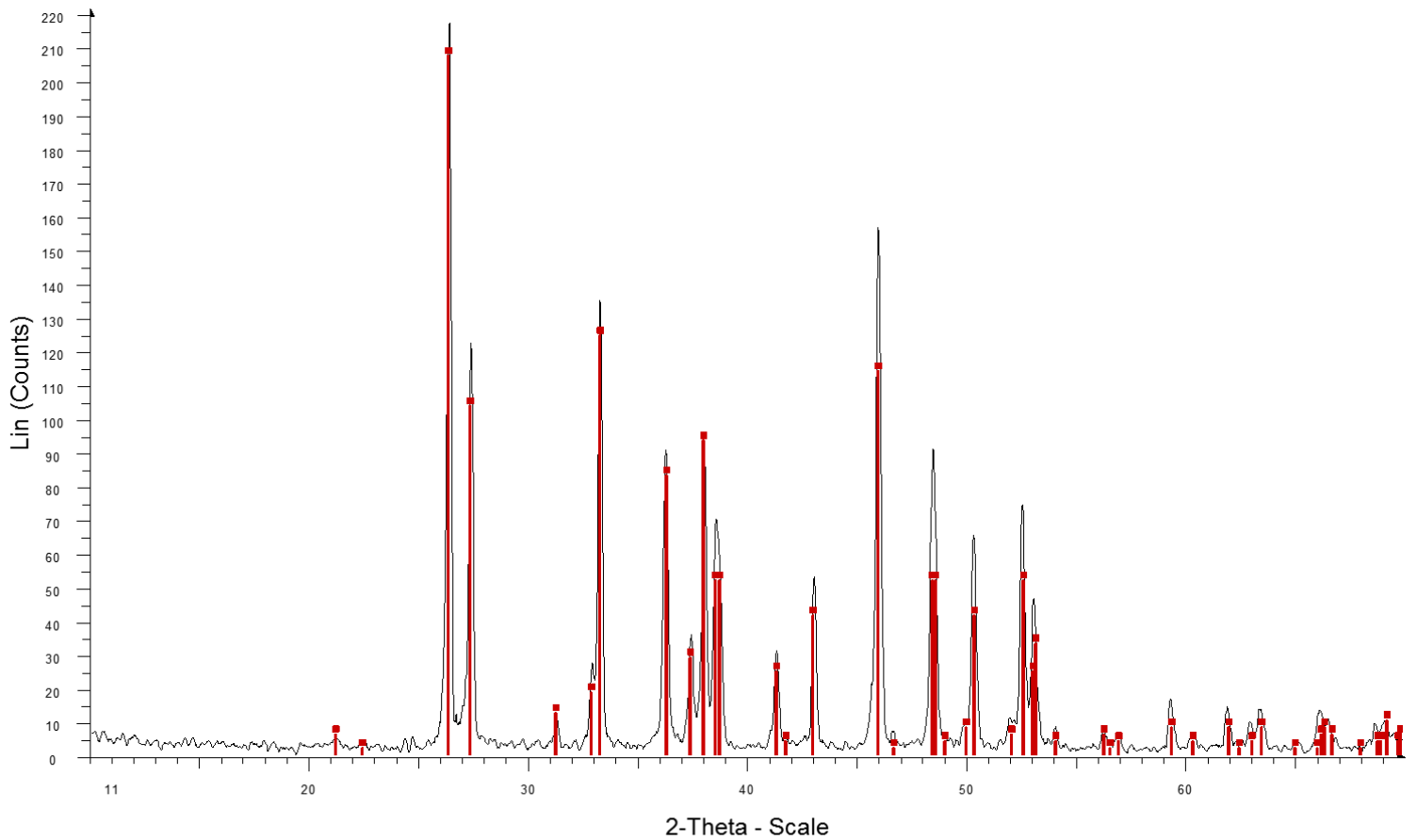


Appendix 5: Densitometry analysis of MZ-172 coral sample. Average growth rate for this coral was 1.32 mm/year.



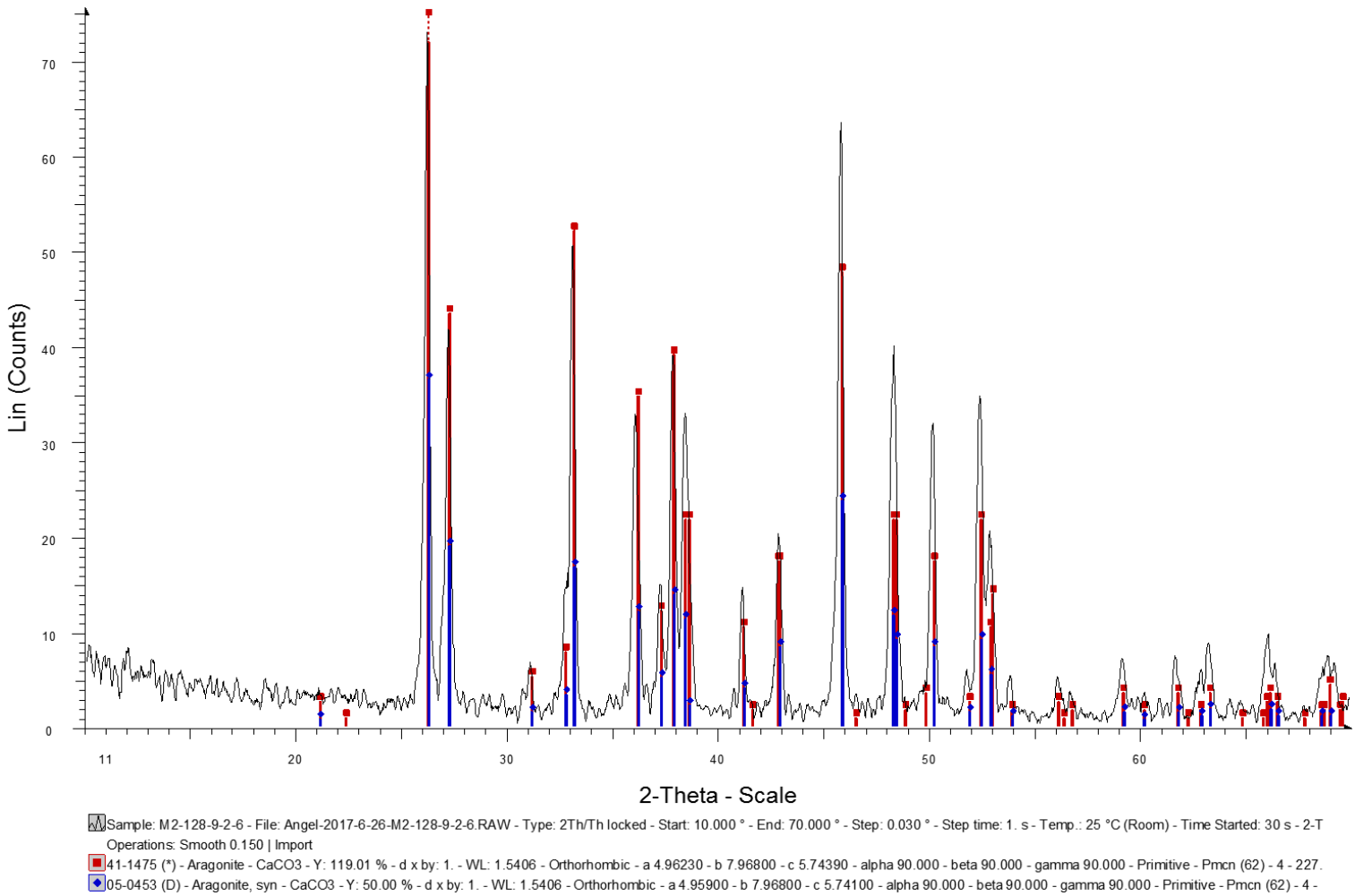
Sample: MZ-157-3-0-6 - File: Angel-2017-6-26-MZ-157-3-0-6.RAW - Type: 2Th/Th locked - Start: 10.000 ° - End: 70.000 ° - Step: 0.030 ° - Step time: 1. s - Temp.: 25 °C (Room) - Time Started: 16 s - 2-T
 Operations: Smooth 0.150 | Import
 41-1475 (*) - Aragonite - CaCO₃ - Y: 84.09 % - d x by: 0.9977 - WL: 1.5406 - Orthorhombic - a 4.96230 - b 7.96800 - c 5.74390 - alpha 90.000 - beta 90.000 - gamma 90.000 - Primitive - Pmcn (62) - 4 - 2

Appendix 6: XRD results of MZ-157 coral sample.

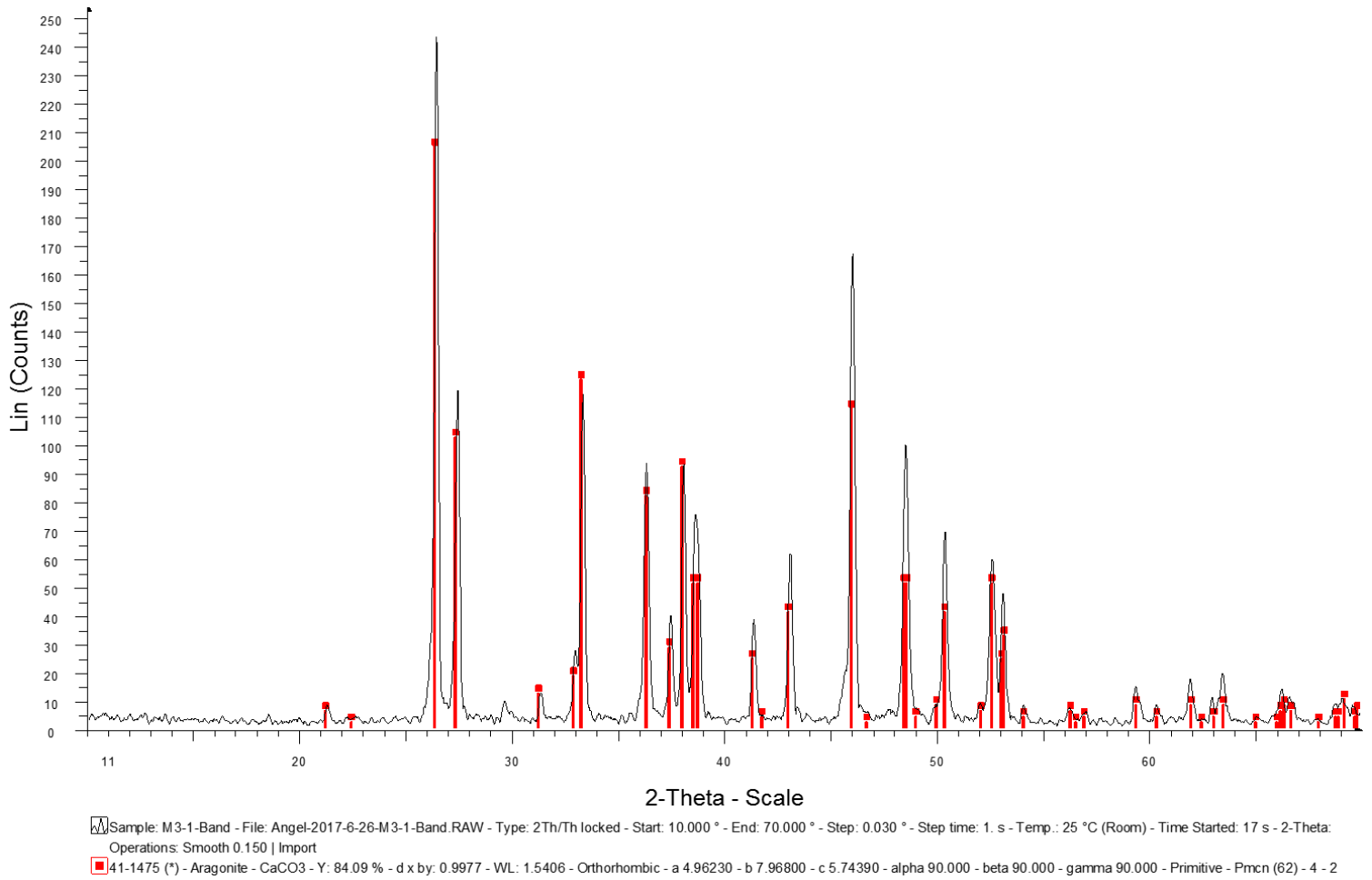


Sample: M3-4 - File: Angel-2017-6-26-M3-4.RAW - Type: 2Th/Th locked - Start: 10.000 ° - End: 70.000 ° - Step: 0.030 ° - Step time: 1. s - Temp.: 25 °C (Room) - Time Started: 16 s - 2-Theta: 10.000 ° - T
 Operations: Smooth 0.150 | Import
 41-1475 (*) - Aragonite - CaCO₃ - Y: 95.45 % - d x by: 0.9977 - WL: 1.5406 - Orthorhombic - a 4.96230 - b 7.96800 - c 5.74390 - alpha 90.000 - beta 90.000 - gamma 90.000 - Primitive - Pmcn (62) - 4 - 2

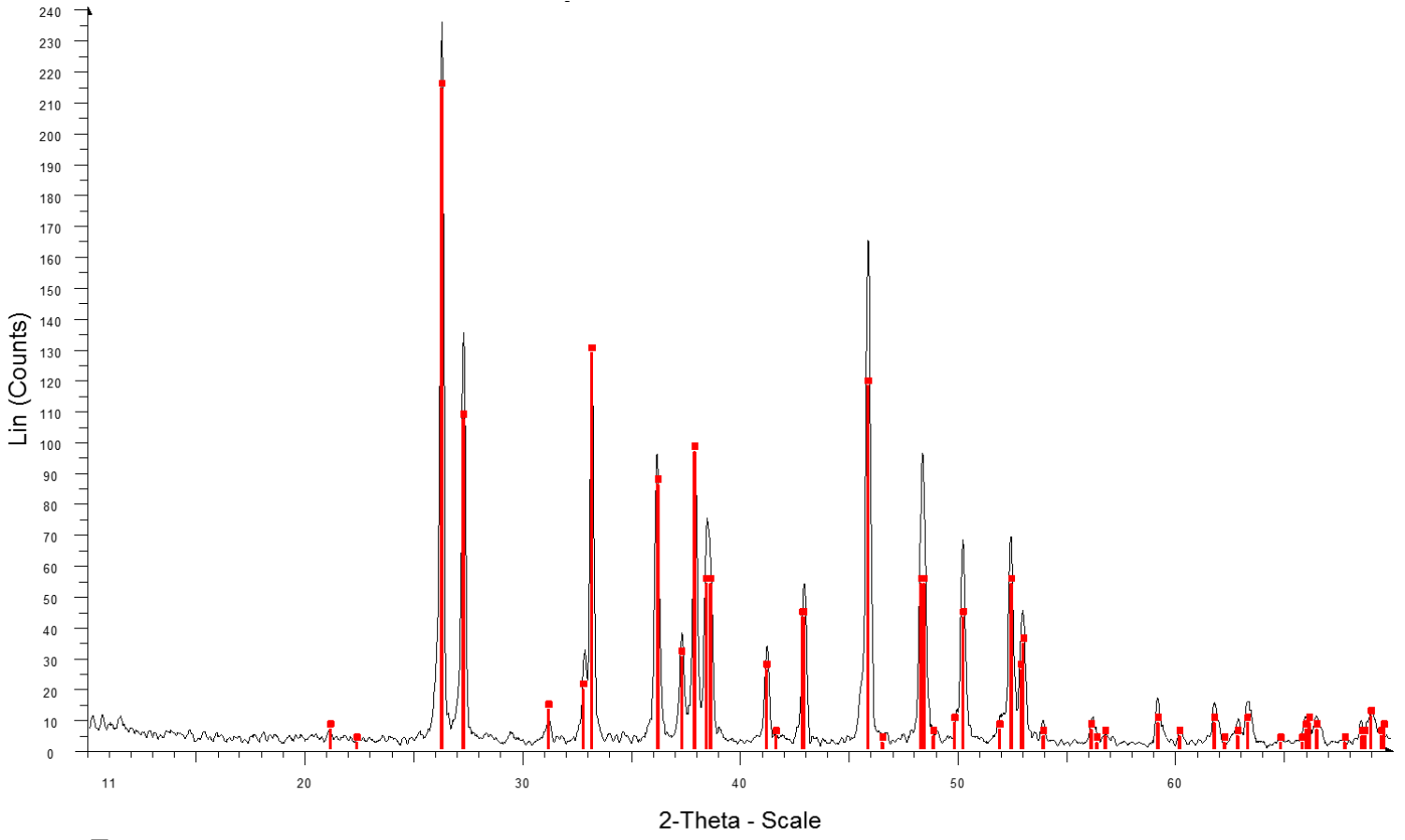
Appendix 7: XRD results of M3-4 coral sample.



Appendix 8: XRD results of M2-146 coral sample.

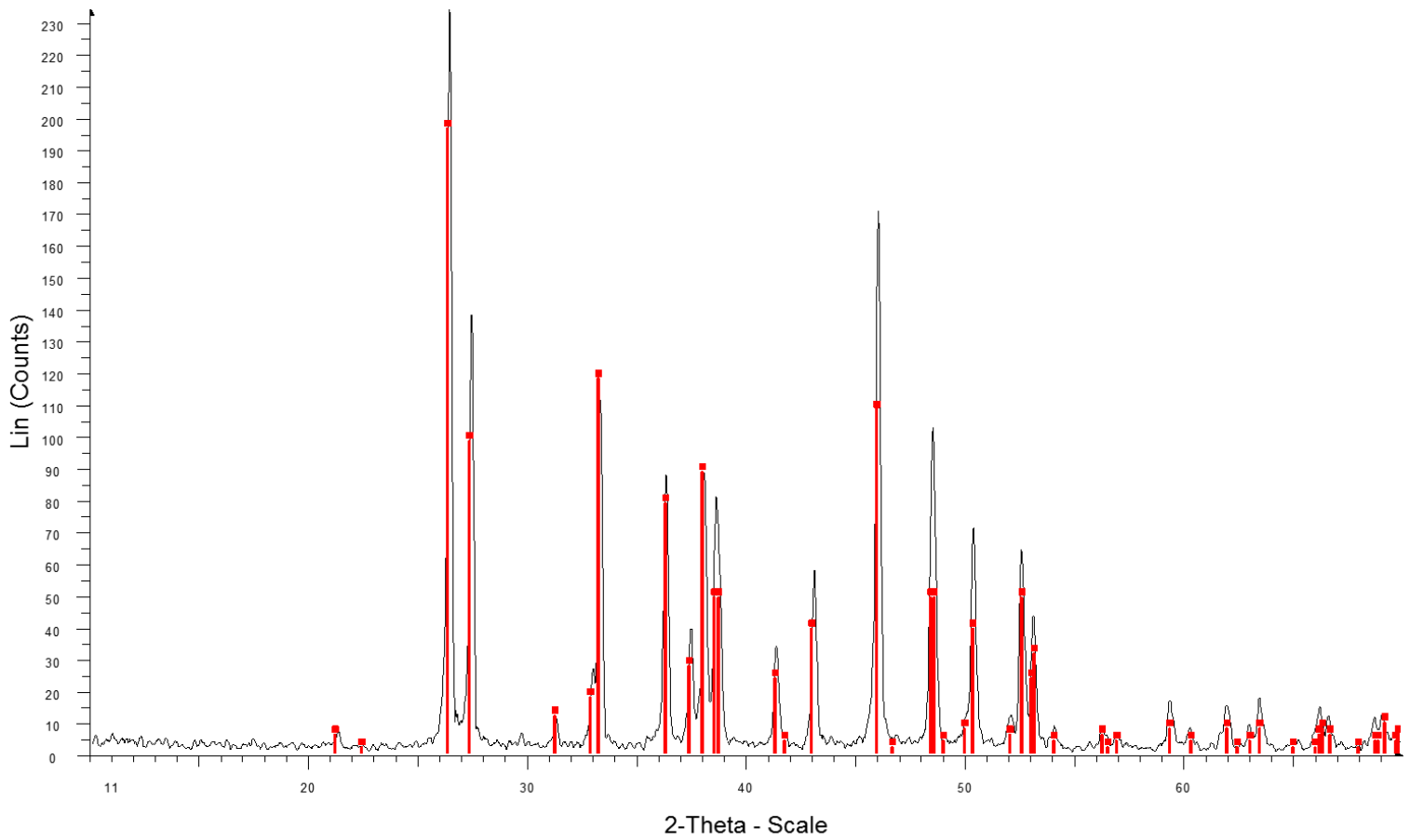


Appendix 9: XRD results of M3-1 band coral sample.



Sample: M3-1-Bottom - File: Angel-2017-6-26-M3-1-Bottom.RAW - Type: 2Th/Th locked - Start: 10.000 ° - End: 70.000 ° - Step: 0.030 ° - Step time: 1. s - Temp.: 25 °C (Room) - Time Started: 16 s - 2-The
 Operations: Smooth 0.150 | Import
 41-1475 (*) - Aragonite - CaCO3 - Y: 90.91 % - d x by: 1. - WL: 1.5406 - Orthorhombic - a 4.96230 - b 7.96800 - c 5.74390 - alpha 90.000 - beta 90.000 - gamma 90.000 - Primitive - Pmcn (62) - 4 - 227.1

Appendix 10: XRD results of M3-1 bottom coral sample.



Sample: M3-1-Top - File: Angel-2017-6-26-M3-1-Top.RAW - Type: 2Th/Th locked - Start: 10.000 ° - End: 70.000 ° - Step: 0.030 ° - Step time: 1. s - Temp.: 25 °C (Room) - Time Started: 16 s - 2-Theta: 10.
 Operations: Smooth 0.150 | Import
 41-1475 (*) - Aragonite - CaCO3 - Y: 84.09 % - d x by: 0.9977 - WL: 1.5406 - Orthorhombic - a 4.96230 - b 7.96800 - c 5.74390 - alpha 90.000 - beta 90.000 - gamma 90.000 - Primitive - Pmcn (62) - 4 - 2

Appendix 11: XRD results of M3-1 top coral sample.

Appendix 12: Sample M3-1 data.

Chronology M3 1	Schrag Sr/Ca (mMol/Mol)	SST this study M3-1	SST Swart M3-1	SSTFlannery13M3-1
0.3	8.99	26.57	24.93	30.97
0.6	8.62	32.01	32.74	40.36
0.9	8.92	27.61	26.43	32.78
1.2	8.77	29.83	29.61	36.60
1.5	8.97	26.85	25.33	31.46
1.8	9.23	23.05	19.88	24.91
2.1	9.20	23.45	20.45	25.60
2.4	9.22	23.22	20.13	25.21
2.7	9.16	24.03	21.29	26.60
3	9.17	23.95	21.17	26.46
3.3	9.14	24.29	21.66	27.04
3.6	9.20	23.40	20.39	25.52
3.9	8.88	28.25	27.35	33.88
4.2	8.90	27.88	26.81	33.24
4.5	8.99	26.64	25.04	31.10
4.8	8.98	26.74	25.17	31.27
5.1	9.01	26.31	24.56	30.53
5.4	8.95	27.18	25.81	32.03
5.7	8.87	28.31	27.43	33.98
6	8.90	27.91	26.86	33.30
6.3	8.98	26.72	25.15	31.24
6.6	8.98	26.67	25.08	31.15
6.9	8.93	27.41	26.14	32.43
7.2	8.87	28.35	27.49	34.05
7.5	9.02	26.10	24.26	30.16
7.8	8.96	27.02	25.58	31.75
8.1	9.08	25.24	23.02	28.68
8.4	9.03	26.06	24.20	30.10
8.7	9.00	26.43	24.73	30.74
9	9.04	25.83	23.87	29.70
9.3	9.14	24.31	21.69	27.08
9.6	9.16	24.09	21.38	26.71
9.9	9.12	24.61	22.12	27.60
10.2	9.13	24.53	22.00	27.46
10.5	9.14	24.43	21.86	27.29
10.8	9.06	25.58	23.51	29.27
11.1	9.06	25.49	23.38	29.12
11.4	9.04	25.86	23.91	29.75
11.7	9.16	24.04	21.31	26.62
12	9.15	24.18	21.50	26.86

12.3	9.14	24.43	21.86	27.29
12.6	9.16	24.03	21.28	26.59
12.9	9.15	24.25	21.60	26.97
13.2	9.22	23.22	20.12	25.20
13.5	9.07	25.43	23.30	29.01
13.8	9.03	25.95	24.04	29.91
14.1	9.07	25.34	23.17	28.85
14.4	8.94	27.37	26.08	32.35
14.7	8.90	27.89	26.84	33.26
15	8.89	28.11	27.14	33.63
15.3	8.98	26.71	25.14	31.23
15.6	9.03	25.93	24.02	29.88
15.9	8.87	28.41	27.57	34.15
16.2	8.64	31.82	32.47	40.03
16.5	8.86	28.47	27.66	34.26
16.8	8.81	29.25	28.78	35.60
17.1	8.88	28.27	27.37	33.91
17.4	8.79	29.51	29.16	36.06
17.7	8.89	28.03	27.04	33.50
18	8.90	27.89	26.83	33.25
18.3	8.76	30.02	29.89	36.94
18.6	8.89	28.07	27.09	33.56
18.9	8.90	27.95	26.91	33.36
19.2	8.86	28.53	27.74	34.36
19.5	8.84	28.73	28.04	34.71
19.8	8.90	27.92	26.87	33.31
20.1	8.87	28.31	27.44	33.98
20.4	8.80	29.43	29.04	35.91
20.7	8.82	29.04	28.48	35.24
21	8.86	28.46	27.65	34.24
21.3	8.82	29.13	28.60	35.39
21.6	8.87	28.39	27.54	34.11
21.9	8.90	27.98	26.95	33.41
22.2	8.89	28.06	27.08	33.55
22.5	8.85	28.70	27.99	34.65
22.8	8.79	29.54	29.20	36.10
23.1	8.83	28.98	28.40	35.14
23.4	9.04	25.91	23.98	29.84
23.7	9.11	24.83	22.44	27.98
24	8.92	27.60	26.41	32.76
24.3	8.89	28.10	27.13	33.61
24.6	8.92	27.55	26.34	32.67
24.9	8.91	27.79	26.69	33.09

25.2

8.96

26.99

25.54

31.71

Appendix 13: Sample M2-146 data.

Chronology M2 146	Schrag Sr/Ca (mMol/Mol) M2-146	SST This study M2-146	SST Swart M2- 146	SSTFlannery13M2- 146
0.3	9.304	21.93	18.27	22.97
0.6	9.192	23.59	20.66	25.85
0.9	9.186	23.68	20.79	26.00
1.2	9.248	22.77	19.48	24.42
1.5	9.227	23.07	19.91	24.95
1.8	9.251	22.72	19.41	24.34
2.1	9.300	22.00	18.37	23.09
2.4	9.242	22.86	19.61	24.58
2.7	9.168	23.95	21.17	26.46
3	9.226	23.08	19.93	24.96
3.3	9.282	22.26	18.75	23.55
3.6	9.253	22.68	19.36	24.28
3.9	9.281	22.28	18.78	23.58
4.2	9.395	20.58	16.34	20.66
4.5	9.274	22.38	18.93	23.76
4.8	9.200	23.47	20.49	25.64
5.1	9.226	23.08	19.93	24.96
5.4	9.420	20.22	15.82	20.02
5.7	9.264	22.53	19.13	24.01
6	9.274	22.38	18.92	23.75
6.3	9.276	22.34	18.86	23.69
6.6	9.340	21.40	17.51	22.06
6.9	9.334	21.49	17.64	22.21
7.2	9.263	22.54	19.16	24.04

7.5	9.231	23.01	19.83	24.85
7.8	9.286	22.20	18.67	23.45
8.1	9.250	22.73	19.42	24.36
8.4	9.246	22.80	19.52	24.48
8.7	9.228	23.06	19.90	24.93
9	9.189	23.63	20.71	25.91
9.3	9.249	22.75	19.45	24.39
9.6	9.238	22.91	19.68	24.66
9.9	9.250	22.73	19.42	24.35
10.2	9.259	22.60	19.24	24.14
10.5	9.261	22.57	19.20	24.09
10.8	9.261	22.57	19.19	24.07
11.1	9.220	23.18	20.07	25.14
11.4	9.283	22.25	18.73	23.52
11.7	9.258	22.62	19.27	24.17
12	9.307	21.90	18.23	22.92
12.3	9.320	21.70	17.95	22.59
12.6	9.286	22.21	18.67	23.45
12.9	9.302	21.97	18.33	23.04
13.2	9.283	22.25	18.73	23.52
13.5	9.296	22.06	18.46	23.20
13.8	9.369	20.98	16.91	21.33
14.1	9.327	21.60	17.80	22.41
14.4	9.285	22.22	18.69	23.47
14.7	9.316	21.75	18.02	22.68
15	9.317	21.74	18.00	22.65
15.3	9.272	22.41	18.96	23.80
15.6	9.323	21.65	17.87	22.50

15.9	9.340	21.40	17.52	22.07
16.2	9.293	22.10	18.51	23.26
16.5	9.317	21.74	18.00	22.65
16.8	9.282	22.26	18.75	23.55
17.1	9.364	21.04	17.00	21.45
17.4	9.368	20.99	16.92	21.36
17.7	9.332	21.51	17.68	22.26
18	9.375	20.88	16.77	21.18
18.3	9.240	22.88	19.64	24.62
18.6	9.279	22.30	18.81	23.62
18.9	9.329	21.56	17.75	22.35
19.2	9.317	21.74	18.00	22.65
19.5	9.317	21.74	18.00	22.64
19.8	9.292	22.11	18.54	23.29
20.1	9.263	22.53	19.14	24.02
20.4	9.300	22.00	18.37	23.09
20.7	9.277	22.34	18.86	23.68
21	9.299	22.01	18.39	23.12
21.3	9.318	21.72	17.98	22.62
21.6	9.281	22.27	18.76	23.56
21.9	9.229	23.05	19.88	24.91
22.2	9.224	23.11	18.98	25.02
22.5	9.287	22.19	17.32	23.42
22.8	9.241	22.87	18.55	24.60
23.1	9.253	22.69	18.22	24.28
23.4	9.267	22.47	17.84	23.92
23.7	9.357	21.16	15.48	21.64
24	9.384	20.75	14.74	20.94

24.3	9.309	21.87	16.75	22.87
24.6	9.225	23.10	18.97	25.00
24.9	9.225	23.09	18.95	24.99
25.2	9.313	21.81	16.64	22.76
25.5	9.278	22.31	17.55	23.64
25.8	9.187	23.66	19.96	25.96
26.1	9.148	24.24	21.01	26.96
26.4	9.180	23.77	20.17	26.16
26.7	9.229	23.05	18.87	24.90
27	9.260	22.59	18.04	24.11
27.3	9.255	22.66	18.17	24.23
27.6	9.250	22.74	18.31	24.37
27.9	9.283	22.25	17.44	23.53
28.2	9.190	23.62	19.89	25.89
28.5	9.248	22.77	18.36	24.42
28.8	9.381	20.79	14.82	21.01
29.1	9.275	22.36	17.64	23.73
29.4	9.221	23.16	19.07	25.10
29.7	9.337	21.44	15.99	22.14
30	9.290	22.14	17.23	23.33
30.3	9.290	22.15	17.25	23.35
30.6	9.278	22.31	17.55	23.64
30.9	9.300	21.99	16.97	23.08
31.2	9.167	23.96	20.50	26.48
31.5	9.205	23.40	19.49	25.51
31.8	9.281	22.27	17.47	23.56

Appendix 14: Sample MZ-172 data.

Chronology MZ-172	Schrag Sr/Ca (mMol/Mol) MZ-172	SST This Study MZ-172	SST Swart MZ-172	SSTFlannery13MZ-172
0.4	9.03	25.94	24.02	29.89
0.8	8.97	26.86	25.36	31.49
1.2	9.08	25.26	23.05	28.72
1.6	9.20	23.50	20.52	25.68
2	9.02	26.09	24.25	30.16
2.4	9.02	26.20	24.40	30.34
2.8	9.10	24.94	22.59	28.16
3.2	9.12	24.69	22.24	27.75
3.6	9.09	25.13	22.87	28.50
4	9.08	25.27	23.07	28.73
4.4	9.22	23.22	20.13	25.20
4.8	9.20	23.43	20.43	25.57
5.2	9.10	24.92	22.57	28.14
5.6	9.19	23.63	20.72	25.91
6	9.07	25.46	23.34	29.07
6.4	9.09	25.12	22.85	28.48
6.8	9.03	26.05	24.20	30.09
7.2	9.00	26.37	24.65	30.64
7.6	9.07	25.37	23.21	28.90
8	9.10	24.98	22.65	28.23
8.4	8.99	26.51	24.84	30.87
8.8	8.93	27.41	26.14	32.42
9.2	9.14	24.33	21.73	27.12
9.6	9.18	23.78	20.92	26.16
10	9.12	24.65	22.18	27.67
10.4	9.14	24.40	21.82	27.24
10.8	9.09	25.14	22.88	28.51
11.2	9.10	24.92	22.57	28.14
11.6	9.03	25.96	24.06	29.93
12	9.27	22.45	19.02	23.87
12.4	9.09	25.05	22.75	28.35
12.8	9.03	25.94	24.03	29.89
13.2	9.13	24.51	21.97	27.42
13.6	9.02	26.13	24.30	30.22
14	8.98	26.77	25.22	31.32
14.4	9.02	26.14	24.32	30.24
14.8	9.01	26.23	24.44	30.39
15.2	8.98	26.71	25.14	31.23
15.6	8.91	27.80	26.70	33.11

16	8.90	27.86	26.79	33.21
16.4	8.99	26.55	24.91	30.95
16.8	8.87	28.30	27.42	33.97
17.2	8.93	27.47	26.23	32.53
17.6	8.95	27.10	25.70	31.90
18	8.92	27.54	26.33	32.66
18.4	8.92	27.61	26.43	32.77
18.8	8.98	26.71	25.14	31.22
19.2	8.97	26.90	25.41	31.55
19.6	9.02	26.12	24.29	30.21
20	9.07	25.35	23.18	28.88
20.4	8.96	26.98	25.52	31.68
20.8	9.09	25.16	22.91	28.54
21.2	9.01	26.34	24.60	30.58
21.6	9.03	25.93	24.02	29.88
22	8.94	27.30	25.98	32.23
22.4	8.96	27.00	25.55	31.73
22.8	8.96	26.97	25.50	31.66
23.2	9.01	26.34	24.61	30.59
23.6	8.88	28.23	27.32	33.85
24	8.89	28.11	27.14	33.63
24.4	8.96	27.05	25.62	31.81
24.8	8.94	27.30	25.99	32.25
25.2	8.87	28.30	27.42	33.96
25.6	8.89	28.12	27.16	33.65
26	8.92	27.61	26.43	32.78
26.4	8.99	26.56	24.93	30.97
26.8	8.90	27.88	26.81	33.24
27.2	8.94	27.39	26.11	32.39
27.6	8.91	27.69	26.54	32.91
28	8.99	26.63	25.02	31.09
28.4	8.91	27.74	26.61	32.99
28.8	8.91	27.72	26.58	32.95
29.2	8.90	27.90	26.85	33.28
29.6	8.89	28.04	27.82	33.52
30	8.95	27.13	26.19	31.95
30.4	8.91	27.69	27.19	32.91
30.8	9.01	26.31	24.72	30.53
31.2	8.96	26.99	25.94	31.71
31.6	8.95	27.16	26.25	32.00
32	8.91	27.72	27.24	32.96
32.4	8.82	29.14	29.79	35.41
32.8	8.95	27.13	26.18	31.94

33.2	8.93	27.50	26.86	32.59
33.6	8.93	27.53	26.90	32.63
34	8.93	27.48	26.81	32.54
34.4	8.99	26.51	25.08	30.88
34.8	8.95	27.18	26.28	32.03
35.2	8.98	26.66	25.35	31.14
35.6	8.92	27.56	26.97	32.70
36	9.05	25.74	23.70	29.55
36.4	8.97	26.88	25.73	31.51
36.8	8.95	27.11	26.15	31.91
37.2	8.92	27.60	27.03	32.75
37.6	8.98	26.75	25.51	31.30
38	8.93	27.48	26.81	32.54
38.4	8.92	27.55	26.94	32.67
38.8	8.88	28.21	28.12	33.80
39.2	8.83	28.92	29.39	35.02
39.6	8.90	27.96	27.68	33.38
40	8.83	28.98	29.51	35.14
40.4	8.89	28.00	27.75	33.45
40.8	8.81	29.17	29.85	35.47
41.2	8.77	29.82	31.01	36.59
41.6	8.87	28.29	28.27	33.95
42	8.94	27.38	26.64	32.38
42.4	8.89	28.01	27.76	33.46
42.8	8.98	26.70	25.41	31.20
43.2	8.92	27.56	26.96	32.69
43.6	8.88	28.26	28.21	33.89
44	8.95	27.19	26.29	32.05
44.4	8.89	28.03	27.80	33.49
44.8	9.02	26.17	24.47	30.29
45.2	9.03	25.92	24.02	29.86
45.6	8.95	27.19	26.30	32.05
46	9.03	25.95	24.07	29.91
46.4	9.05	25.71	23.64	29.49
46.8	9.12	24.58	21.62	27.56
47.2	9.04	25.77	23.75	29.61
47.6	9.05	25.62	23.48	29.35
48	8.97	26.83	25.65	31.43
48.4	9.03	26.04	24.23	30.06
48.8	8.97	26.85	25.68	31.46
49.2	8.97	26.83	25.64	31.42
49.6	9.01	26.26	24.63	30.44
50	9.10	24.88	22.16	28.07

50.4	9.05	25.63	23.50	29.36
50.8	9.01	26.29	24.69	30.51
51.2	9.11	24.77	21.95	27.87
51.6	9.14	24.32	21.15	27.10
52	9.09	25.12	22.58	28.48
52.4	9.10	24.98	22.33	28.24
52.8	9.07	25.35	23.00	28.88
53.2	9.29	22.15	17.25	23.35
53.6	9.18	23.74	20.10	26.10
54	9.00	26.39	24.87	30.68
54.4	9.16	24.09	20.73	26.70
54.8	9.13	24.45	21.39	27.33
55.2	9.10	24.93	22.24	28.15
55.6	9.11	24.85	22.11	28.02
56	9.18	23.80	20.21	26.20
56.4	9.06	25.48	23.22	29.09
56.8	9.08	25.29	22.88	28.77
57.2	9.08	25.31	22.92	28.80
57.6	8.96	27.01	25.97	31.74
58	9.02	26.08	24.31	30.14
58.4	8.88	28.13	27.99	33.67
58.8	8.91	27.82	27.42	33.13
59.2	9.04	25.78	23.77	29.62
59.6	9.01	26.28	24.67	30.48
60	9.05	25.74	23.69	29.55
60.4	9.08	25.27	22.86	28.74
60.8	9.14	24.31	21.13	27.08
61.2	9.08	25.30	22.90	28.79
61.6	9.22	23.20	19.15	25.17
62	9.15	24.26	21.04	27.00
62.4	9.00	26.50	25.05	30.86
62.8	8.94	27.36	26.61	32.35
63.2	9.01	26.35	24.79	30.60
63.6	9.05	25.70	23.62	29.47
64	9.11	24.75	21.91	27.83
64.4	9.09	25.14	22.62	28.51
64.8	9.11	24.88	22.15	28.06
65.2	9.04	25.90	23.99	29.83
65.6	9.01	26.27	24.65	30.47
66	9.05	25.70	23.62	29.47
66.4	9.05	25.62	23.49	29.35

66.8	9.04	25.78	23.77	29.62
67.2	9.05	25.66	23.55	29.41
67.6	9.15	24.26	21.04	26.99
68	9.00	26.37	24.83	30.64
68.4	9.03	26.00	24.15	29.99
68.8	9.15	24.23	21.00	26.95
69.2	9.07	25.41	23.10	28.97
69.6	9.17	23.96	20.50	26.48
70	9.12	24.69	21.82	27.74
70.4	9.06	25.59	23.43	29.30
70.8	8.88	28.16	28.04	33.72
71.2	9.00	26.36	24.80	30.62
71.6	9.02	26.13	24.40	30.23
72	8.97	26.89	25.76	31.53
72.4	9.09	25.16	22.65	28.54
72.8	9.13	24.55	21.57	27.51
73.2	9.04	25.90	23.98	29.82
73.6	9.06	25.48	23.23	29.11
74	9.18	23.76	20.14	26.13
74.4	9.22	23.13	19.02	25.05
74.8	9.16	24.12	20.80	26.76
75.2	9.08	25.25	22.82	28.71
75.6	9.08	25.24	22.80	28.69
76	9.01	26.24	24.59	30.41
76.4	9.12	24.67	21.78	27.71
76.8	9.03	26.01	24.17	30.01
77.2	8.98	26.73	25.48	31.26
77.6	9.20	23.51	19.70	25.71
78	9.28	22.33	17.57	23.66
78.4	9.26	22.66	18.17	24.23
78.8	9.20	23.44	19.58	25.59
79.2	9.32	21.75	16.55	22.67
79.6	9.33	21.61	16.30	22.44
80	9.39	20.73	14.71	20.91
80.4	9.27	22.39	17.69	23.78
80.8	9.35	21.22	15.59	21.75
81.2	9.27	22.46	17.81	23.89
81.6	9.26	22.53	17.94	24.02
82	9.30	22.00	16.99	23.10
82.4	9.32	21.63	16.32	22.46
82.8	9.31	21.81	16.66	22.78
83.2	9.36	21.05	15.29	21.46

83.6	9.36	21.13	15.42	21.59
84	9.24	22.93	18.66	24.71
84.4	9.17	23.98	20.55	26.52
84.8	9.15	24.17	20.88	26.84
85.2	9.06	25.54	23.34	29.20
85.6	9.03	25.97	24.10	29.94
86	8.92	27.67	27.16	32.88
86.4	9.00	26.48	25.03	30.83
86.8	9.02	26.19	24.50	30.33
87.2	8.98	26.68	25.38	31.17
87.6	9.02	26.12	24.37	30.20
88	9.09	25.12	22.58	28.48
88.4	9.09	25.12	22.58	28.48
88.8	9.14	24.42	21.32	27.27
89.2	9.05	25.76	23.74	29.59
89.6	9.13	24.44	21.37	27.31
90	9.05	25.63	23.51	29.37
90.4	9.09	25.14	22.63	28.52
90.8	9.01	26.35	24.79	30.60
91.2	9.14	24.42	21.33	27.27
91.6	9.09	25.12	22.59	28.48
92	9.14	24.30	21.11	27.07
92.4	9.11	24.80	22.01	27.93
92.8	9.15	24.28	21.08	27.03
93.2	9.10	24.90	22.18	28.09
93.6	8.98	26.74	25.48	31.27
94	9.00	26.46	24.99	30.79
94.4	8.97	26.89	25.75	31.53
94.8	8.92	27.63	27.09	32.81
95.2	8.87	28.38	28.42	34.09
95.6	8.88	28.19	28.10	33.78
96	9.06	25.48	23.23	29.10
96.4	9.09	25.14	22.62	28.52
96.8	9.07	25.36	23.02	28.90
97.2	8.98	26.76	25.53	31.31
97.6	9.01	26.35	24.78	30.59
98	8.99	26.57	25.18	30.97
98.4	9.01	26.26	24.62	30.44
98.8	9.02	26.20	24.51	30.34
99.2	8.99	26.64	25.32	31.11
99.6	8.91	27.72	27.24	32.96
100	9.07	25.35	23.00	28.88
100.4	8.99	26.59	25.21	31.01

100.8	9.01	26.33	24.75	30.56
101.2	9.12	24.65	21.75	27.67
101.6	9.16	24.13	20.81	26.77
102	8.93	27.44	26.75	32.49
102.4	8.99	26.61	25.25	31.05
102.8	9.08	25.27	22.85	28.74
103.2	9.12	24.68	21.79	27.71
103.6	9.05	25.75	23.71	29.57
104	9.02	26.12	24.37	30.20
104.4	9.01	26.26	24.63	30.44
104.8	9.03	25.92	24.01	29.85
105.2	9.10	24.98	22.33	28.23
105.6	9.04	25.82	23.84	29.69
106	8.99	26.64	25.30	31.09
106.4	9.08	25.27	22.85	28.74
106.8	9.11	24.85	22.10	28.01
107.2	9.03	26.00	24.16	29.99
107.6	9.06	25.56	23.37	29.24
108	8.94	27.26	26.43	32.18
108.4	8.94	27.38	26.63	32.38
108.8	9.00	26.48	25.03	30.83
109.2	8.98	26.74	25.49	31.27
109.6	8.96	27.01	25.98	31.74
110	9.03	26.02	24.20	30.03
110.4	9.04	25.89	23.97	29.81
110.8	9.05	25.73	23.67	29.52
111.2	9.09	25.17	22.67	28.56

Appendix 15: Sample M3-4 data.

Chronology M3 4	Schrag Sr/Ca (mMol/Mol)M3-4	SST This Study M3-4	SST Swart M3-4	SSTFlannery13M3-4
0.3	9.02	26.09	24.25	30.16
0.6	9.01	26.29	24.53	30.50
0.9	9.00	26.41	24.70	30.70
1.2	9.05	25.70	23.68	29.48
1.5	8.99	26.64	25.03	31.09
1.8	9.03	26.04	24.18	30.07
2.1	8.93	27.43	26.17	32.47
2.4	8.98	26.69	25.11	31.19
2.7	8.97	26.82	25.29	31.40
3	8.97	26.82	25.30	31.41
3.3	8.96	27.03	25.60	31.77
3.6	9.06	25.52	23.42	29.16
3.9	9.05	25.71	23.70	29.50
4.2	9.03	25.97	24.07	29.94
4.5	9.05	25.74	23.74	29.54
4.8	8.99	26.55	24.91	30.95
5.1	9.01	26.26	24.49	30.45
5.4	9.00	26.49	24.82	30.84
5.7	9.03	25.99	24.10	29.98
6	8.98	26.72	25.15	31.23
6.3	8.99	26.62	25.00	31.06
6.6	9.02	26.20	24.40	30.34
6.9	9.07	25.39	23.24	28.94
7.2	9.20	23.44	20.45	25.59
7.5	9.02	26.18	24.38	30.31
7.8	9.11	24.78	22.37	27.90
8.1	9.06	25.47	23.36	29.09
8.4	9.06	25.55	23.48	29.23
8.7	9.09	25.09	22.81	28.43
9	9.02	26.12	24.29	30.20
9.3	9.08	25.30	23.12	28.79
9.6	9.21	23.37	20.34	25.46
9.9	9.02	26.20	24.40	30.34
10.2	9.07	25.42	23.28	28.99
10.5	9.04	25.80	23.83	29.66
10.8	9.14	24.43	21.87	27.29
11.1	9.22	23.13	19.99	25.04
11.4	9.13	24.48	21.94	27.38
11.7	9.32	21.65	17.87	22.49

12	9.09	25.07	22.78	28.39
12.3	9.07	25.34	23.17	28.86
12.6	9.12	24.59	22.09	27.57
12.9	9.15	24.20	21.54	26.90
13.2	9.06	25.48	23.37	29.10
13.5	9.08	25.21	22.98	28.63
13.8	8.98	26.70	25.12	31.21
14.1	8.98	26.76	25.21	31.31
14.4	9.06	25.53	23.45	29.20
14.7	9.04	25.85	23.91	29.75
15	9.02	26.07	24.22	30.13
15.3	9.12	24.60	22.11	27.58
15.6	9.10	24.97	22.63	28.21
15.9	9.20	23.54	20.59	25.76
16.2	9.11	24.74	22.31	27.83
16.5	9.06	25.57	23.50	29.26
16.8	9.11	24.86	22.48	28.03
17.1	9.11	24.73	22.29	27.81
17.4	9.08	25.23	23.01	28.67
17.7	9.03	26.04	24.18	30.07
18	9.08	25.19	22.96	28.60
18.3	9.14	24.31	21.70	27.09
18.6	9.08	25.29	23.10	28.77
18.9	9.05	25.67	23.65	29.44
19.2	9.06	25.60	23.55	29.31
19.5	9.04	25.84	23.89	29.73
19.8	9.09	25.03	22.72	28.32
20.1	9.08	25.25	23.03	28.70
20.4	9.07	25.40	23.25	28.96
20.7	9.11	24.76	22.33	27.85
21	9.17	23.90	21.10	26.38
21.3	9.20	23.47	20.49	25.64
21.6	9.15	24.19	21.52	26.87
21.9	9.16	24.13	21.43	26.77
22.2	9.17	23.86	20.32	26.30
22.5	9.18	23.76	20.14	26.13
22.8	9.06	25.49	23.24	29.11
23.1	9.06	25.48	23.24	29.11
23.4	9.10	25.02	22.41	28.31
23.7	9.07	25.42	23.12	28.99
24	9.03	26.05	24.26	30.09
24.3	8.98	26.80	25.59	31.37
24.6	8.98	26.75	25.51	31.29

24.9	9.05	25.71	23.64	29.49
25.2	9.10	24.93	22.25	28.16
25.5	9.02	26.19	24.50	30.32
25.8	9.03	26.01	24.18	30.01
26.1	9.03	26.01	24.18	30.01
26.4	9.07	25.42	23.11	28.99
26.7	9.08	25.26	22.83	28.72
27	9.00	26.45	24.97	30.77
27.3	9.07	25.40	23.09	28.97
27.6	9.14	24.43	21.35	27.29
27.9	9.14	24.33	21.17	27.12
28.2	9.11	24.77	21.96	27.88
28.5	9.03	26.00	24.17	30.01
28.8	9.03	26.03	24.22	30.05
29.1	9.11	24.86	22.11	28.03

Appendix 16: Modern coral data.

Age Model Mo	Sr/Ca (mMol/Mol) Mo	SST This Study Mo	SST Swart Mo	SSTFlannery13Mo
1996.923892	8.91	27.76	26.65	33.04
1996.992339	8.97	26.87	25.37	31.51
1997.04162	9.1	24.95	22.61	28.19
1997.101853	8.95	27.17	25.80	32.02
1997.159349	8.98	26.73	25.16	31.25
1997.214106	8.99	26.58	24.95	30.99
1997.257912	8.98	26.73	25.16	31.25
1997.312669	9.01	26.28	24.52	30.48
1997.329097	8.99	26.58	24.95	30.99
1997.361951	8.9	27.91	26.86	33.29
1997.416709	8.87	28.35	27.49	34.06
1997.493369	8.9	27.91	26.86	33.29
1997.520748	8.84	28.80	28.13	34.82
1997.572767	8.81	29.24	28.77	35.59
1997.630262	8.81	29.24	28.77	35.59
1997.778107	8.79	29.54	29.19	36.10
1997.824651	8.81	29.24	28.77	35.59
1997.879409	8.81	29.24	28.77	35.59
1997.953331	8.83	28.95	28.34	35.08
1998.008089	8.88	28.21	27.28	33.80
1998.040943	8.98	26.73	25.16	31.25
1998.10939	8.96	27.02	25.58	31.76
1998.161409	8.98	26.73	25.16	31.25
1998.213429	8.98	26.73	25.16	31.25
1998.306517	8.9	27.91	26.86	33.29
1998.325682	8.91	27.76	26.65	33.04
1998.396866	8.86	28.50	27.71	34.31
1998.407818	8.88	28.21	27.28	33.80
1998.462575	8.81	29.24	28.77	35.59
1998.555663	8.81	29.24	28.77	35.59
1998.714459	8.77	29.83	29.62	36.61
1998.761003	8.87	28.35	27.49	34.06
1998.804809	8.83	28.95	28.34	35.08
1998.823974	8.91	27.76	26.65	33.04
1998.840401	8.89	28.06	27.07	33.55
1998.856829	8.97	26.87	25.37	31.51
1998.870518	9.01	26.28	24.52	30.48
1998.944441	8.97	26.87	25.37	31.51
1998.990984	8.96	27.02	25.58	31.76

1999.119664	9.01	26.28	24.52	30.48
1999.259296	8.97	26.87	25.37	31.51
1999.377024	8.97	26.87	25.37	31.51
1999.47285	8.94	27.32	26.01	32.27
1999.631646	8.84	28.80	28.13	34.82
1999.691879	8.83	28.95	28.34	35.08
1999.705569	8.98	26.73	25.16	31.25
1999.730209	8.87	28.35	27.49	34.06
1999.75485	8.87	28.35	27.49	34.06
1999.779491	8.89	28.06	27.07	33.55
1999.795918	8.84	28.80	28.13	34.82
1999.842462	8.88	28.21	27.28	33.80
1999.858889	8.92	27.61	26.43	32.78
2000.039589	9.01	26.28	24.52	30.48
2000.066968	8.99	26.58	24.95	30.99
2000.091608	8.97	26.87	25.37	31.51
2000.201123	9.01	26.28	24.52	30.48
2000.294211	8.99	26.58	24.95	30.99
2000.34623	8.98	26.73	25.16	31.25
2000.425629	9	26.43	24.73	30.74
2000.455745	8.9	27.91	26.86	33.29
2000.540619	8.84	28.80	28.13	34.82
2000.595377	8.83	28.95	28.34	35.08
2000.647396	8.82	29.09	28.56	35.33
2000.787028	8.76	29.98	29.83	36.86
2000.871902	8.88	28.21	27.28	33.80
2000.929397	9.02	26.13	24.31	30.23
2001.025222	8.97	26.87	25.37	31.51
2001.11831	9	26.43	24.73	30.74
2001.211398	9.02	26.13	24.31	30.23
2001.329126	8.93	27.47	26.22	32.53
2001.359243	8.94	27.32	26.01	32.27
2001.403049	8.91	27.76	26.65	33.04
2001.414	8.93	27.47	26.22	32.53
2001.435903	8.86	28.50	27.71	34.31
2001.455068	8.84	28.80	28.13	34.82
2001.646719	8.85	28.65	27.92	34.57
2001.693263	8.82	29.09	28.56	35.33
2001.715166	8.82	29.09	28.56	35.33
2001.988953	8.94	27.32	26.01	32.27
2002.04371	8.95	27.17	25.80	32.02
2002.197031	8.98	26.73	25.16	31.25
2002.454391	8.94	27.32	26.01	32.27

2002.5201	8.93	27.47	26.22	32.53
2002.566644	8.9	27.91	26.86	33.29
2002.613188	8.87	28.35	27.49	34.06
2002.667945	8.92	27.61	26.43	32.78
2002.681634	8.89	28.06	27.07	33.55
2002.695324	8.82	29.09	28.56	35.33
2002.733654	8.83	28.95	28.34	35.08
2002.782936	8.74	30.28	30.25	37.37
2002.824004	8.75	30.13	30.04	37.12
2002.85412	8.8	29.39	28.98	35.84
2002.884237	8.83	28.95	29.44	35.08
2002.94447	8.88	28.21	28.12	33.80
2003.026606	8.98	26.73	25.46	31.25
2003.138859	9	26.43	24.93	30.74
2003.352413	8.97	26.87	25.73	31.51
2003.412646	8.93	27.47	26.79	32.53
2003.472879	8.89	28.06	27.85	33.55
2003.544064	8.87	28.35	28.38	34.06
2003.628938	8.83	28.95	29.44	35.08
2003.648103	8.83	28.95	29.44	35.08
2003.667268	8.83	28.95	29.44	35.08
2003.711074	8.8	29.39	30.24	35.84
2003.746666	8.8	29.39	30.24	35.84
2003.779521	8.8	29.39	30.24	35.84
2003.842492	8.83	28.95	29.44	35.08
2003.861657	8.85	28.65	28.91	34.57
2003.878084	8.86	28.50	28.65	34.31
2003.924628	8.96	27.02	25.99	31.76
2003.979385	8.9	27.91	27.59	33.29
2004.03688	8.93	27.47	26.79	32.53
2004.083424	8.97	26.87	25.73	31.51
2004.121754	8.99	26.58	25.20	30.99
2004.195677	9.02	26.13	24.40	30.23
2004.313405	8.95	27.17	26.26	32.02
2004.398279	8.95	27.17	26.26	32.02
2004.480416	8.86	28.50	28.65	34.31
2004.557076	8.85	28.65	28.91	34.57
2004.636474	8.82	29.09	29.71	35.33
2004.663853	8.85	28.65	28.91	34.57
2004.702183	8.81	29.24	29.97	35.59
2004.713135	8.85	28.65	28.91	34.57
2004.724086	8.85	28.65	28.91	34.57
2004.787057	8.84	28.80	29.18	34.82

2004.877407	8.93	27.47	26.79	32.53
2005.02799	8.98	26.73	25.46	31.25
2005.11834	9	26.43	24.93	30.74
2005.200476	8.99	26.58	25.20	30.99
2005.252495	8.96	27.02	25.99	31.76
2005.318204	8.92	27.61	27.06	32.78
2005.422243	8.91	27.76	27.32	33.04
2005.441408	8.92	27.61	27.06	32.78
2005.460573	8.87	28.35	28.38	34.06
2005.518069	8.89	28.06	27.85	33.55
2005.561875	8.88	28.21	28.12	33.80
2005.635797	8.83	28.95	29.44	35.08
2005.712458	8.77	29.83	31.03	36.61
2005.791856	8.83	28.95	29.44	35.08
2005.865778	8.84	28.80	29.18	34.82
2005.947914	8.93	27.47	26.79	32.53
2006.041002	9.03	25.99	24.14	29.97
2006.117662	9.05	25.69	23.61	29.46
2006.169682	9.02	26.13	24.40	30.23
2006.224439	9.08	25.25	22.81	28.70
2006.284673	8.98	26.73	25.46	31.25
2006.325741	8.96	27.02	25.99	31.76
2006.364071	8.93	27.47	26.79	32.53
2006.413352	8.9	27.91	27.59	33.29
2006.462634	8.89	28.06	27.85	33.55
2006.536557	8.92	27.61	27.06	32.78
2006.703567	8.87	28.35	28.38	34.06
2006.793917	8.9	27.91	27.59	33.29
2006.848674	8.96	27.02	25.99	31.76
2006.878791	8.9	27.91	27.59	33.29
2007.023898	8.95	27.17	26.26	32.02
2007.078655	9.08	25.25	22.81	28.70
2007.138888	9.09	25.10	22.55	28.44
2007.179956	9.05	25.69	23.61	29.46
2007.204597	9.09	25.10	22.55	28.44
2007.231976	8.98	26.73	25.46	31.25
2007.256617	8.95	27.17	26.26	32.02
2007.283995	8.94	27.32	26.53	32.27
2007.311374	8.92	27.61	27.06	32.78
2007.336015	8.91	27.76	27.32	33.04
2007.360656	8.91	27.76	27.32	33.04

2007.385297	8.86	28.50	28.65	34.31
2007.409938	8.86	28.50	28.65	34.31
2007.423627	8.87	28.35	28.38	34.06
2007.456481	8.84	28.80	29.18	34.82
2007.48386	8.85	28.65	28.91	34.57
2007.511239	8.84	28.80	29.18	34.82
2007.538617	8.83	28.95	29.44	35.08
2007.565996	8.81	29.24	29.97	35.59
2007.61254	8.86	28.50	28.65	34.31
2007.659084	8.91	27.76	27.32	33.04
2007.700152	8.77	29.83	31.03	36.61
2007.771336	8.89	28.06	27.85	33.55
2007.880851	8.87	28.35	28.38	34.06
2007.962987	8.97	26.87	25.73	31.51
2008.195706	9.01	26.28	24.67	30.48
2008.228561	8.89	28.06	27.85	33.55
2008.258678	8.95	27.17	26.26	32.02
2008.286056	8.99	26.58	25.20	30.99
2008.321649	8.95	27.17	26.26	32.02
2008.368192	8.95	27.17	26.26	32.02
2008.420212	8.89	28.06	27.85	33.55
2008.458542	8.88	28.21	28.12	33.80
2008.540678	8.9	27.91	27.59	33.29
2008.62829	8.85	28.65	28.91	34.57
2008.702213	8.85	28.65	28.91	34.57
2008.762446	8.9	27.91	27.59	33.29
2008.798038	8.85	28.65	28.91	34.57
2008.874698	8.88	28.21	28.12	33.80
2008.973262	8.97	26.87	25.73	31.51
2009.055398	9.01	26.28	24.67	30.48
2009.156699	9.06	25.54	23.34	29.21
2009.195029	9.18	23.77	20.16	26.15
2009.288117	9.05	25.69	23.61	29.46
2009.351088	9	26.43	24.93	30.74
2009.397632	8.93	27.47	26.79	32.53
2009.416797	8.96	27.02	25.99	31.76
2009.471554	8.92	27.61	27.06	32.78
2009.564642	8.91	27.76	27.32	33.04
2009.68237	8.96	27.02	25.99	31.76
2009.73439	8.9	27.91	27.59	33.29
2009.882235	8.92	27.61	27.06	32.78
2009.950682	8.97	26.87	25.73	31.51

2010.038294	8.99	26.58	25.20	30.99
2010.128643	8.99	26.58	25.20	30.99
2010.161498	8.99	26.58	25.20	30.99
2010.21078	8.97	26.87	25.73	31.51
2010.32577	8.92	27.61	27.06	32.78
2010.383265	8.88	28.21	28.12	33.80
2010.435285	8.83	28.95	29.44	35.08
2010.509207	8.79	29.54	30.50	36.10
2010.536586	8.8	29.39	30.24	35.84
2010.629674	8.78	29.68	30.77	36.35
2010.703596	8.81	29.24	29.97	35.59
2010.793946	8.82	29.09	29.71	35.33
2010.895247	8.92	27.61	27.06	32.78
2011.002024	8.95	27.17	26.26	32.02
2011.193675	8.98	26.73	25.46	31.25
2011.371637	8.96	27.02	25.99	31.76
2011.39354	8.92	27.61	27.06	32.78
2011.459249	8.89	28.06	27.85	33.55
2011.541385	8.89	28.06	27.85	33.55
2011.582453	8.84	28.80	29.18	34.82
2011.623521	8.8	29.39	30.24	35.84
2011.667327	8.83	28.95	29.44	35.08
2011.711133	8.79	29.54	30.50	36.10
2011.798745	8.8	29.39	30.24	35.84
2011.875405	8.86	28.50	28.65	34.31
2011.990396	8.95	27.17	26.26	32.02
2012.042415	8.96	27.02	25.99	31.76
2012.083483	8.97	26.87	25.73	31.51
2012.127289	8.98	26.73	25.46	31.25
2012.201212	8.95	27.17	26.26	32.02
2012.288824	8.95	27.17	26.26	32.02
2012.368222	8.96	27.02	25.99	31.76
2012.458572	8.92	27.61	27.06	32.78
2012.70498	8.81	29.24	29.97	35.59
2012.798068	8.84	28.80	29.18	34.82
2012.844611	8.89	28.06	27.85	33.55
2012.874728	8.85	28.65	28.91	34.57
2012.907582	8.91	27.76	27.32	33.04
2012.937699	8.89	28.06	27.85	33.55
2013.00067	9.01	26.28	24.67	30.48
2013.055427	9.04	25.84	23.87	29.72
2013.09102	8.95	27.17	26.26	32.02
2013.12935	8.99	26.58	25.20	30.99

2013.184107	8.99	26.58	25.20	30.99
2013.241603	9.01	26.28	24.67	30.48
2013.29636	8.96	27.02	25.99	31.76
2013.34838	8.94	27.32	26.53	32.27
2013.375758	8.91	27.76	27.32	33.04
2013.518128	8.89	28.06	27.85	33.55
2013.627642	8.84	28.80	29.18	34.82
2013.674186	8.87	28.35	28.38	34.06
2013.789177	8.82	29.09	29.71	35.33
2013.857624	8.85	28.65	28.91	34.57
2013.956187	8.95	27.17	26.26	32.02
2014.123197	8.96	27.02	25.99	31.76
2014.342227	8.92	27.61	27.06	32.78
2014.449004	8.88	28.21	28.12	33.80
2014.484596	8.92	27.61	27.06	32.78
2014.544829	8.86	28.50	28.65	34.31
2014.624227	8.9	27.91	27.59	33.29
2014.766597	8.82	29.09	29.71	35.33
2014.867898	8.84	28.80	29.18	34.82
2014.950034	8.88	28.21	28.12	33.80
2015.037646	8.89	28.06	27.85	33.55
2015.204656	8.94	27.32	26.53	32.27
2015.34155	8.88	28.21	28.12	33.80
2015.374404	8.92	27.61	27.06	32.78
2015.437375	8.9	27.91	27.59	33.29
2015.481181	8.89	28.06	27.85	33.55
2015.538676	8.81	29.24	29.97	35.59
2015.639978	8.77	29.83	31.03	36.61
2015.722114	8.72	30.57	32.36	37.88
2015.760444	8.75	30.13	31.56	37.12
2015.779609	8.8	29.39	30.24	35.84
2015.796036	8.86	28.50	28.65	34.31
2015.869959	8.82	29.09	29.71	35.33
2015.990425	8.93	27.47	26.79	32.53
